Cation-Controlled Diastereo- and Enantioselective Synthesis of Indolines: An Autocatalytic Process

Krishna Sharma

A dissertation presented in partial fulfilment of the requirements for the award of the degree of

Master of Science (by Research)

of the

University of Oxford





Chemistry Research Laboratory
12 Mansfield Road
Oxford OX1 3TA

St Peter's College
New Inn Hall St
Oxford OX1 2DL

March 2014

Declaration

This dissertation describes the work carried out at the Chemistry Research Laboratory, University of Oxford, between October 2011 and January 2014. The dissertation is the result of my own work and includes nothing which is the outcome of work done in collaboration except where specifically indicated in the text.

Krishna Sharma

Acknowledgements

I would like to take this opportunity to thank my supervisor, Dr Martin Smith for his constant motivation, encouragement and for always bringing me hope by saying "this chemistry will definitely work, we're almost getting there". He has been an excellent mentor and I have managed to learn quite a lot from him. Without his guidance and support it would not have been possible to carry out the research work described in this thesis.

Thanks to Dr Meiling Li for being an amazing co-supervisor during the first year of my research and for setting such high standards by working more than 12 hours in a day. Thanks for teaching all the skills and for having made me feel comfortable in the lab.

Thanks to Dr Peter Knipe, Dr Craig Johnston and Roly Armstrong for taking out their precious time to proof-read this thesis. I also thank Dr Russell Driver for his help with X-ray crystallography. Thanks to all the members of the Smith group: Dr Jamie Wolstenhulme, Dr Craig Campbell, Alan Lamb, Emily Kiss, Alex Cavell, Philip Gerken, Antti Lahdenperä, Shuyu Chu, John Joliffe, Ben Rahemtulla, Elliot Smith and Danielle Bunting; for their support, invaluable advice and creating a cheerful and friendly atmosphere in the lab. Thanks to the past members of the group: Dr Phil Woods, Dr Caroline Stovold and Dr Melissa D'Ascenzio for all the good times.

A big thank you goes to my family for having supported me at all times. My maternal grandparents: Prof. V. N. Dixit and Dr Manorama Dixit have always been a great source of support and motivation and have played an integral role in shaping my life. My parents: Prof. R. K. Sharma and Dr Ranjana Sharma, who happen to be chemist have been a tremendous source of inspiration and enthusiasm and it would not have been possible to pursue my studies without their support. I also thank my brother Pranav Sharma for all the cheerful times we have had. Thanks to all my friends in Oxford and in India.

Thanks to the Tata Trusts for the scholarship.

Thanks to the Almighty!

List of abbreviations

Å	Ångström
a	antarafacial
app.	apparent
Alk	alkyl
aq.	aqueous
Ar	Aromatic
Bn	Benzyl
br.	broad
Bu	Butyl
C	Celcius
c	centi
c	concentration
cat.	catalyst
COSY	^{1}H-^{1}H Correlation Spectroscopy
d	doublet
deg	degree
δ	chemical shift
DEPT	Distortionless Enchancement by Polarization Transfer
DMF	*N*,*N*-dimethylformamide
d.r.	Diastereomeric ratio
e.e.	Enantiomeric excess
eq	equivalents
ESI	electrospray ionization
Et	Ethyl
EWG	Electron-withdrawing group
FI	field ionization
FT	Fourier transform
G	grams
H	Hertz
h	Planck's constant
h	Hour(s)
HMBC	Heteronuclear Multiple Bond Correlation Spectroscopy
HPLC	High Performance Liquid Chromatography Spectroscopy
HRMS	High Resolution Mass Spectrometry

HSQC	Heteronuclear Single Quantum Correlation Spectroscopy
i	iso
IPA	isopropyl alcohol (propan-2-ol)
IR	infrared
IUPAC	International Union of Pure and Applied Chemistry
J	coupling constant
L	Litres
λ	wavelength
lit.	literature
LRMS	low resolution mass spectrometry
M	mega
M	Molar
m	*meta*
m	metre
m	milli
m	multiplet
Me	methyl
min	minutes
mol	moles
mp	melting point
μ	micro
n	normal
NMR	nuclear magnetic resonance
ν	frequency
o	*ortho*
p	*para*
PE	petroleum ether
Ph	phenyl
ppm	parts per million
Pr	propyl
PTC	Phase-transfer Catalysis
q	quartet
®	registered trademark
R	generic substituent
R_f	retention Factor
RT	room temperature

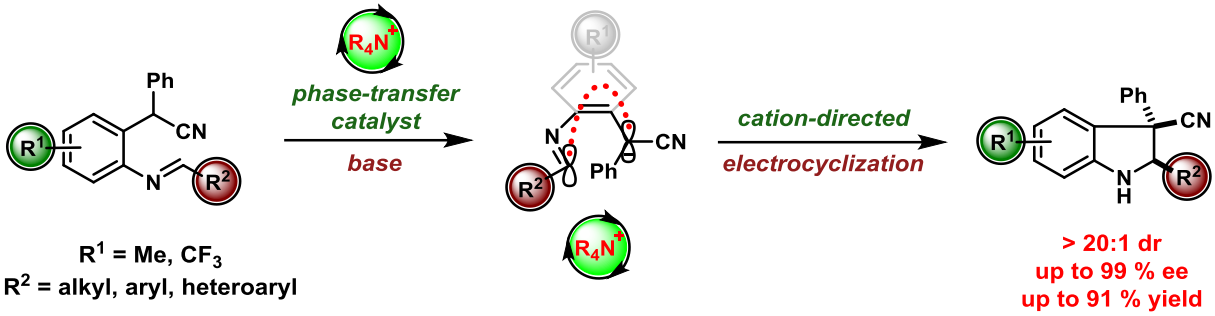
s	singlet
s	suprafacial

Cation-Controlled Diastereo- and Enantioselective Synthesis of Indolines: An Autocatalytic Process

Krishna Sharma MSc (by Research), Hilary 2014 St Peter's College

Abstract

Asymmetric phase-transfer catalysis is a powerful technique that enables a wide range of transformations under mild conditions, often using inexpensive and environmentally benign reagents. By extending the applications of phase-transfer catalysis we have developed a highly diastereo- and enantioselective synthesis of functionalized indolines bearing two contiguous stereocentres, one of which is quaternary and all carbon, in a single synthetic step. The reaction proceeds with complete diastereoselectivity and with high levels of enantioselectivity (up to 99% ee).



Cation-directed diastereo- and enantioselective synthesis of indolines

Despite the development of phase-transfer catalysis as a primary synthetic tool in organic synthesis, the mechanistic understanding of these reactions still remains a challenge, due mainly to the difficulty of studying the complex multi-phase systems. Therefore, a further aim of this project was to understand the reaction mechanism of our phase-transfer catalysed transformation. Investigations into the mechanism of our phase-transfer catalysed reaction have been carried out by studying the reaction kinetics. These have shown that the reaction follows a sigmoidal curve with an induction period present. A detailed kinetic investigation was carried out which demonstrated that an autocatalytic mechanism is operational.

Table of Contents

Declaration i

Acknowledgements ii

List of abbreviations iii

Abstract vi

Table of Contents vii

1. Introduction 1

1.1 Pericyclic reactions 1

1.1.1 Stereochemistry of electrocyclizations 5

1.2 Literature 6

1.2.1 Asymmetric 4π Nazarov 7

1.2.2 6π Electrocyclizations 12

1.2.3 Asymmetric 6π Electrocyclizations 14

1.3 Project Aims 17

2. Results and Discussion 18

2.1 Retrosynthesis 20

2.2 Synthesis of substrates 21

2.2.1 Synthesis of phenylnitrile substituted anilines 21

2.2.2 Imine formation 22

2.3 Initial attempts at cyclization 23

2.4 Optimization of the reaction conditions 24

2.4.1 Screening of different temperatures 25

2.4.2 Screening of base 27

2.4.3 Catalyst screening 28

2.4.4 Catalyst loading 30

2.4.5 Solvent screen 31

2.4.6 Concentration effects 33

2.5 Cyclization with optimized reaction conditions 34

2.6 Stereochemical model 39

3. Mechanism of Phase-Transfer Catalysis 41

3.1 Introduction: Phase-transfer catalysis 41

3.1.1 Mechanism of phase-transfer catalysis 42

3.1.1.1 Starks' extraction mechanism 42

3.1.1.1.1 Brandstrom-Montanari modification 43

3.1.1.2 Mąkosza's interfacial mechanism 44

3.1.1.3 Modified interfacial mechanism 46

3.1.2 Kinetic factors influencing PTC reactions 47

3.1.2.1 Catalyst structure 47

3.1.2.2 Effect of anions 49

3.1.2.3 Stirring speed 49

3.1.2.4 Kinetic order with respect to catalyst concentration 50

3.1.3 Mechanistic Investigations: Phase-transfer catalysis 51

3.1.3.1 Investigations by Starks 51

3.1.3.2 Kinetic investigations by Merck 52

3.1.3.3 Kinetic investigations by Denmark 57

3.2 Mechanistic Investigations on our phase-transfer catalysed cyclization 58

3.2.1 Catalyst-Dependent Diastereoselectivity 58

3.2.1.1 Interconversion Experiments 59

3.2.1.1.1 Investigations on ester-substituted system 59

3.2.1.1.2 Investigations on nitrile-substituted system 60

3.2.1.2 Interconversion Experiments- Conclusions 62

3.2.2 Kinetic Investigations 64

3.2.2.1 Initial investigations 64

3.2.2.1.1 Initial attempts at monitoring reaction 64

3.2.2.1.2 Modification of reaction conditions 65
3.2.2.2 Kinetic investigation experiments 67
3.2.2.2.1 Order of addition experiments 67
3.2.2.2.2 Background cyclization 70
3.2.2.2.2.1 Kinetic profile- background cyclization 70
3.2.2.2.3 Chiral catalyst loading 72
3.2.2.2.4 Cyclization with –OH protected catalyst 74
3.2.2.2.5 Stirring rate experiments 75
3.2.2.2.6 Autocatalysis investigation 78
3.2.2.2.6.1 with indolinyl anion 78
3.2.2.2.6.2 with product indoline 81
3.2.2.2.6.3 Influence of chirality 82
3.2.3 Proposed Mechanism 83
3.2.3.1 Catalyst-dependent diastereoselectivity 85
4. Conclusion and Future work 87
5. Experimental 91
5.1 General Information 91
5.1.1 Solvents and Reagents 91
5.1.2 Chromatography 91
5.1.3 NMR Spectroscopy 91
5.1.4 IR Spectroscopy 92
5.1.5 Mass Spectroscopy 92
5.1.6 Polarimetry 92
5.1.7 Melting Points 92
5.1.8 HPLC 92
5.1.9 Naming and Numbering of Compounds 93
5.2 General Procedures 94

5.3 Experimental Procedures and Data 96

5.4 Calibration of HPLC system for kinetic analysis 137

5.5 Kinetic experiments data 139

5.5.1 Modified asymmetric cyclization 139

5.5.2 Order of addition 140

5.5.3 Background cyclization 143

5.5.4 Chiral catalyst loading 144

5.5.5 Log [Cat] vs. Log k plot 149

5.5.6 Cyclization with –OH protected catalyst 150

5.5.7 Stirring rate experiments 151

5.6 X-Ray Crystallographic Data 159

5.7 Crystallographic information files 163

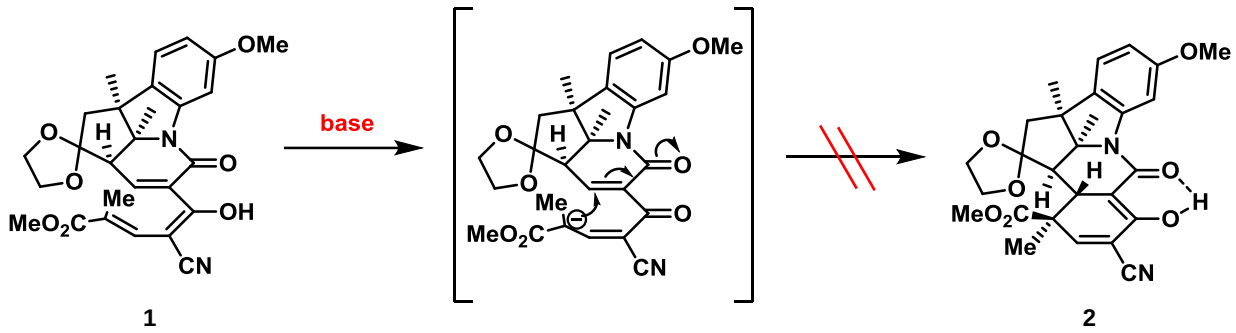
6. References 164

1. Introduction

1.1 Pericyclic Reactions

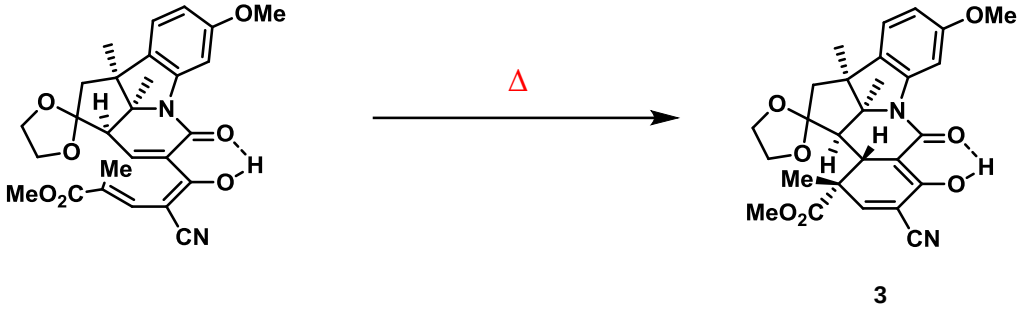
Most reactions in organic chemistry can be classified into one of three, more or less exclusive categories: ionic, radical and pericyclic. The third distinct class, pericyclic reactions, is defined as a process that proceeds *via* a cyclic transition state and progresses in a concerted fashion; i.e. bond formation and breaking occurs simultaneously.[1] Pericyclic reactions encompass four different reaction classes, namely *cycloadditions*, *sigmatropic rearrangements*, *group transfer reactions*, and *electrocyclic reactions*, each of which possesses special features not shared by others.[1,2]

Pericyclic reactions were only recognized as a separate class in the late 1950's. Curly arrows were used to show the movement of electrons in these reactions, and the absence of a sense of direction to these arrows was unsettling to the chemists. Hence, in the early 1960's, Doering termed these reactions as, 'no mechanism reactions'.[3] This lack of understanding developed an interest amongst chemists to study the mechanism of these reactions. In 1963, one of the greatest organic chemists of the 20th century, R. B. Woodward disclosed his landmark synthesis of Vitamin B_{12}.[4] Woodward came across a set of puzzling reactions during the course of this synthesis. He planned to use an intramolecular Michael addition under basic conditions to close a six membered ring and introduce two new stereogenic centres. Unfortunately, the desired reaction did not take place under these conditions (Scheme **1**).



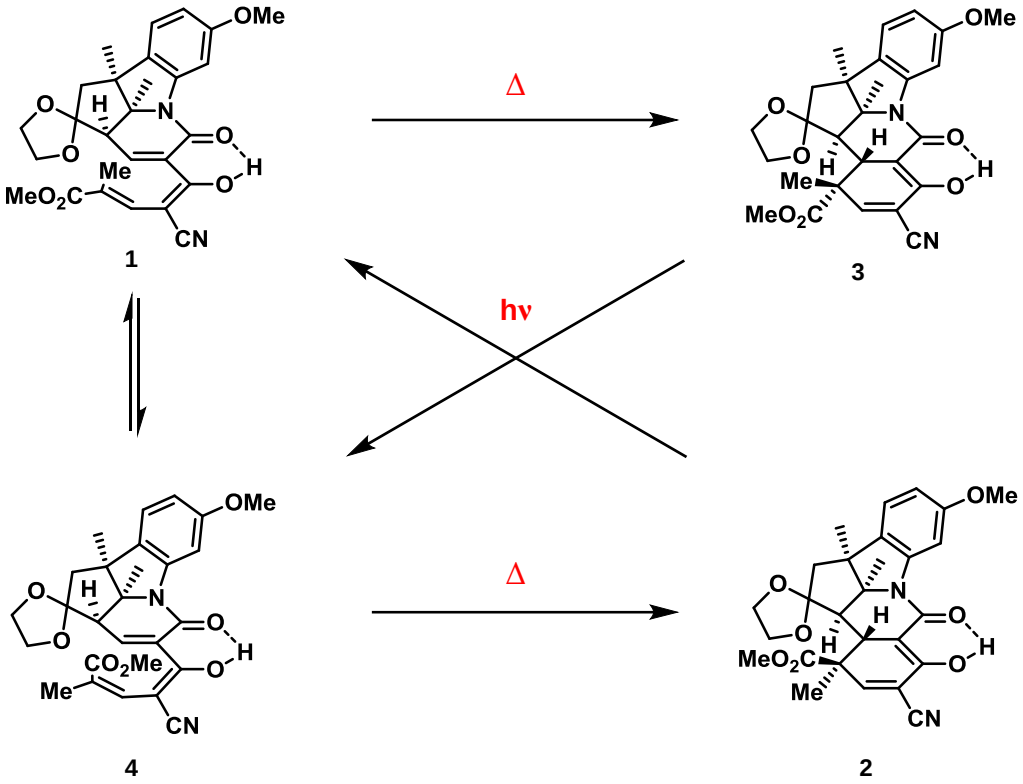
Scheme 1: Proposed Intramolecular Michael Reaction

However, when he attempted to take the melting point of the crystalline cyano-enol **1**, the desired cyclization was found to take place! This thermal reaction gave the opposite diastereomer **3** to the one postulated **2** on steric grounds (Scheme **2**).



Scheme 2: Cyclization observed during melting point determination

Further examination of the reaction revealed that the starting material undergoes thermally induced olefin isomerisation, and that each olefin isomer **1** and **4** undergoes stereospecific cyclization to give rise to two distinct diastereomers of the product **3** and **2** respectively. However, irradiation of each of these products **3** and **2** triggered a retro-cyclization affording starting materials **4** and **1** with the opposite double bond geometry to the olefin from which it was formed (Scheme **3**).



Scheme 3: Electrocyclization during Woodward's Vitamin B_{12} Synthesis

The above thermal and photochemical transformations are now recognised as a thermal disrotatory and photochemical conrotatory 6π electrocyclizations respectively.[5]

These results, along with some other examples of "no mechanism" reactions led Woodward, in collaboration with Hoffmann, in 1965 to lay down some fundamental principles for the theoretical treatment of all concerted reactions. The basic principle is that reactions occur readily when there is congruence between orbital symmetry of reactants and products, and only with difficulty when that congruence is not present. This can be put in simple terms: "*orbital symmetry is conserved in concerted reactions*".[5]

In the following years, these ideas were generalized to the ubiquitous Woodward-Hoffmann rules, which provide a simple and general prediction of the stereochemical outcome of all pericyclic reactions.[1,5,6]

A general way of stating the Woodward Hoffmann rules for thermal pericyclic reactions is:

"*A ground-state pericyclic change is symmetry-allowed when the total number of* $(4q + 2)_s$ *and* $(4r)_a$ *components is odd*"*

The rule for photochemical reactions is simply the reverse of the rule for thermal reactions:

"*A pericyclic change in the first electronically excited state is symmetry-allowed when the total number of* $(4q + 2)_s$ *and* $(4r)_a$ *components is even*"

Our work is focussed on ring-closing electrocyclizations, which are characterized by the formation of a ring from an acyclic, conjugated precursor by means of thermal or photochemical initiation. The characteristic feature of an electrocyclization is the formation of a σ-bond across the ends of a conjugated system, at the expense of a π-bond, to give a cyclic product.

* q, r – integers, s – suprafacial, a – antarafacial, component – a bond(s) or an orbital(s) taking part in the pericyclic reaction as a single unit.

1.1.1 Stereochemistry of Electrocyclizations

Application of the Woodward-Hoffmann rules to electrocyclic reactions leads to a specific set of simple rules:

"*Thermal electrocyclic reactions involving (4n+2)π electrons are disrotatory processes*", in which the π-orbitals at the ends of the conjugated system rotate in opposite directions to form a new σ-bond where the R_1 and R_2 substituents are *syn* (Figure **1a**).

Conversely, "*thermal electrocyclic reactions involving (4n)π electrons are conrotatory processes*", in which the π-orbitals at the ends of the conjugated system rotate in the same direction to form a new σ-bond where the R_1 and R_2 substituents are *anti* (Figure **1b**).

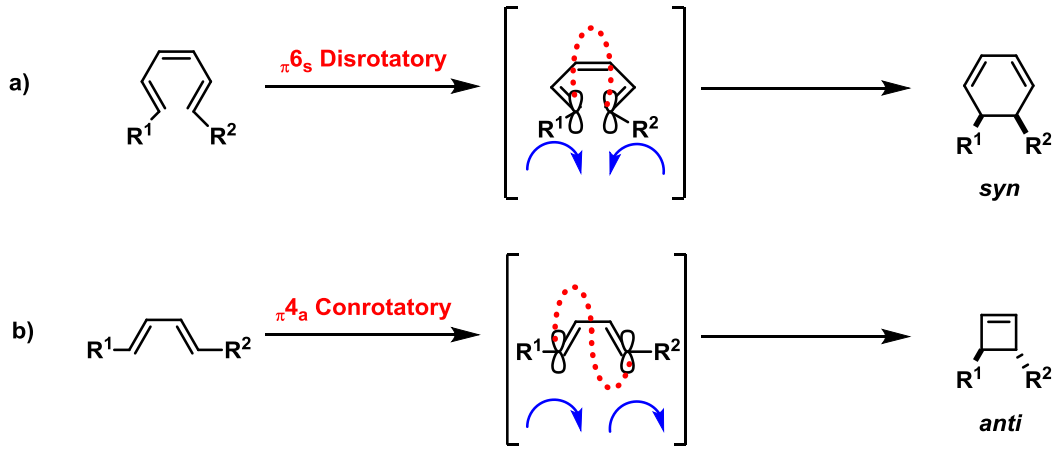


Figure 1: Conrotatory and disrotatory electrocyclizations

These orbital symmetry constraints are reversed when the reaction proceeds under conditions of photochemical initiation.

The Woodward-Hoffmann rules have become a powerful synthetic tool as they provide an explanation for the stereoselectivity of electrocyclic reactions. Hoffmann was awarded the

1981 Nobel Prize in Chemistry for this work, shared with Kenichi Fukui who developed a similar model using frontier molecular orbital (FMO) theory. Woodward had died two years before so he was not eligible to win what would have been his second Nobel Prize in Chemistry.

Among the classes of pericyclic reactions, cycloadditions and sigmatropic rearrangements have been widely studied. In contrast, electrocyclizations have not been fully explored and have been given little attention by the synthetic chemists due to the problems associated with the requirement of high temperatures to initiate these reactions and with assembling the conjugated polyene precursors. More importantly, there are no general methods for the asymmetric catalysis of electrocyclic reactions, resulting in limited opportunities for exerting stereocontrol in these transformations and hence, rendering research in this field challenging.[7,8,9]

1.2 Literature

As discussed above, the Woodward-Hoffmann rules govern the relative stereochemistry of electrocyclic reactions i.e. a particular substrate will form a specific isomer of the product depending upon the relative sense of rotation of the π-orbitals across the ends of the conjugated system involved in the electrocyclization step.

These rules do not have any influence on the absolute stereochemistry of the products formed. For example, an electrocyclic ring closing reaction that is conrotatory can still rotate in two directions, producing enantiomeric products. Hence, in order to exert enantioselectivity in an electrocyclic ring closing reaction it is therefore necessary to control

the absolute direction of rotation of the orbitals (the torquoselectivity)*,[10] in the ring closing process.

This introduction highlights the relevant examples to date for exerting stereocontrol in electrocyclic ring closing reactions in which the enantioselectivity has been influenced by a chiral substrate or catalyst.

A review published by Smith *et al.* offers an in-depth overview of asymmetric electrocyclic processes.[11]

1.2.1 Asymmetric 4π Nazarov

The Nazarov cyclization is a thermal 4π conrotatory electrocyclization that converts divinyl ketones to cyclopentenones by activation with a Lewis acid (Figure **2**).[12] The potential synthetic utility of this reaction is considerable and this method represents one of the most versatile methods for the synthesis of five-membered carbocycles.

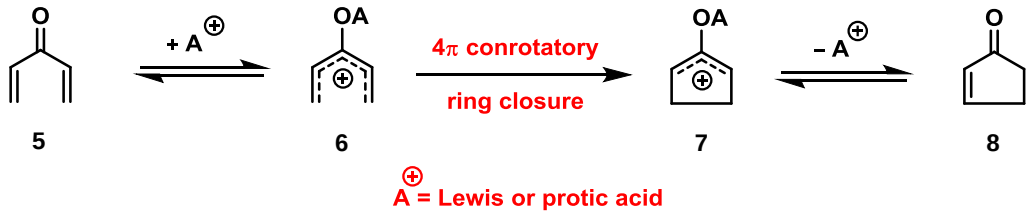


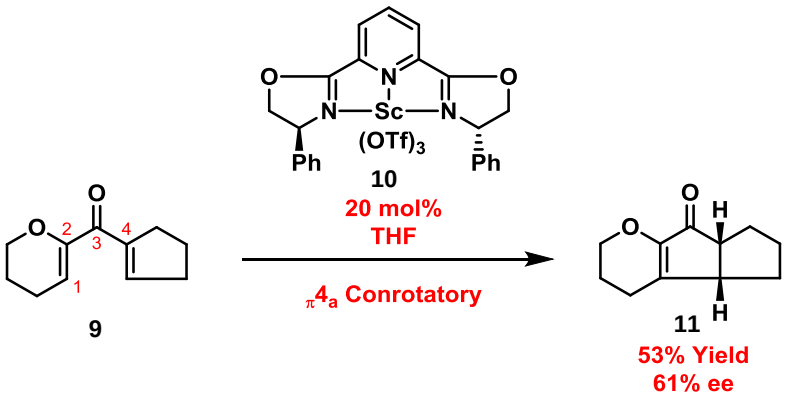
Figure 2: Mechanism of Nazarov Cyclization

* IUPAC define torquoselectivity as "the preference for 'inward' or 'outward' rotation of substituents in conrotatory or disrotatory electrocyclic ring opening reactions".[10] We extend this definition to describe the absolute direction of rotation of substituents in an electrocyclic ring closure in a manner consistent with – but not identical to – the IUPAC definition.

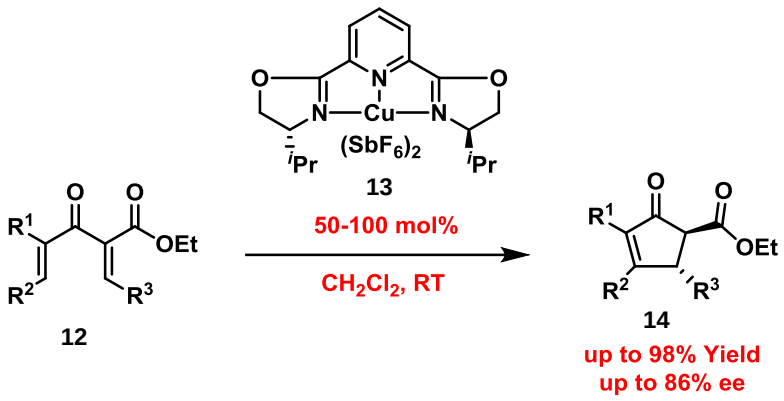
Trauner[13,14] and Aggarwal[15] independently developed examples of catalytic asymmetric variant of the Nazarov cyclization reactions.

Trauner employed the use of α-oxygenated dienones **9** as substrates in his reaction utilizing their propensity for bidendate chelation with chiral scandium Lewis acid catalyst **10** and thereby facilitating selective binding to the catalyst (Scheme **4**). This preorganises one side of the molecule in the reactive s-*trans* conformation. The second enone moiety can also be organised in the s-*trans* conformation by allowing substitution in the 4-position, which will lead to a further increasing in the reactivity.[13]

Trauner observed that 2-alkoxy substituents render the substrate highly reactive, allowing the reaction to occur within minutes at room temperature. The products **11** were obtained in moderate yields and enantioselectivities under optimized conditions (up to 53% yield, up to 61% ee).

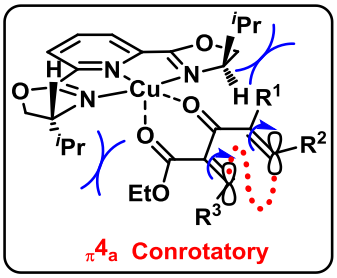


Scheme 4: Trauner's Lewis acid catalysed asymmetric Nazarov reaction



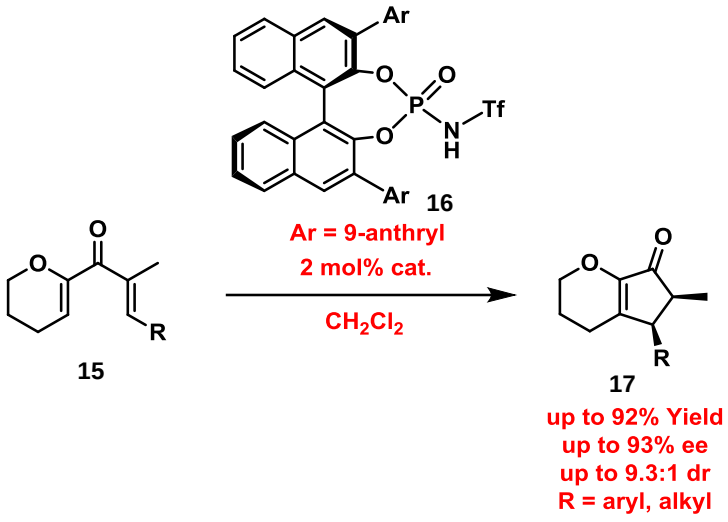
Scheme 5: Aggarwal's Lewis acid catalysed asymmetric Nazarov reaction

Aggarwal demonstrated that the direction of conrotation of orbitals during Nazrov cyclization of a 1,3-dicarbonyl system would be controlled with a copper bisoxazoline complex (Scheme **5**).[16] The presence of an α-ester group will, however, result in retardation of the reaction rate because the presence of an electron-withdrawing group in the α-position destabilizes intermediate **6** (Figure **2**) which is formed in the RDS. This reaction affords the cyclized product **14** in high yields (up to 92%) and good enantioselectivities (up to 87%). Reduction in the catalyst loading reduces the yield without affecting the ee. This may be due to binding of the product 1,3-dicarbonyl to the catalyst **13** which would inhibit catalysis of the reaction. The authors proposed the following stereochemical model for this transformation (Scheme **6**). It is proposed that the steric bulk of the bisoxazoline ligand distorts the plane of the cationic divinyl ketone intermediate (**6**, Figure **2**), resulting in pushing of the alkene substituents R^2 and R^3 away from the ^{i}Pr groups of the ligand, which places the bonding lobes of the two corresponding orbitals in close proximity and hence forces one mode of conrotation to be favoured over the other.



Scheme 6: Stereochemical model for Aggarwal's 4π electrocyclization[15]

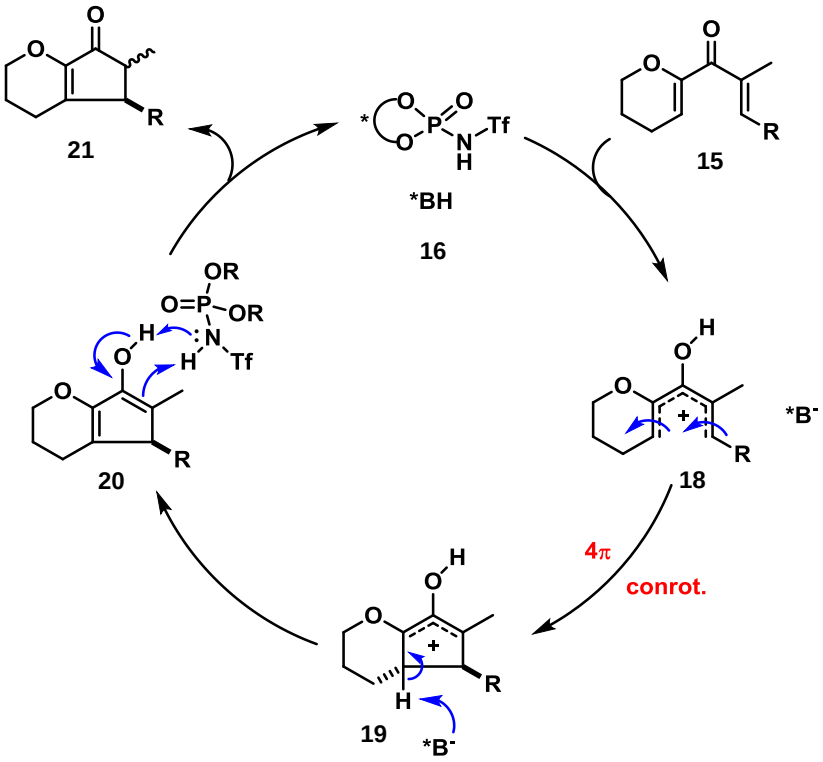
Rueping *et al.* developed the first organocatalytic asymmetric Nazarov cyclization reaction using a chiral Brønsted acid derived from BINOL (Scheme **7**).[17]



Scheme 7: Rueping's organocatalytic asymmetric Nazarov reaction

Rueping made use of substrates similar to those employed by Trauner in his earlier work, relying on the reactivity of an α-alkoxy dienone. The catalytic cycle for this reaction was envisaged to involve protonation of the divinyl ketone moiety **15** by the *N*-triflyl phosphoramide. This results in the formation of cyclopentadienyl cation **18** which is then

stabilized by the formation of an adduct with the phosphoramide anion. The chiral phosphate anion binds preferentially to one of the two faces of the cyclopentadienyl cation **18** and hence renders the subsequent 4π electrocyclization of the adduct enantioselective. The resulting oxyallyl cation **19** undergoes elimination of a proton to form the enolate **20**. Catalyst mediated protonation of this cyclic enol **20** proceeds diastereoselectively, affording the substituted cyclopentenone product and regenerating the Brønsted acid catalyst **16** (Scheme **8**). When compared to the metal-catalysed reaction, the main features of this organocatalytic asymmetric 4π electrocyclization reaction developed by Rueping are: the lower catalyst loadings (2 mol%) required for the transformation, high enantioselectivities, mild reaction conditions and fast reaction times.



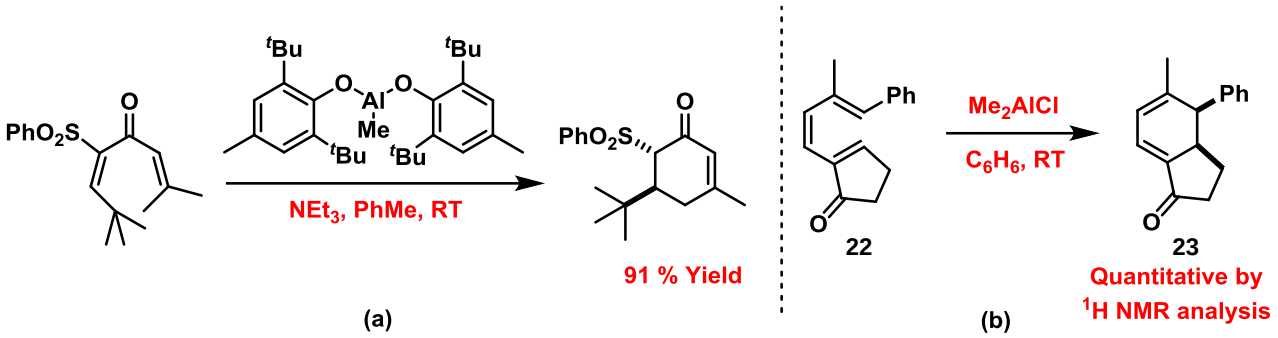
Scheme 8: Proposed catalytic cycle for Rueping's Nazarov cyclization

1.2.2 6π Electrocyclizations

Research in our group is focussed on the development of catalytic asymmetric 6π electrocyclic ring closing reactions. The absence of any general approaches for controlling the absolute stereochemistry of 6π electrocyclic reactions, and the importance of these transformations make research in this field challenging and interesting.

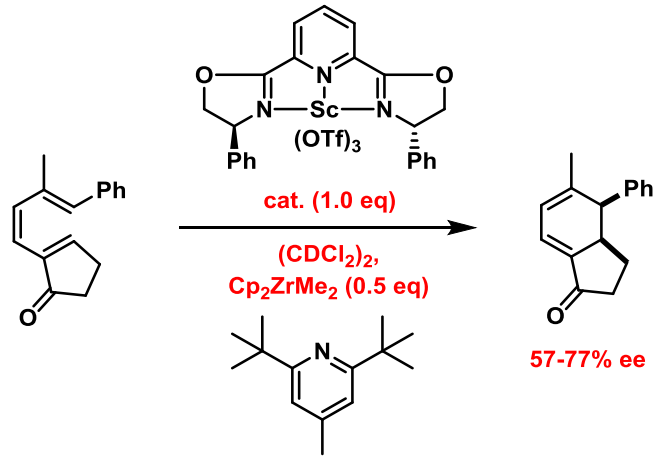
The simplest example of a thermal disrotatory 6π electrocyclization is the conversion of 1,3,5-hexatriene to 1,3-cyclohexadiene. As discussed previously, high temperatures are required to initiate such transformations, often preluding their use in the synthesis of complex molecules. However, an interesting finding by Magomedov *et al*. demonstrates that synergistic combinations of electron-withdrawing and donating groups around the extended π-system can significantly lower the activation energy of 6π electrocyclization, thereby allowing the reaction to occur under mild conditions (Scheme **9 a**).[1819] This hypothesis has been supported with theoretical calculations by Fu *et al.*[20]

Trauner *et al.*[21] carried out some experimental and computational studies to demonstrate that the rate of 6π electrocyclizations can be influenced by varying the electronics of the substituents on the hexatriene system (Scheme **9 b**). They observed that the presence of an electron-withdrawing group at the 2-position of hexatriene lowers the electrocyclization energy barrier by up to 10 kcal/mol[20]. They exploited this effect to carry out a Lewis acid catalysed cyclization of **22**, which was substituted at the 2-position with a carbonyl group. This reaction could be carried out in quantitative yield at room temperature.



Scheme 9: Effect of substitutions on 6π electrocyclizations

This observed reduction of the electrocyclization energy barrier in the presence of Lewis acid catalyst suggested that asymmetric Lewis acid catalysis would provide a viable handle to carry out catalytic asymmetric electrocycliztion. Using a PyBOX ligand with scandium(III) as the Lewis acid metal, Trauner *et al*. were able to carry out the following reaction in up to 55-77% ee (Scheme **10**).[22]

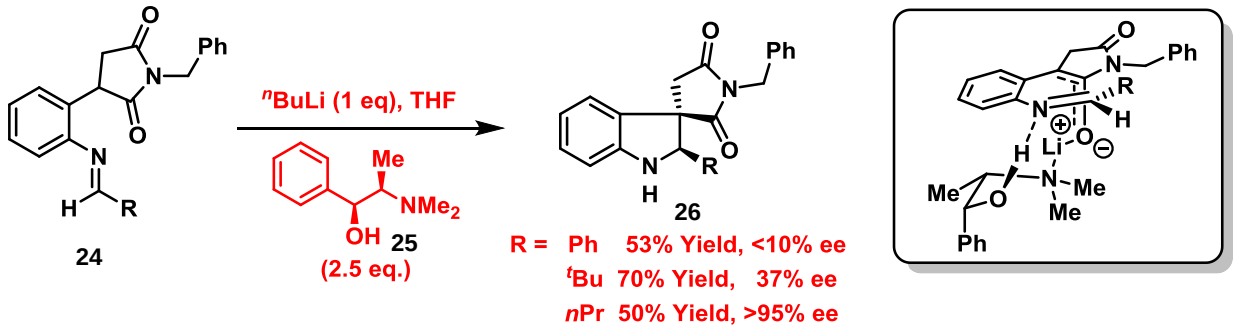


Scheme 10: Trauner's Lewis acid catalysed asymmetric 6π electrocyclization

1.2.3 Asymmetric 6π Electrocyclizations

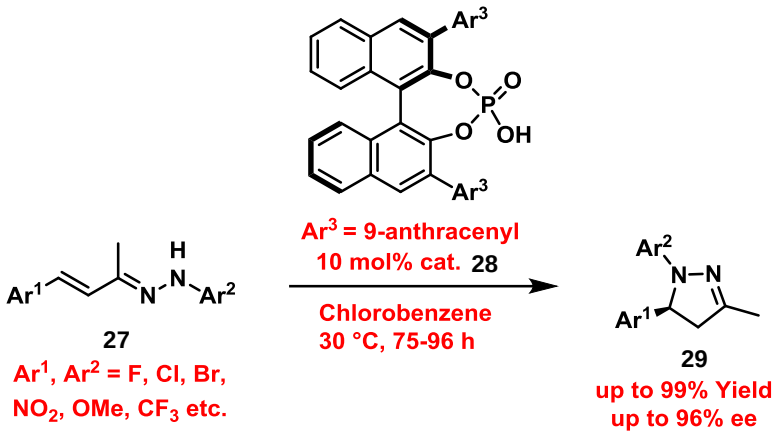
Only a few examples have been reported for the asymmetric variants of 6π electrocyclizations despite the importance of these transformations in synthetic chemistry.

In the 1980s pioneering work by Speckamp *et al.* presented the first attempts at rendering a 6π process asymmetric (Scheme **11**).[23,24] They demonstrated that azomethines **24** in the presence of *n*BuLi and *N*-methylephedrine **25** in THF at 0-20 °C undergo cyclization to form spirocyclic indolines **26** in moderate yields (up to 53%) and high enantioselectivities (up to 98% ee). Speckamp *et al*. proposed a model to rationalize the stereochemical outcome of the reaction. Their model suggests that *n*BuLi deprotonates the substrate **24** at the benzylic position which then binds to *N*-methylephedrine **25**. This binding is caused by (i) the interaction of Li^+ ion of enolate with the nitrogen of *N*-methylephedrine **25** and (ii) the interaction of imine portion of the substrate with the hydroxyl group of *N*-methylephedrine **25** *via* hydrogen-bonding. This puts the azomethine and enolate oxygen in a helical conformation, hence giving rise to the *cis*-spirocyclic product *via* a disrotatory 1,5-electrocyclic ring closure. A slight variation in the substrate or catalyst reduces the enantioselectivity of the reaction considerably, making the reaction extremely sensitive. For example, replacing Li^+ with Na^+ leads to a drastic reduction in the enantioselectivity (20% ee).



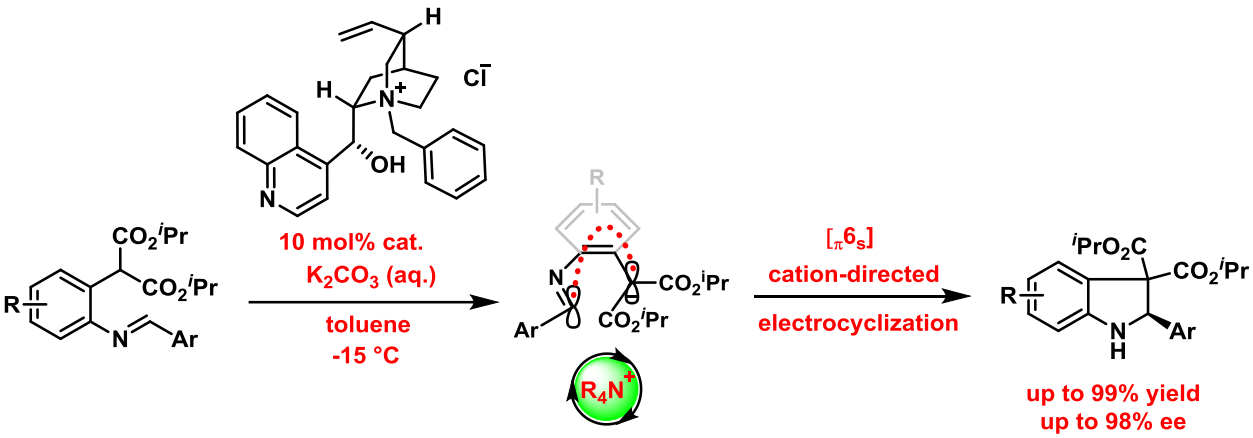
Scheme 11: Speckamp *et al.* electrocyclization

In 2009 List *et al.* developed another catalytic asymmetric 6π electrocyclization.[25] They demonstrated that hydrazones **27** undergo a 6π electrocyclization when exposed to the chiral phosphoric acid **28** furnishing 2-pyrazolines **29** in excellent yields and in high enantioselectivities. It is proposed that the chiral phosphoric acid catalyst **28** forms a tight ion-pair with the protonated imine portion of the substrate and hence transfers the stereochemical information.



Scheme 12: List *et al.* electrocyclization

From the foundations laid in the literature, research within the Smith group led to the development of a catalytic asymmetric 6π electrocyclization of benzaldimines under phase-transfer conditions to form indolines, with high levels of enantioselectivity (Scheme **13**).[26] The stereoinduction of the electrocyclization can be rationalized by means of tight-ion pairing of the substrate anion to the cinchona derived chiral phase-transfer catalyst[27] in an organic solvent. This causes one of the π-faces of the substrate to be blocked, thus controlling the direction of rotation of orbitals during cyclization and hence the enantioselectivity of the reaction (Figure **3**).



Scheme 13: Catalytic asymmetric 6π electrocyclization by Smith *et al.*

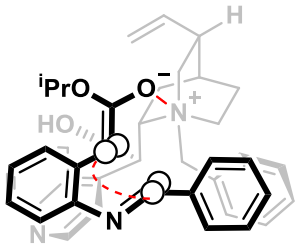
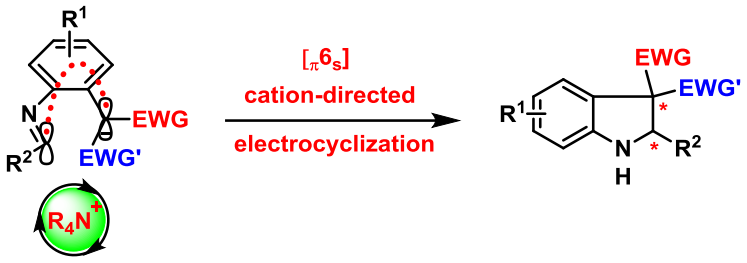


Figure 3: Proposed binding model (one ester omitted for clarity)

These few examples described in this introduction give an idea of the great potential for asymmetric catalysis of 6π electrocyclizations.

1.3 Project Aims

This project will focus on the development of a cation-directed diastereo- and enantioselective synthesis of indolines bearing two contiguous asymmetric centres, one of which is quaternary and all carbon, in a single synthetic step. In order to achieve this we propose to make use of two electronically different electron-withdrawing groups at the benzylic position of the substrate imine, to introduce a second stereocentre into the product (Scheme **14**).

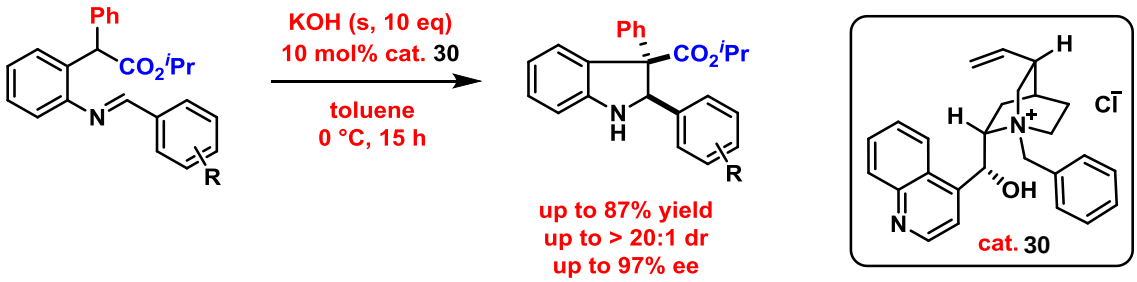


Scheme 14: Diastereo- and enantioselective electrocyclization

A further aim of this project was to investigate the reaction mechanism of this phase-transfer catalysed transformation.

2. Results and Discussion

Initial investigations within the Smith group have demonstrated that a combination of phenyl and ester anion stabilizing groups at the benzylic position of substrate imine gave rise to indolines in high diastereo- and enantioselectivity (> 20:1 dr, up to 97% ee, Scheme **15a**).[28]



Scheme 15a: Diastereo- and enantioselective electrocyclization with phenyl-ester system

The scope of the electrocyclization reaction was investigated by introducing different substituents on the aryl ring of the aromatic imine moiety. The influence of electron-withdrawing groups at the *o*-, *m*- and *p*- position of the aryl ring was explored (Table **1**).

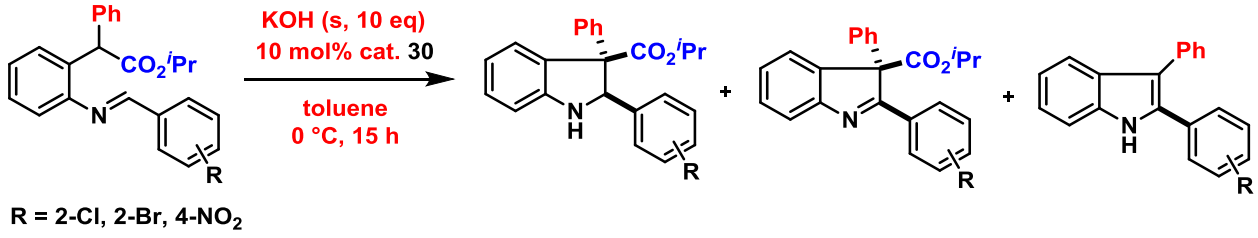
R	Time (h)	Yield[(a)] (%)	dr[(b)]	ee[(c)] (%)
H	15	45	6:1	92
4-NO_2	15	57	> 20:1	n.d.
4-Cl	6	73	> 20:1	95
4-Br	4	87	5:1	88
3-NO_2	4	40	2:1	41
3-Cl	12	74	> 20:1	79
2-Cl	20	87	> 20:1	97
2-Br	20	80	> 20:1	95

Table 1: Diastereo- and enantioselective electrocyclization with *iso*-propyl ester group

(a) Yield of isolated product
(b) dr determined by ^{1}H NMR
(c) ee determined by chiral stationary phase HPLC

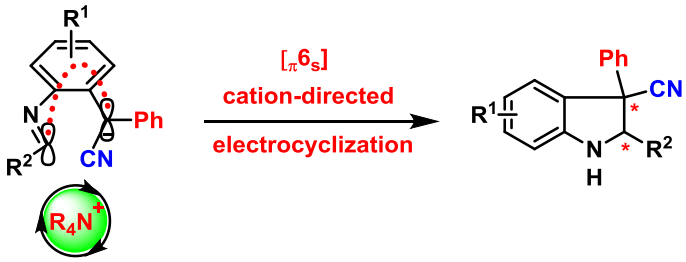
Further investigations carried out on this system within the group have shown some interesting results. Chiral phase-transfer catalyst **30** leads to the formation of an indoline with a high diastereomeric preference in favour of the *anti*-isomer (in which the C-2 arene and the C-3 phenyl groups are on the opposite side of the indoline core). This enantioenriched *anti*-isomer of indoline when subjected to the achiral phase-transfer catalyst TBAHS at room temperature resulted in the formation of the opposite diastereoisomer *syn*-isomer as a racemate. The starting material imine when subjected to achiral phase-transfer catalyst TBAHS also leads to the formation of *syn*-isomer of indoline as a racemate. These observations suggested that *anti*-isomer of indoline is the kinetic isomer which under achiral phase-transfer conditions is converting to give the thermodynamically more stable *syn*-isomer as a racemate, *via* a cycloreversion mechanism. These investigations have been extended and will be discussed in detail under mechanistic studies in Chapter **3**.

We observed that some substrates (R = 2-Cl, 2-Br, 4-NO_2) underwent uncontrollable oxidation after forming the product indoline in the reaction mixture or on standing to generate indolenines (Scheme **15b**). These materials also slowly decompose to give complex mixtures of products including indoles, which are presumably generated through decarboxylation. Whilst this undesired reactivity could possibly be prevented through further functionalization, we realized that this significantly compromised the potential utility of these building blocks, and we decided that a change of substrate might offer an alternative reactivity profile.



Scheme 15b: Uncontrollable oxidation with phenyl-ester system

Our aim was to develop a highly diastereo- and enantioselective system without such limitations and hence we decided to investigate an alternative electron withdrawing group, and we initially focussed on changing the *iso*-propyl ester for a nitrile functional group (Scheme **16**).



Scheme 16: Diastereo- and enantioselective electrocyclization with nitrile group

2.1 Retrosynthesis

Retrosynthetic analysis of the desired substrate indicated that the imine required for the cyclization could be synthesized from the requisite aniline. This compound could be generated *via* a S_NAr from commercially available fluoronitro aromatics followed by reduction of the phenylnitrile substituted nitroarene (Figure **4**).

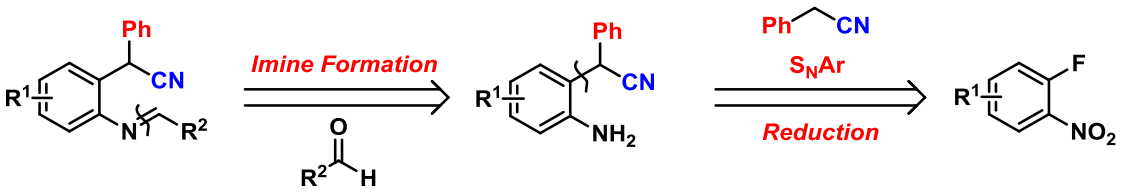


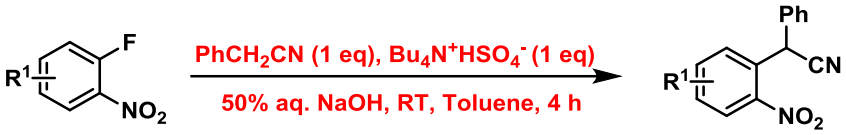
Figure 4: Retrosynthetic analysis of imine substrate

2.2 Synthesis of substrates

2.2.1 Synthesis of phenylnitrile substituted anilines

The nitro-compounds **32a-c** were synthesized by a phase-transfer catalysed nucleophilic aromatic substitution reaction of commercially available 2-fluoronitrobenzene compounds **31a-c** with phenylacetonitrile in the presence of stoichiometric TBAHS and 50% aqueous NaOH in toluene (Scheme **17**).[29] Substituents on the aryl ring are well tolerated with good yields obtained for a 5-CH_3 substituent and 4-CF_3 group.

It is however important to note that stoichiometric amounts of TBAHS are used in this reaction as the product can form a lipophilic ion-pair (soluble in organic phase) with the quaternary ammonium ion in a similar way as the substrate and hence arresting the catalytic process of the reaction leading to poor yields of the desired product.

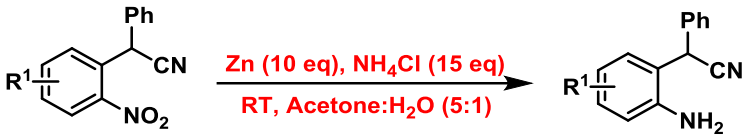


Fluoronitro compound		Nitroarenes	Yield (%)
31a	R^1=H	**32a**	76
31b	R^1=5-CH_3	**32b**	86
31c	R^1=4-CF_3	**32c**	77

Scheme 17: Synthesis of nitroarene compounds

The aniline derivatives **33a-c** were synthesized by reducing the nitro-compounds **32a-c** with Zn metal and NH_4Cl in an acetone/water mixture (5:1) (Scheme **18**).[30] Reduction of the nitro group to the aniline occurred smoothly without any over-reduction of the nitrile. This

method of reduction is much quicker and cost effective compared to the Pd/H_2 reduction.[31] Substitutions in the ring are well tolerated giving 73% yield for 5-CH_3 substituent and 60% yield for 4-CF_3 group.

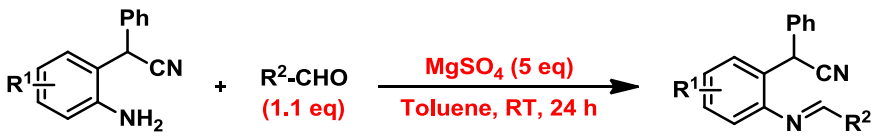


Nitroarenes		Anilines	Yield (%)
32a	R^1=H	**33a**	79
32b	R^1=5-CH_3	**33b**	73
32c	R^1=4-CF_3	**33c**	60

Scheme 18: Synthesis of phenylnitrile substituted anilines

2.2.2 Imine formation

With anilines **33a-c** in hand, a variety of imines were synthesized using aromatic and aliphatic aldehydes **34-46** (Table **2**). Excellent conversion was observed using 1.1 equivalents of the aldehyde with $MgSO_4$ (5 eq) as a dessicant and Lewis acid catalyst (Scheme **19**). Imines synthesized from aliphatic aldehydes were unstable and were used immediately after formation in the cyclization.



Scheme 19: Imine formation

After filtration and concentration *in vacuo* the imines did not require any further purification. The reaction is tolerant of both electron-withdrawing and electron-donating substituents on the aryl ring of the aromatic aldehyde moiety.

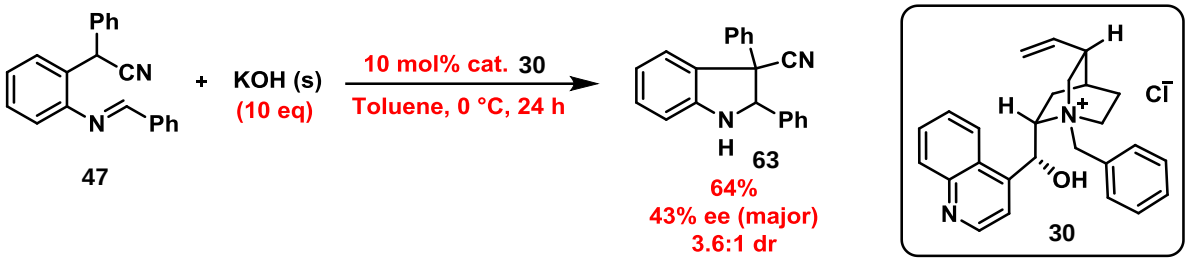
Aniline		Aldehyde	Imine
33a	**34**	R^2=Ph	**47**
33a	**35**	R^2=2-naphthyl	**48**
33a	**36**	R^2=*p*-(Me)C_6H_4	**49**
33a	**37**	R^2=*o*-(Me)C_6H_4	**50**
33a	**38**	R^2=*m*-(OMe)C_6H_4	**51**
33a	**39**	R^2=*p*-(OMe)C_6H_4	**52**
33a	**40**	R^2=2-furyl	**53**
33b	**40**	R^2=2-furyl	**54**
33c	**40**	R^2=2-furyl	**55**
33a	**41**	R^2=cyclohexyl	**56**
33c	**41**	R^2=cyclohexyl	**57**
33a	**42**	R^2=2-(*tert*-butyl)	**58**
33a	**43**	R^2=PhCH=CH	**59**
33a	**44**	R^2=cyclopentyl	**60**
33a	**45**	R^2=*p*-BrC_6H_4	**61**
33a	**46**	R^2=*p*-(NO_2)C_6H_4	**62**

Table 2

2.3 Initial Attempts at Cyclization

With the desired imines **47-62** in hand, we attempted cyclization under phase-transfer conditions which had proved to be successful with previous systems in the group (Scheme **20**).

Imine **47** was subjected to asymmetric phase-transfer conditions using cinchonidine catalyst **30** in toluene with 10 equivalents of powdered KOH (Scheme **20**). After 24 hours, the reaction cleanly provided a 64% yield of indoline **63** as a 3.6:1 mixture of diastereomers in 43% ee (major diastereomer).



Scheme 20: Electrocyclization of imine **47**

2.4 Optimization of the reaction conditions

Unfortunately, as evident from the results obtained the levels of stereocontrol were not ideal and hence we decided to optimize the reaction conditions in order to improve the stereoselectivity of the reaction. In an attempt to attain a diastereo- and enantioselective reaction we planned to carry out reaction optimization by evaluating a number of reaction parameters: catalyst, catalyst loading, temperature, solvent, base and concentration of the reaction mixture (Figure **5**).

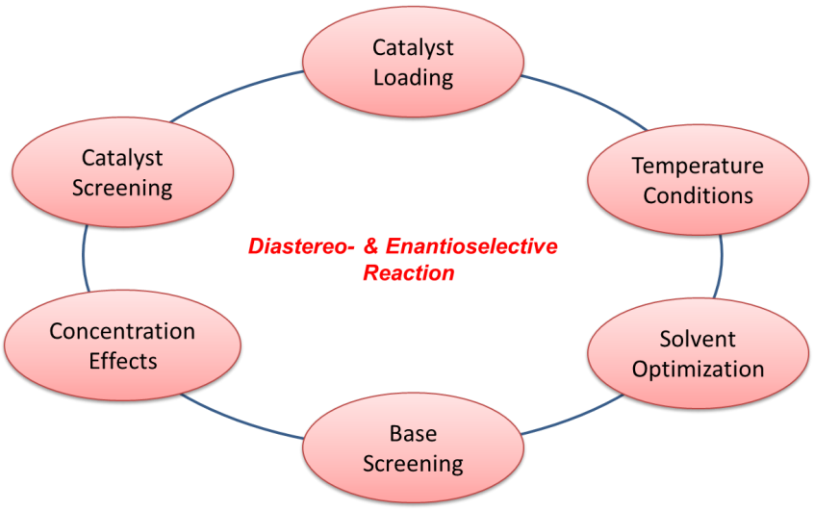
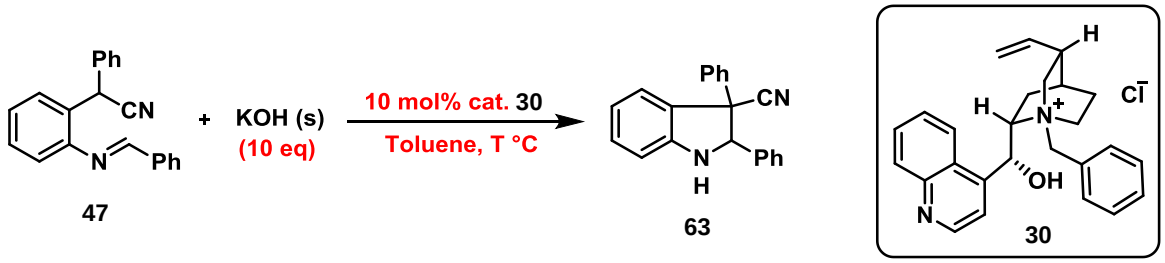


Figure 5: Optimization of the reaction conditions

2.4.1 Screening of different temperatures

Since asymmetric phase-transfer reactions are frequently carried out at reduced temperatures, a screen of different temperatures was conducted to evaluate its impact on the observed stereoselectivity of the reaction (Scheme **21**).



Temp. (°C)	dr[(a)]	ee_{major} (%) [(b)]
0	3.6:1	43
-10	5.5:1	51
-30	19:1	52
-50	21:1	55

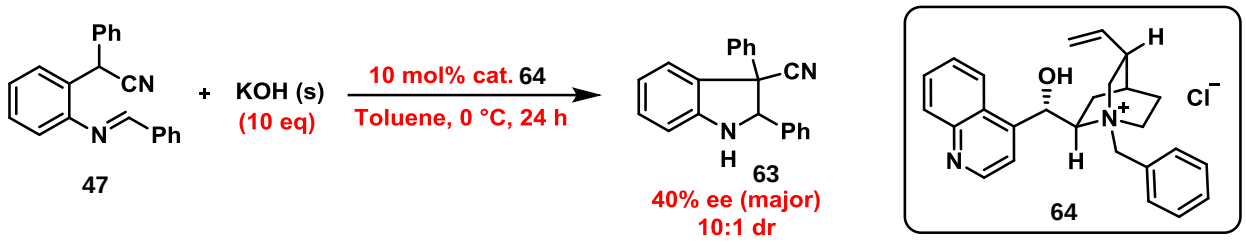
Scheme 21: Screening of temperature with cat. **30**

A slight increase in the stereoselectivity was observed when the temperature was reduced to -30 °C, furnishing the product indoline **63** in 19:1 dr and 52% ee. On reducing the temperature further to -50 °C, no appreciable change in the dr or ee was observed (21:1 dr, 55% ee).

As is evident from Scheme **21** cinchonidine catalyst **30** provided only moderate levels of stereoselectivity even at lower temperatures, giving the indoline **63** in 3.6:1 dr and 43% ee at 0 °C. Hence, we attempted the same reaction at 0 °C with cinchonine catalyst **64** (*pseudo*-

(a) dr determined by ^{1}H NMR.
(b) ee determined by chiral stationary phase HPLC.

enantiomeric form of cinchonidine catalyst **30**), which gave a better diastereoselectivity (10:1 dr), but it did not show any appreciable change in the enantioselectivity of the reaction (Scheme **22**). However, catalyst **64** gave the opposite major enantiomer of indoline **63** as expected.

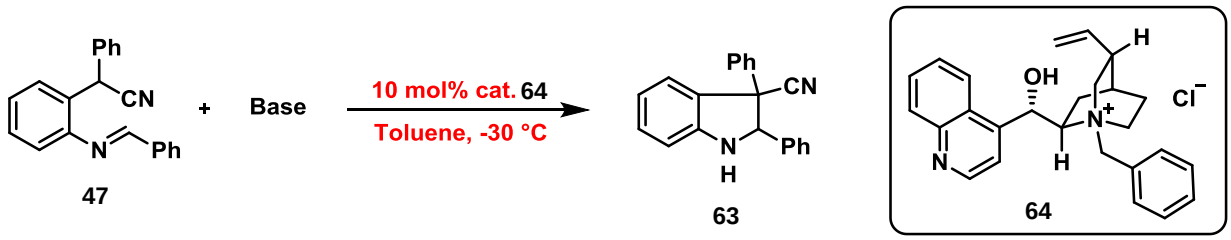


Scheme 22: Electrocyclization with catalyst **64**

As greater diastereoselectivity was observed with catalyst **64**, further optimization was carried out using catalyst **64** at -30 °C.

2.4.2 Screening of base

Subsequently, we then investigated the effect of base on the reaction by employing a variety of different solid and aqueous bases for the cyclization (Scheme **23**).



Base	Base equivalents	Rxn Time (h)	dr[(a)]	ee (%)[(b)]
None	0	No Rxn	-	-
KOH (s)	1	72	2:1	55
30% aq. KOH	1	< 5% conversion	-	-
K_2CO_3 (s)	1	<5% conversion	-	-
30% aq. KOH	5	48	4:1	55
K_2CO_3 (s)	5	72	3:1	50
$CsOH{\cdot}H_2O$ (s)	2	48	4:1	61

Scheme 23: Base Screening

From the results obtained, it was shown that $CsOH{\cdot}H_2O$(s) was the optimal base for the reaction as it gives better diastereoselectivity (4:1 dr) and enantioselectivity (61% ee) when compared to similar reaction conditions.

(a) dr determined by ^{1}H NMR.
(b) ee determined by chiral stationary phase HPLC.

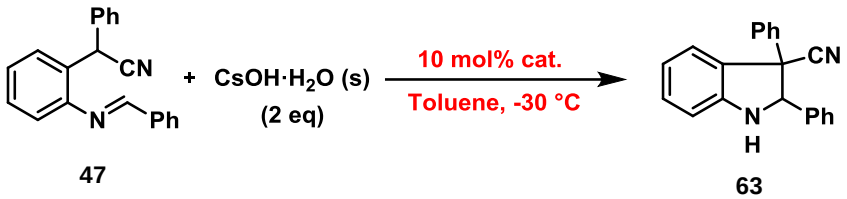
2.4.3 Catalyst screening

We then turned our attention to optimization of the catalyst structure. The cyclization reaction was attempted with a number of different cinchona alkaloid derived phase-transfer catalysts (Scheme **24**).[32]

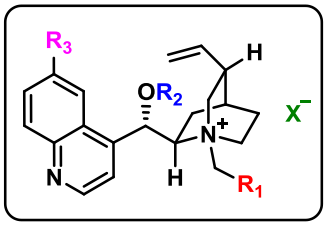
The cinchonine catalyst **65** in which the *N*-benzyl moiety is *para*-substituted with an electron-withdrawing CF_3 group shows a slight reduction in enantioselectivity (50% ee) compared to the unsubstituted catalyst **64** (61% ee). This implies that the presence of an electron poor *N*-benzyl group on the cinchonine catalyst is detrimental for the enantioselectivity of the reaction (Scheme **24**).

The cinchonidine catalyst **66** where the free hydroxyl group is capped with an allyl group shows a marked drop in enantioselectivity (0% ee), which potentially indicates the importance of hydrogen-bonding *via* the catalyst hydroxyl group to the imine portion of the substrate.

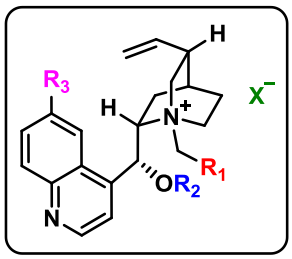
The cinchonidine catalyst **67** where the benzyl group is replaced by 9-anthracenyl, shows a significant drop in the enantioselectivity of the reaction, furnishing the product in 12% ee under identical reaction conditions. This could be due to steric clashes between the substrate **47** and the large anthracenyl group of the catalyst leading to poorer binding.



47 63



Catalyst	R^1	R^2	R^3	X^-	ee[a] (%)	dr[b]
64	Ph	H	H	Cl^-	61	4:1
65	*p*-$(CF_3)C_6H_4$	H	H	Cl^-	50	5:1



Catalyst	R^1	R^2	R^3	X^-	ee[a] (%)	dr[b]
66	Ph	allyl	H	Br^-	0	3:1
67	9-anthracenyl	H	H	Cl^-	12	1:1
68	Ph	H	OMe	Cl^-	78	14:1
69	*p*-BrC_6H_4	H	OMe	Br^-	78	14:1
70	C_6F_5	H	OMe	Br^-	54	9.5:1
71	*p*-$(OMe)C_6H_4$	H	OMe	Br^-	71	9.5:1
72	Ph	H	O^{i}Pr	Br^-	80	16:1

Scheme 24: Phase-transfer catalysts examined

(a) ee determined by chiral stationary phase HPLC.
(b) dr determined by ^{1}H NMR.

The quinine derived catalyst **68** with a methoxy group on the quinoline ring demonstrated improved enantioselectivity (78% ee) and diastereoselectivity (14:1 dr) relative to catalyst **64**.

A few derivatives (**69-72**) of quinine catalyst **68**, with different substituents on the *N*-benzyl and quinoline ring units were synthesized within the group.[33] These were tested in the cyclization, but unfortunately did not show any considerable improvement in the stereoselectivity of the reaction when compared to the quinine catalyst **68**.

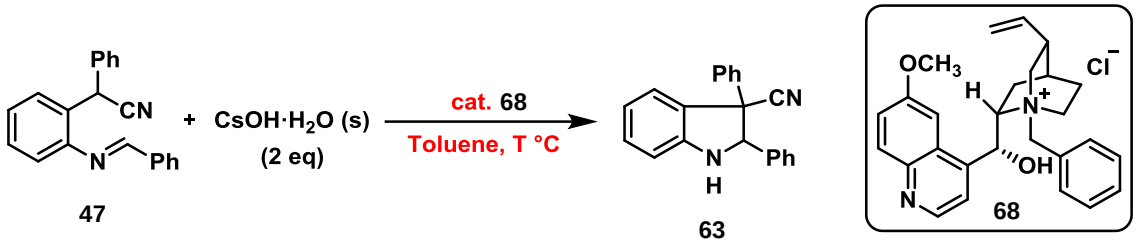
Hence, we reverted back to the commercially available quinine catalyst **68** for further optimization.

2.4.4 Catalyst loading

With the optimal catalyst (**68**) in hand we investigated the effect of catalyst loading at reduced reaction temperatures (Scheme **25**).

Reduction in the catalyst loading from 20 to 5 mol% and lowering of the temperature from -30 °C to -50 °C led to an improvement in both diastereoselectivity (to >20:1 dr) and enantioselectivity (to 89% ee) of the reaction (Scheme **25**).

However, lowering the catalyst loading further from 5 to 2 mol% led to a reduction in the diastereoselectivity (> 20:1 to 7:1 dr) and enantioselectivity (89% to 45% ee). Therefore, we maintained a loading of 5 mol% in all of our subsequent reactions.



Temp. (° C)	Catalyst Loading (mol%)	dr [a]	ee [b] (%)	Rxn Time (h)
-30	20	9:10	48	20
	10	14:1	78	26
-50	10	> 20:1	87	90
	5	> 20:1	89	48
	2	7:1	45	24

Scheme 25: Catalyst loading

2.4.5 Solvent screen

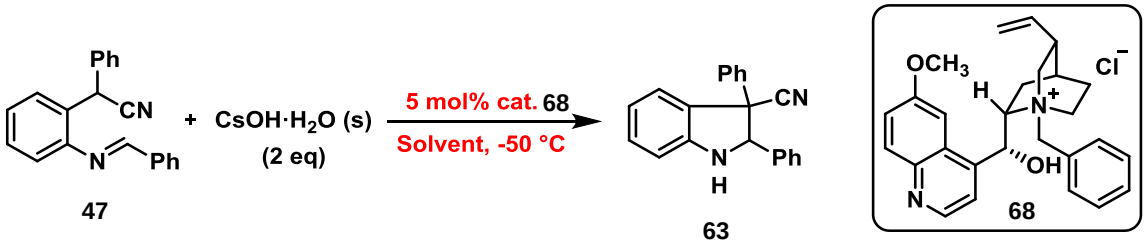
With the optimal temperature and catalyst loading conditions in hand, we performed a screen of solvents on the cyclization reaction. We employed a number of different solvent systems for the reaction (Scheme **26**).

From the results we observed that chlorinated solvents gave good enantioselectivities (68% ee with chloroform, 82% ee with dicloromethane) but poor diastereoselectivities (1.6:1 dr with chloroform, 2:1 dr with dichloromethane). THF gave slightly greater diastereoselectivity (5:1 dr) but reduced enantioselectivity (45% ee) when compared to

(a) dr determined by ^{1}H NMR.
(b) ee determined by chiral stationary phase HPLC.

chlorinated solvents. We also observed that the substrate **47** was completely insoluble in hexane.

Mixed solvent systems such as toluene and hexane (4:1) were also evaluated and gave reasonable enantioselectivity (74% ee) and diastereoselectivity (14:1 dr), but did not improve upon what was observed with pure toluene (> 20:1 dr, 88% ee).



Solvent	Dipole Moment (D)	dr [a]	ee [b] (%)	Yield [c] (%)	Rxn Time (h)
Chloroform	1.04	1.6:1	68	60	24
Dichloromethane	1.60	2:1	82	88	24
Tetrahydrofuran	1.75	5:1	45	85	24
Hexane	0.00		Compound **47** insoluble		
Toluene & Hexane (4:1)	-	14:1	74	-	24
Toluene	0.36	> 20:1	88	75	48

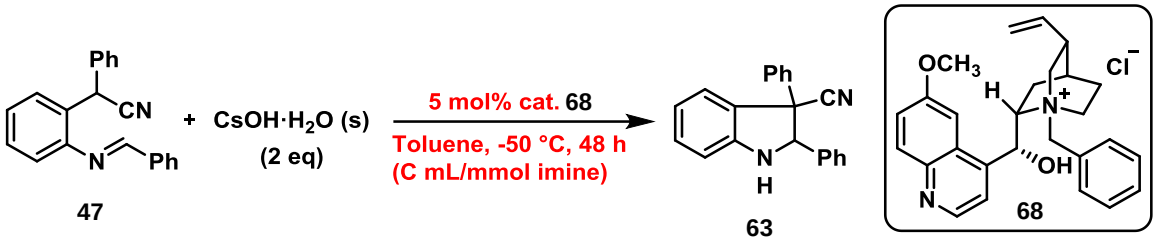
Scheme 26: Solvent screen

(a) dr determined by ^{1}H NMR.
(b) ee determined by chiral stationary phase HPLC.
(c) Yield of isolated product.

2.4.6 Concentration effects

Next, we investigated the effect of concentration with respect to the substrate on the stereoselectivity of the reaction (Scheme **27**). Diluting the reaction mixture by increasing the amount of toluene from 13 mL/(mmol of substrate) to 26 mL/(mmol of substrate) demonstrated a marked drop in enantioselectivity (88% to 48% ee). Concentrating the reaction mixture by decreasing the quantity of solvent from 13 mL/(mmol of substrate) to 6.5 mL/(mmol of substrate), showed a slight reduction in enantioselectivity (88% to 81% ee), but a significant drop in diastereoselectivity (> 20:1 to 9:1 dr).

Hence, we maintained an optimal reaction concentration of 13 mL/(mmol of substrate) in toluene for all further cyclization reactions.



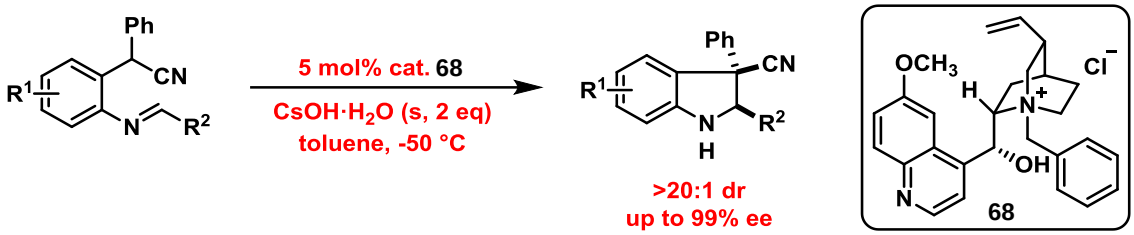
Solvent Concentration C (mL / mmol of substrate)	dr[(a)]	ee[(b)] (%)
13	> 20:1	88
26	> 20:1	48
6.5	9:1	81

Scheme 27: Concentration effects

(a) dr determined by ^{1}H NMR.
(b) ee determined by chiral stationary phase HPLC.

2.5 Cyclization with optimized reaction conditions

With these optimized reaction conditions in hand we investigated the cyclization of the previously synthesized imines. We were delighted to find that this procedure could be used to generate a variety of substituted indolines, essentially as a single diastereomer (> 20:1 dr) and with excellent levels of enantioselectivity (up to 99% ee), (Scheme **28**).



Product	R^1	R^2	Yield (%)	ee[a] (%)
63	H	Ph	75	89
73	H	2-naphthyl	84	80
74	H	*p*-(Me)C_6H_4	86	90
75	H	*o*-(Me)C_6H_4	94	76
76	H	*m*-(Me)C_6H_4	92	60
78	H	*p*-(OMe)C_6H_4	83	90
79	H	2-furyl	91	98
80	6-CH_3	2-furyl	89	97
81	7-CF_3	2-furyl	81	95
82	H	cyclohexyl	32[b]	94
83	7-CF_3	cyclohexyl	78	99
84	H	2-(*tert*-butyl)	30	67
85	H	PhCH=CH	50[c]	90
86	H	cyclopentyl	29	70
87	H	*p*-BrC_6H_4	76	55
88	H	*p*-(NO_2)C_6H_4	64	55

Scheme 28: Optimized cyclization process

(a) ee determined by chiral stationary phase HPLC.
(b) 66% conversion of starting material **56** to product **82** observed by ^{1}H NMR.
(c) partial conversion of starting material **59** to product **85** observed by ^{1}H NMR.

We observed that increasing the size of the aryl substituent to a 2-naphthyl group (**73**) led to a decrease in enantioselectivity (to 80% ee), (Scheme **29**).



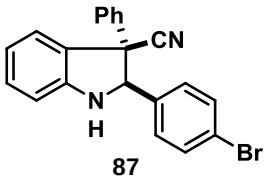
Scheme 29: Electrocyclization with larger aromatic ring

Electron-rich aromatic rings such as *p*-methoxyphenyl (**78**) and *p*-methylphenyl (**74**) were well tolerated, giving high enantioselectivities (up to 90% ee), (Scheme **30**).

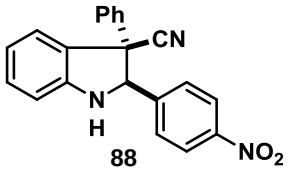


Scheme 30: Electrocyclization with electron-rich aromatic rings

However, electron-poor aromatic rings such as *p*-bromophenyl (**87**) or *p*-nitrophenyl (**88**) gave lower enantioselectivities (55% ee), (Scheme **31**).



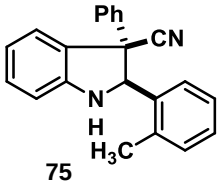
87
76% Yield
>20:1 dr
55% ee



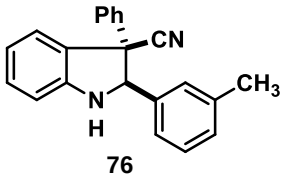
88
64% Yield
>20:1 dr
55% ee

Scheme 31: Electrocyclization with electron-poor aromatic rings

Ortho- and *meta*- substituted aryl rings such as *o*-methylphenyl (71% ee) and *m*-methylphenyl (60% ee) gave reduced enantioselectivity compared to the unsubstituted phenyl ring **63** (89% ee).



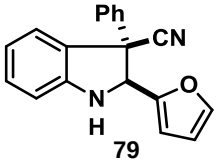
75
94% Yield
>20:1 dr
76% ee



76
92% Yield
>20:1 dr
60% ee

Scheme 32: Electrocyclization with *ortho*- and *meta*- substituted aryl ring

An electron-rich heteroaromatic 2-furyl ring is also well tolerated providing indoline **79** as a single diastereomer and with excellent enantioselectivities (98% ee), (Scheme **33**).



79
91% Yield
>20:1 dr
98% ee

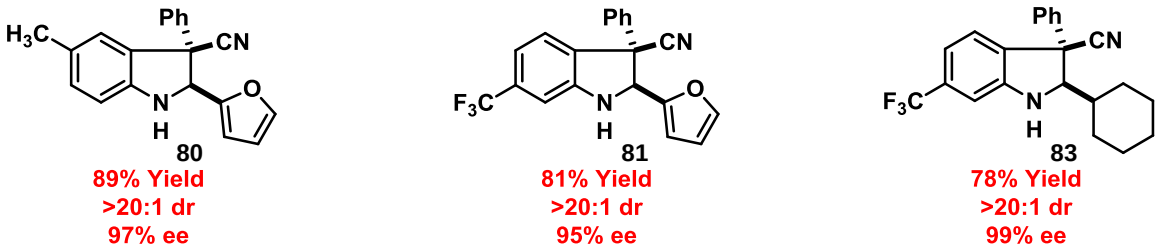
Scheme 33: Electrocyclization with heteroaromatic 2-furyl ring

An aliphatic cyclohexyl ring (**82**) also provided indoline as a single diastereomer with excellent enantioselectivity (94% ee). However, a cyclopentyl ring (**86**) gave a reduced enantioselectivity of 70% ee (Scheme **34**).



Scheme 34: Electrocyclization with cycloaliphatic rings

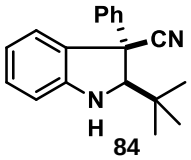
Both electron withdrawing and donating substituents are well tolerated on the indolinyl arene without compromising selectivity; the 7-trifluoromethyl substituted indoline bearing a cyclohexyl group at the 2-position (**83**) can be generated in 99% ee. A 6-methyl substituted indoline bearing a furyl group at the 2-position (**80**) was generated in 97% ee (Scheme **35**).



Scheme 35: Electrocyclization with substituted left-aromatic ring

The cyclization of imines derived from alkyl aldehydes proved to be more challenging, as they were unstable under the cyclization conditions and gave rise to unwanted by-products.

The cyclization reactions with imines having either aliphatic straight chain (*n*-butyl) or branched chain (*iso*-butyl) groups were found to give trace amounts of product in a complex mixture of materials. However, we were pleased to observe that an imine having a bulkier alkyl group, aliphatic branched 2-(*tert*-butyl) **84**, was comparatively more stable to the cyclization conditions and furnished the desired product in moderate yield (30%) and enantioselectivity (67% ee, Scheme **36**).

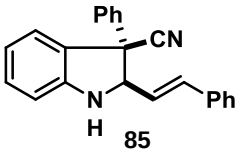


84

30% Yield
>20:1 dr
67% ee

Scheme 36: Electrocyclization with aliphatic branched 2-(*tert*-butyl)

An unsaturated side chain (**85**) is also well tolerated providing indolines with high enantioselectivity (90% ee, Scheme **37**).



85

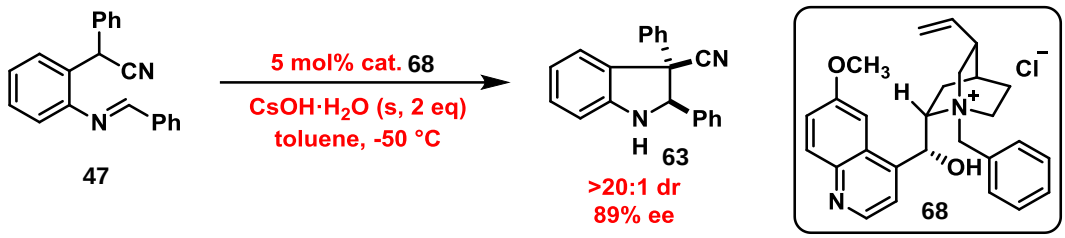
50% Yield
>20:1 dr
90% ee

Scheme 37: Electrocyclization with alkene functionality

In conclusion, we have demonstrated that this cyclization process under optimized reaction conditions is tolerant of a wide variety of substituents giving rise to the desired indolines as a single diastereomer and with high levels of enantioselectivity.

2.6 Stereochemical Model

The cyclization reaction of **47** in the presence of catalyst **68** under optimized phase-transfer conditions proceeds with complete diastereoselectivity and high enantioselectivity, providing the major diastereomer **63** in 89% ee (Scheme **38**).



Scheme 38: Electrocyclization

The relative configuration of the major diastereomer was established by X-ray crystallography (Figure **6**).[34]

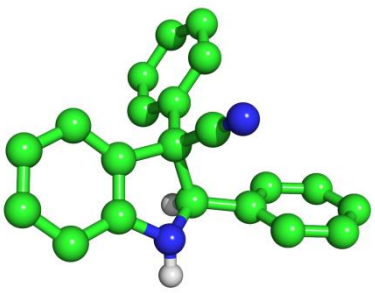
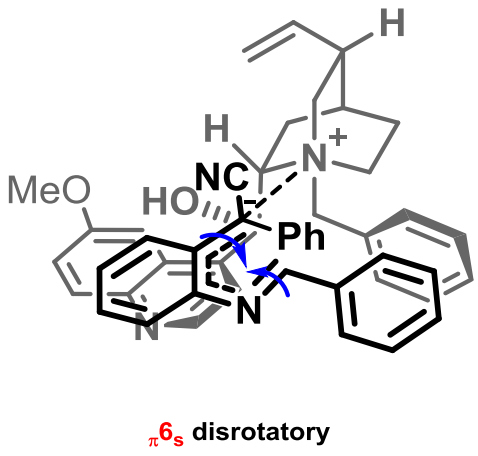


Figure 6: X-ray crystal structure of major diastereomer

The X-ray crystal structure of the major diastereomer denotes that it has an *anti*-arrangement of the two phenyl rings and has been termed as the *anti*-isomer. By analogy, all other indoline products in Scheme **28** were assumed to have the same relative configuration.

Based on the Corey and Lygo model of binding for cinchona alkaloid derived phase-transfer catalysts,[32,35] it has been proposed that our substrate anion binds into the least hindered quadrant of the quaternary catalyst cation (Scheme **39**). This is associated with non-covalent π-stacking interactions between *N*-aryl, quinoline ring units of the catalyst and the aromatic rings of the substrate. These interactions lead to the formation of a tight ion-pair between the substrate and catalyst, and thereby effectively blocking one of the π-faces of the substrate. This causes the aromatic ring of the aldehyde moiety of the substrate to rotate away from the bulk of the catalyst to provide the product indoline having the observed stereochemistry.



Scheme 39: Stereochemical model

3. Mechanism of Phase-Transfer Catalysis

3.1 Introduction: Phase-transfer catalysis

Chemical species located in two or more different phases of a mixture are often prevented to react due to their inability to come together. Traditionally this problem is solved by use of an appropriate mutual solvent.

In 1971, Charles M. Starks presented an alternative solution to this heterogeneity problem by introducing the concept of "*phase-transfer catalysis*".[36] Phase-transfer catalysis is an efficient and powerful technique that allows a great variety of reactions under mild conditions, often using inexpensive and environmentally benign reagents and solvents. Phase-transfer catalysis uses catalytic amounts of a *phase-transfer catalyst* which facilitates the transfer of one of the reactants across the interface into the other phase where it can react with another molecule. For effective phase-transfer catalytic action, it is important that the phase-transfer catalyst is regenerated during the organic reaction; otherwise large amounts of phase-transfer catalyst will be required.[37]

When developing a phase-transfer catalyst, the most important considerations are: stability of the catalyst under the reaction conditions, ease of preparation or availability of the catalyst, cost, ease of removal or recovery and selectivity in catalytic activity.[38]

There are a variety of different phase-transfer catalysts available, such as quaternary ammonium and phosphonium salts, crown ethers and poly-ethylene glycols. Among these, the quaternary ammonium salts are generally the cheapest and simplest to prepare, and hence are widely used.

3.1.1 Mechanism of phase-transfer catalysis

Phase-transfer catalysed reactions generally follow either what Starks described as the "extraction mechanism" or the "interfacial mechanism" as outlined by Mąkosza which have been described below.

3.1.1.1 Starks' extraction mechanism

The simplest phase-transfer catalysed nucleophilic substitution reaction can be written as $RY + X^- \rightarrow RX + Y^-$, where the active nucleophile X^- is being transferred from the aqueous into the organic phase (Figure **6**). A quaternary ammonium phase-transfer catalyst (eg. tetrabutylammonium) possesses an ionic character which makes it partially soluble in the aqueous phase. In addition, the quaternary ammonium cation Q^+ portion of the catalyst is generally substituted with lipophilic hydrocarbon chains, lending an organophilic nature to the catalyst which makes it soluble in the organic phase. Hence the phase-transfer catalyst is distributed between the organic and aqueous phase.

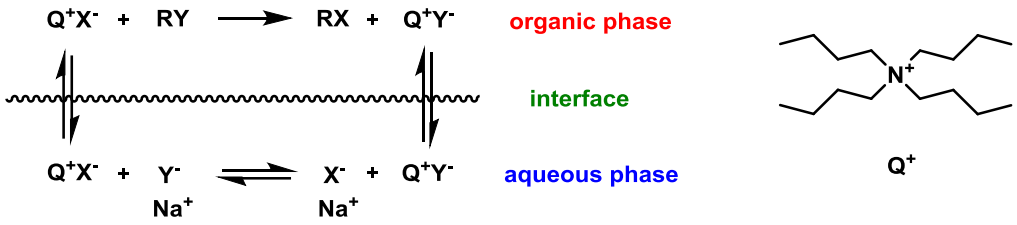


Figure 6: Starks' extraction mechanism

In the Starks extraction mechanism, the quaternary ammonium cation Q^+ forms an ion-pair with nucleophilic anion X^- in the aqueous phase and the ion-pair $[Q^+X^-]$ is extracted into the

organic phase *via* an equilibrium process, where the nucleophilic reaction can now take place. After nucleophilic substitution has occurred the negatively charged leaving group Y^- pairs with the quaternary cation forming an ion-pair, $[Q^+Y^-]$, which can again equilibrate between the two phases, thus establishing a cycle which will continue until all the nucleophilic species X^- or the substrate RY is consumed (Figure **6**).[36,39,40]

3.1.1.1.1 Brandstrom-Montanari modification

In the Brandstrom-Montanari modification of the Starks extraction mechanism, the catalyst is highly organophilic and exists exclusively in the organic phase. The quaternary ammonium cation catalyst Q^+ exchanges Y^- for X^- at the interfacial region of the system followed by the transfer of the exchanged species into the organic phase (Figure **7**).[41,42,43]

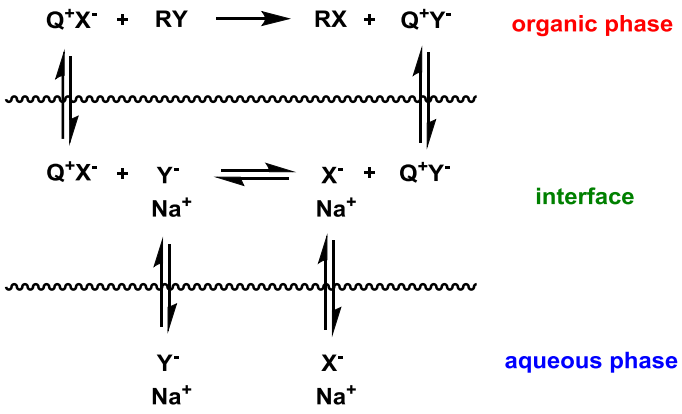


Figure 7: Brandstrom-Montanari modification of Starks' extraction mechanism

3.1.1.2 Mąkosza's interfacial mechanism

A large number of industrially important phase-transfer catalysed reactions are carried out in the presence of a base. One of the advantages of carrying out reactions in the presence of a base in biphasic systems is that it prevents hydrolysis of the reactant present in the organic phase, since OH^- has only limited solubility in the organic phase, and hence the organic substrate does not face the alkaline conditions present in the aqueous phase. This also avoids the use of expensive and corrosive agents like alkali metal hydrides and alkoxides.[44]

Despite the widespread utility of the phase-transfer catalysed reactions carried out in the presence of a base, the mechanism of these reactions was not clearly understood. In general complicated kinetics were observed for hydroxide ion initiated phase-transfer (PTC/OH^-) reactions compared to the simple pseudo-first or second order kinetics associated with the extraction mechanism. Also the reaction rate of PTC/OH^- reactions was found to be highly dependent on the stirring speed of the reaction compared to the independence of the rate of extraction systems on stirring speeds. Hence, the extraction mechanism which was believed to be operative for most PTC systems could not explain the behaviour of PTC systems involving hydroxide ion as the base. This led Mąkosza to propose an alternative mechanism for such systems, called the *interfacial mechanism* (Figure **8**).[45]

Currently, PTC/OH^- reactions operating via both the type of mechanisms (extractive and interfacial) are known.

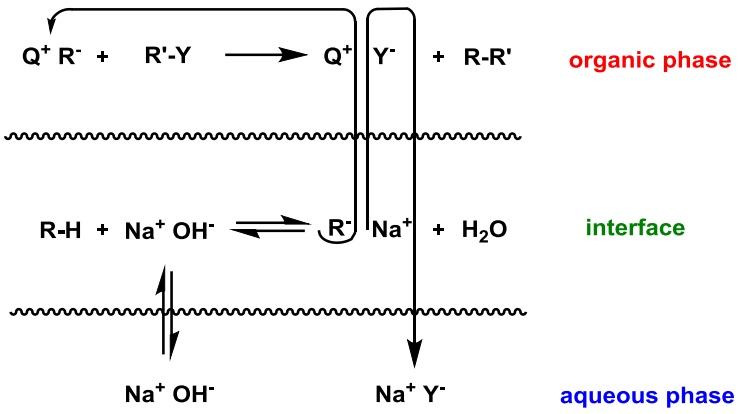


Figure 8: Mąkosza interfacial mechanism for PTC/OH^- reactions

In Mąkosza's interfacial mechanism, the organic substrate RH is deprotonated at the interfacial region by the hydroxide ion located near the interface within the aqueous phase, giving rise to an ion pair, $[Na^+R^-]$, at the interface, which is insoluble in both phases. The quaternary ammonium catalyst cation Q^+ coordinates with the deprotonated substrate and draws it deep into the bulk organic phase in the form of ion pair $[Q^+R^-]$, where it can react with another substrate R'Y to produce the desired product R-R'. The liberated anion Y^- in this process, pairs up with the catalyst cation Q^+ to form ion pair $[Q^+Y^-]$ which can now re-enter the catalytic cycle.

The distinguishing feature of the interfacial mechanism is that the deprotonation of the organic substrate occurs at the interfacial region of the system, in a process which does not involve the phase-transfer catalyst. The only function of the phase-transfer catalyst cation Q^+ is to form an ion pair with the deprotonated substrate and take it into the organic phase for the desired reaction to occur. On the other hand, in the extractive mechanism, the phase-transfer catalyst cation Q^+ extracts the hydroxide ion of the base from the aqueous into the organic phase and the desired reaction takes place.

3.1.1.3 Modified interfacial mechanism

A fourth type of mechanism, known as the modified interfacial mechanism is also possible. In this mechanism, the quaternary ammonium phase-transfer catalyst cation Q^+ which is distributed between the organic and interfacial region of the reaction system, reacts with the hydroxide ion of the base at the interface giving rise to the ion pair of phase-transfer catalyst quaternary ammonium cation with hydroxide anion, $[Q^+OH^-]$. This phase-transfer catalyst hydroxide ion pair deprotonates the substrate at the interface and subsequently takes the substrate anion into the organic phase in the form of phase-transfer catalyst cation-substrate anion ion pair $[Q^+R^-]$ where it can react with electrophilic substrate R'X to produce the desired product R-R' (Figure **9**).[37]

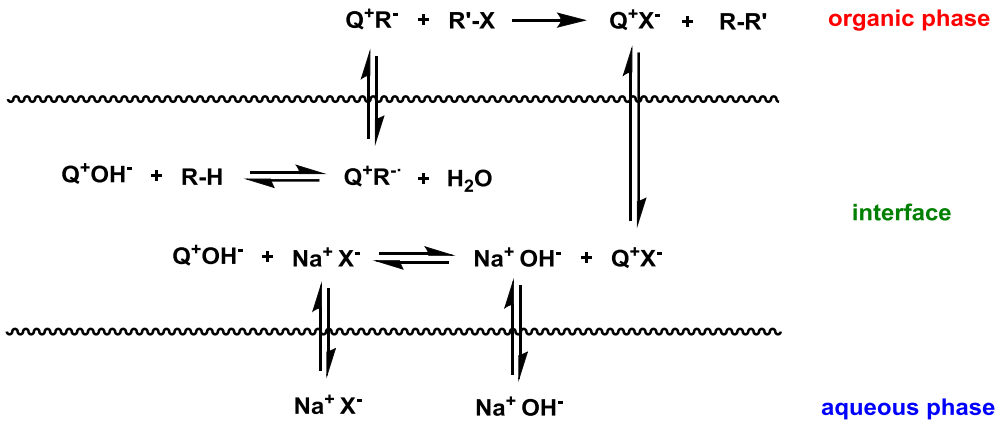


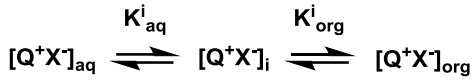
Figure 9: Modified interfacial mechanism for PTC/OH^- reactions

It is important to note that in this mechanism, the phase-transfer catalyst quaternary ammonium cation Q^+ is involved in the deprotonation of substrate. This renders the modified interfacial mechanism distinct from both extractive and interfacial mechanism.

3.1.2 Kinetic factors influencing PTC reactions

3.1.2.1 Catalyst structure

The structure of the catalyst is a critical component of phase-transfer catalysed reactions. In a phase-transfer catalysed reaction system, the quaternary ammonium phase-transfer catalyst ion-pair $[Q^+X^-]$ may be distributed between the aqueous phase, interface, and the organic phase which can be expressed in the form of following equation* (Scheme **40**).



Scheme 40: Distribution of phase-transfer catalyst

For a given anion and organic phase polarity, the distribution constant K of the phase-transfer catalyst will depend on both the structure of the quaternary ammonium part of the catalyst and the counter-ion.

In an interfacial mechanism, the rate-determining step comprises of the formation of phase-transfer catalyst-substrate ion pair $[Q^+R^-]$ followed by its transfer to the organic phase.[46] The phase-transfer catalyst cation Q^+ has to compete with the alkali metal cation of the base in order to successfully form an ion-pair with the substrate anion R^-, and to remove it from the interface and transfer it to the bulk organic phase where the anion is free to react.

* $[Q^+X^-]_{aq}$, $[Q^+X^-]_{i,}$ $[Q^+X^-]_{org}$ – concentration of the phase-transfer catalyst in the aqueous phase, interface, and organic phase respectively.

K^i_{aq} – Distribution constant of the phase-transfer catalyst between aqueous phase and interface.

K^i_{org} – Distribution constant of the phase-transfer catalyst between organic phase and interface.

As the alkyl chains of the quaternary ammonium phase-transfer catalyst cation Q^+ decrease in length, the positive charge on the central nitrogen becomes more electrostatically accessible for interaction with the substrate anion R^-.[47] A quaternary ammonium phase-transfer catalyst in which the positively charged nitrogen centre is more accessible for interaction and can approach the substrate anion R^- site closely may compete with the alkali metal cation of the base more successfully for the formation of catalyst-substrate ion-pair $[Q^+R^-]$. Thus, an ion-pair consisting of an electrostatically available quaternary ammonium cation Q^+ will be of lower energy in comparison to an ion-pair involving a quaternary ammonium cation Q^+ having the positive charge buried deep within four long alkyl chains, and hence will allow faster rates of reaction. Therefore, as the length of the alkyl chains of the quaternary ammonium part of the catalyst decreases the rate of the reaction increases. However, the reaction rate increases until a maximum is attained, after which the rate decreases.

This is because when the lengths of alkyl chains of the quaternary ammonium cation are decreased to an extreme, the catalyst-substrate ion-pair $[Q^+R^-]$ will not be sufficiently organophilic to be soluble in the organic phase, causing a decrease in the rate of the reaction. This is similar to the non-catalysed reaction where the alkali metal-substrate ion pair $[Na^+R^-]$ cannot enter the organic phase.

On the other hand, in cases where the extraction mechanism operates, the main role of the phase-transfer catalyst is to extract the inorganic base into the organic phase in the form of an ion-pair $[Q^+OH^-]$. Hence increasing the organophilicity of the catalyst by increasing the length of the alkyl chains of the quaternary part of the catalyst leads to an increase in the rate of the reaction which is attributed to the increased solubility of the ion-pair $[Q^+OH^-]$ in the organic phase.

3.1.2.2 Effect of anions

The nature of the anions involved in a PTC system has a significant effect on the reaction. The anions involved in the PTC catalytic cycle may have two sources: 1) the counteranion X^- of the phase-transfer catalyst, or 2) the leaving group eliminated from the substrate. The affinity of the anion X^- for association with the quaternary ammonium phase-transfer catalyst cation Q^+ will affect the extent of transfer of the hydroxide ion or substrate anion R^- by the catalyst to the organic phase for the reaction to occur.[37] Phase-transfer catalysed reactions can be totally or partially suppressed by catalyst poisoning[48] when the hydroxide ion (hard base) or substrate anion R^- cannot successfully compete with a soft and highly polarizable lipophilic anion (e.g. I^-) for association with the soft organophilic catalyst cation Q^+ in the organic phase. Extractive PTC reactions are more prone to catalyst poisoning compared to the interfacial PTC reactions. Since in interfacial PTC reactions, the organic substrate anion R^- which is to be transferred to the organic phase by the catalyst, is inherently organophilic in nature (much more than hydroxide ion in the case of extractive PTC) and can compete with other anions for association with the catalyst cation. Dehmlow has arranged different anions according to their lipophilicity, where anions towards the left have a greater affinity for association with the quaternary ammonium cation than those present towards the right.[49]

$I^- > ClO^{3-} > NO^{3-} > Br^- > (CN^-, PhCOO^-) > (NO_2^-, Cl^-) > HSO_4^- > (F^-, OH^-) > SO_4^{2-}$

3.1.2.3 Stirring speed

In principle, a chemical species is required to be in the form of an ion-pair in order to be transferred physically from at least one bulk phase or interface into another bulk phase in a phase-transfer catalysed reaction.

It has been demonstrated that for an interfacial mechanism the rate of the reaction is proportional to the speed of stirring in the range 600-1700 rpm.[50] On the other hand, for an extraction mechanism the reaction rate is independent of stirring speed (> ~300 rpm).[39] This is a powerful criterion for distinguishing between the two mechanisms for a phase-transfer catalysed reaction.

Under the conditions of very slow agitation or stirring, the interfacial area between the phases is minimal and therefore the mass transfer of anions is slow which limits the rate of phase-transfer catalysed reaction.

Also an increase in the stirring speed causes an increase in the degree of dispersion of one phase into the other, leading to an increased rate of reaction until a stage is reached where mass transfer reaches a maximum and the rate becomes independent of the stirring speed.

3.1.2.4 Kinetic order with respect to catalyst concentration

It has been shown that for a phase-transfer catalysed reaction the kinetic order with respect to the catalyst concentration can vary over a wide range of values, since the quaternary ammonium phase-transfer catalyst can exist in the form of a free ion $[Q^+X^-]$, ion-pairs $[Q^+X^-]_2$, or more complex aggregates $[Q^+X^-]_n$. For instance, if the quaternary catalyst is present as a monomeric ion pair $[Q^+X^-]$ and the monomeric ion pair is the reactive species then the kinetic order with respect to the catalyst would be unity. However, if a higher aggregate of the catalyst ($[Q^+X^-]_n$) is the dominant species present but a small equilibrium concentration of the monomeric catalyst $[Q^+X^-]$ is the reactive species, then the kinetic order with respect to the catalyst would be more complex.[37]

On the basis of kinetic studies it has been postulated that extractive reactions generally show first order with respect to the catalyst.[46] On the other hand, interfacial reactions show fractional order with respect to the phase-transfer catalyst. It has also been observed that the hydroxide ion initiated phase-transfer reactions show complicated kinetics in general.[51,52,53]

3.1.3 Mechanistic Investigations: Phase-transfer catalysis

Despite the development of phase-transfer catalysis as a primary synthetic tool in organic synthesis, the mechanism of these reactions is not completely understood. Relatively few examples concerning the study of mechanism of phase-transfer catalysed reactions have been reported. The kinetic analysis of these phase-transfer reactions remains a challenge, due mainly to the difficulty of studying the complex multi-phase systems.

3.1.3.1 Investigations by Starks

As stated already, Starks first introduced the term "phase-transfer catalysis" in 1971 to explain the critical role of quaternary ammonium or phosphonium salts [Q^+X^-] in the reactions between two substances located in different immiscible phases.[36] Starks carried out a detailed kinetic investigation on the displacement reaction of 1-chlorooctane with aqueous sodium cyanide in the presence of quaternary phosphonium or ammonium salts as a phase-transfer catalyst (Figure **10**).[53]

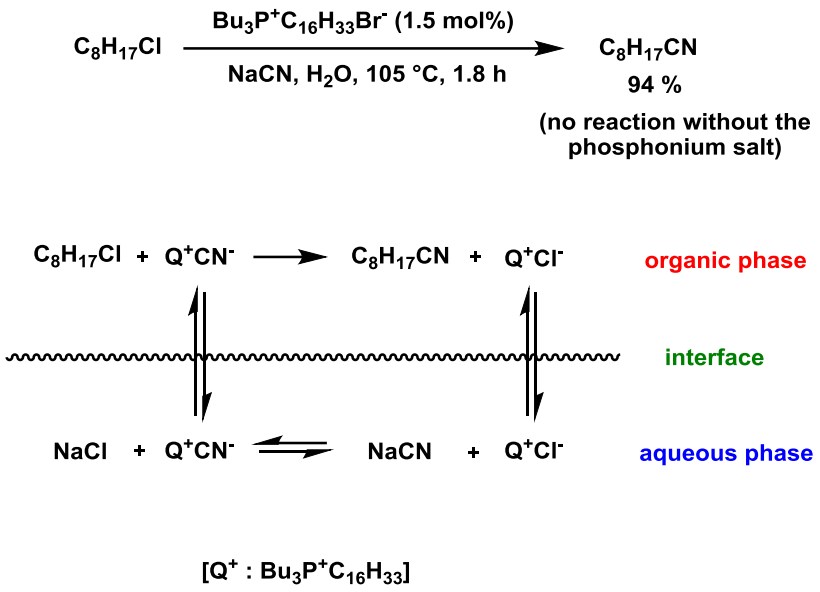


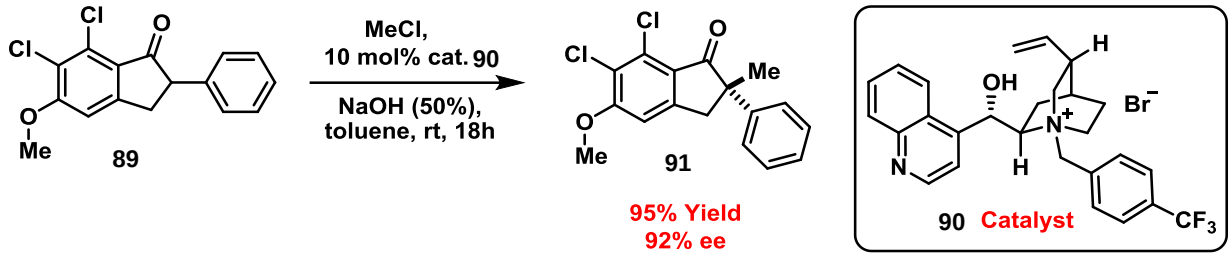
Figure 10: Investigations by Starks

He found that the rate of substitution reaction is directly proportional to the concentration of phase-transfer catalyst, indicating a pseudo-first order kinetic behaviour of the reaction in quaternary salt concentration (assuming all of Q^+ to be in the organic phase). Starks also observed that the rate of the reaction rapidly reaches a maximum with a stirring rate of *ca.* 250-300 rpm and is virtually invariant above this range. These results suggested that the substitution reaction is taking place in the bulk of the organic phase and the equilibration of the associated ion-pairs in the aqueous phase and their partition across the phase-boundary is faster than the substitution reaction. Later, the term "Starks Extraction Mechanism" was proposed to describe the mechanism followed by such reactions.

3.1.3.2 Kinetic investigations by Merck

In 1984, pioneering studies by a Merck research group led to the development of an asymmetric phase-transfer catalysed alkylation reaction.[54] Subjecting indanone **89** to

asymmetric phase-transfer catalysed alkylation conditions using cinchona derived phase-transfer catalyst **90** yielded the alkylated indanone derivative **91** in 92% ee (Scheme **41**).



Scheme 41: Asymmetric phase-transfer catalysed alkylation by Merck

The proposed model for catalysis suggests that the chiral catalyst **90** forms a tight ion-pair with the enolate portion of the substrate and thereby transfers stereochemical information. Molecular modelling studies suggested a three-point interaction model between the substrate and catalyst (Figure **11**). It was postulated that the *N*-benzyl and quinolone rings of the catalyst interact with the π-electrons of the phenyl and the dichloromethoxy aromatic ring, respectively. The hydroxyl group of the catalyst offers hydrogen bonding with the negatively charged enolate oxygen of the substrate. As a result, the alkylating agent can approach the substrate anion only from one side.

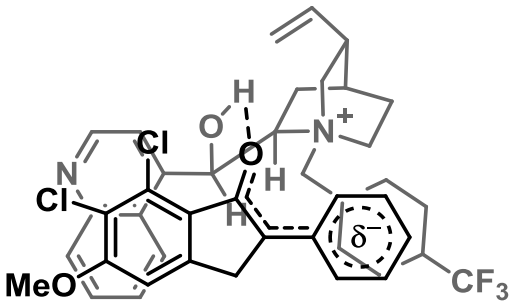
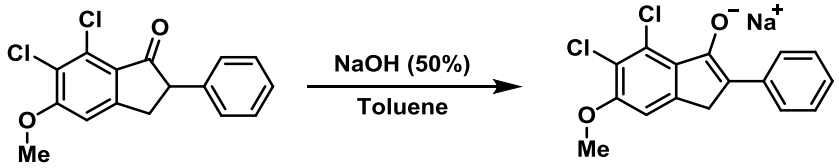


Figure 11: Stereochemical model- asymmetric phase-transfer alkylation

Kinetic and mechanistic studies were later carried out by the Merck research group to understand the mechanism of this asymmetric alkylation reaction.[55] The following three basic steps of the reaction sequence were studied in detail:

(a) Enolate formation

The indanone, present solely in organic layer, is deprotonated in the presence of aqueous NaOH to form the corresponding sodium enolate which exists as a separate solid phase between the organic and the aqueous phases (Scheme **42**).



Scheme 42: Formation of enolate

The deprotonation was found to occur even in the absence of the phase-transfer catalyst which suggests that deprotonation occurs at the interface of the organic and aqueous phase without mediation by the catalyst.

(b) Transfer of the enolate ion into the organic phase

The solubilities of *N*-benzylcinchoninium halides in toluene are so low that they cannot be detected even after vigorous stirring in the solvent for several hours. Yet, the presence of catalyst is detected by LC in the quenched organic layer of phase-transfer reactions indicating that some sort of transformation of the catalyst is taking place which makes the catalyst more soluble under phase-transfer conditions. Experimental studies suggested that the catalyst exists as a dimer in toluene in the presence of aq. NaOH (Figure **12**).

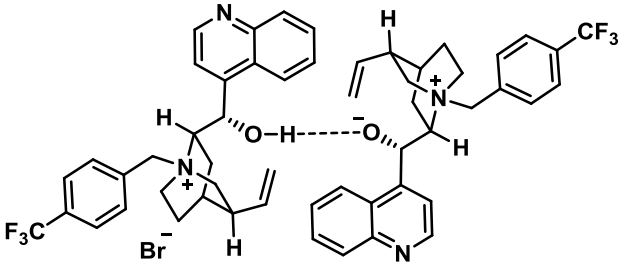


Figure 12: Dimeric phase-transfer catalyst

It is believed that a small amount of catalyst dissolves in the aqueous phase where it is partially deprotonated at the hydroxyl functionality by the strong base, forming a zwitterion. This zwitterion forms a complex with another molecule of phase-transfer catalyst producing a dimeric species, which has a relatively high solubility in the organic phase (Scheme **43**). This enhanced solubility of the catalyst promotes the transfer of the enolate to the organic phase.

$$(Q\text{-}OH)^{+}(Br^{-})_{solid} \rightleftharpoons (Q^{+}\text{-}OH)_{aq} + (Br^{-})_{aq}$$

$$(Q^{+}\text{-}OH)_{aq} + (OH^{-})_{aq} \rightleftharpoons (Q^{+}\text{-}O^{-})_{aq} + H_2O$$

$$(Br^{-})_{aq} + (Q^{+}\text{-}OH)_{aq} + (Q^{+}\text{-}O^{-})_{aq} \rightleftharpoons (Q^{+}OH\text{---}^{-}O\text{-}Q^{+}Br^{-})_{org}$$

Scheme 43: Dimerization pathway

(c) Asymmetric alkylation in the organic phase

The kinetics of the methylation step were found to be complex as an induction period was observed when the chiral phase-transfer catalyst is present at the start of the reaction. This induction period simply disappears when the catalyst is added to the reaction mixture after

the formation of the enolate. Detailed kinetic investigations were performed by the Merck research group in order to understand this complex reaction system. The results are summarised below:

i. The rate of alkylation is zero order in substrate indanone.

ii. Variation of stirring speed in the range 500-1200 rpm had no effect on enantioselectivity and the rate of reaction suggesting that the rate-determining step is occurring in the toluene layer. This indicates that interfacial deprotonation of substrate indanone followed by its transfer to the organic phase is not a rate-determining step.

iii. A bilogarithmic plot of rate constant for alkylation vs. concentration of catalyst added to the reaction mixture resulted in a straight line with a slope of 0.56±0.05. This result is consistent with the mechanism in which the catalyst dimer has to dissociate to the active monomer to catalyse the reaction.

iv. A bilogarithmic plot of rate constant vs. concentration of alkylating species (MeCl) resulted in a straight line with a slope of 0.67±0.06.

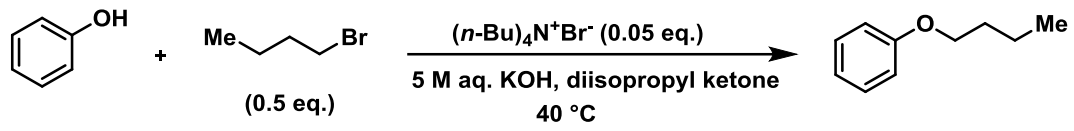
v. An order of unity with respect to the concentration of catalyst and alkylating agent (MeCl) was observed when the reaction is performed in the presence of an achiral phase-transfer catalyst (Aliquat 336). This suggests that the mechanisms for formation of chiral and racemic products are different due to the differences in catalyst structure.

A major change in the kinetics of the alkylation reaction was observed when the aq. base was further diluted from 50% NaOH to 30% NaOH. The bilogarithmic plot of rate constant vs. concentration of alkylating species (MeCl) was found to have a slope of 0.94±0.02, indicating that alkylation is the sole rate-determining step. It was suggested that the amount of water present in the reaction system in the case of 30% NaOH was greater in comparison

to the corresponding system with 50% NaOH, thus, favouring the hydration of the phase-transfer catalyst at the hydroxyl functionality and in turn lowering the extent of catalyst dimer formation.

3.1.3.3 Kinetic investigations by Denmark

Recently, Denmark *et al.*[56] reported kinetic studies to support the extraction mechanism being operational for the phase-transfer catalysed alkylation of phenols (Scheme **44**).[57]



Scheme 44: Phase-transfer catalysed alkylation of phenols

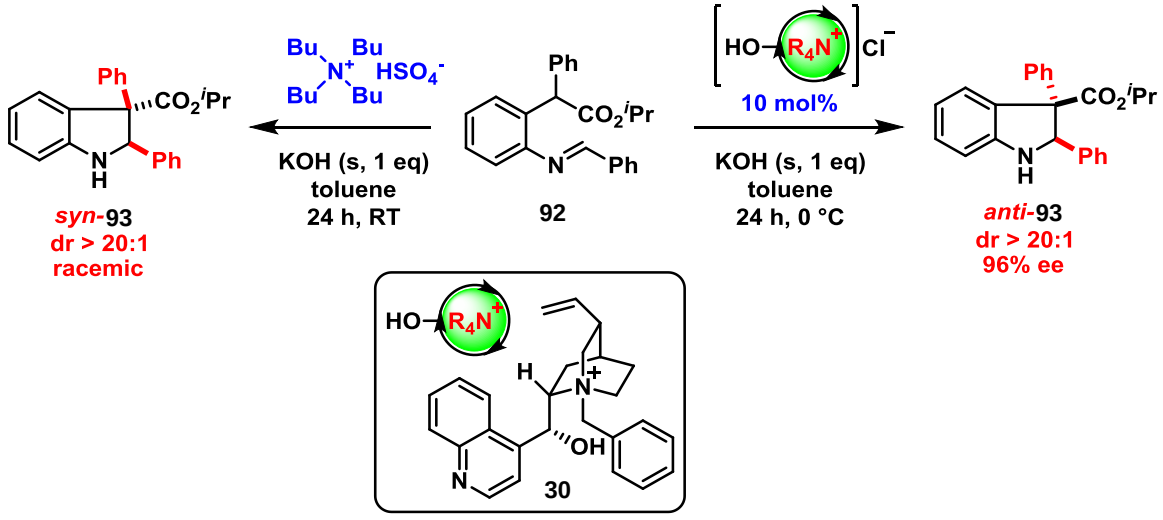
Kinetic investigations demonstrated a linear relationship between the reaction rate and concentration of the alkylating agent (*n*-butyl bromide). This indicates a first order rate dependence in electrophile under phase-transfer conditions, confirming that the bond-forming reaction is the rate-determining step. First order kinetics with respect to the phase-transfer catalyst was observed. Variation of stirring speed in the range 500-2000 rpm had no effect on the rate of reaction suggesting that an extractive mechanism is operational and that the phase-transfer catalysed alkylation reaction is intrinsic reaction rate limited (i.e. the overall reaction rate is limited by the rate of intrinsic organic phase reaction).

These results supports the fact that phase-transfer catalysed alkylation of phenol is operating by an extraction mechanism and is an intrinsic reaction rate-limited process.

3.2 Mechanistic Investigations on our phase-transfer catalysed cyclization

3.2.1 Catalyst-Dependent Diastereoselectivity

As discussed previously in brief, a catalyst dependent diastereoselectivity was observed with the ester-substituted benzhydryl system (Scheme **45**). The use of chiral phase-transfer catalysts allows the conversion of substrate imine to the product indoline with a high diastereomeric preference in the favour of isomer *anti*-**93** (C-2 arene and the C-3 phenyl being on opposite sides of the indoline). On the other hand, use of achiral phase-transfer conditions led to the formation of the other diastereomer *syn*-**93**.



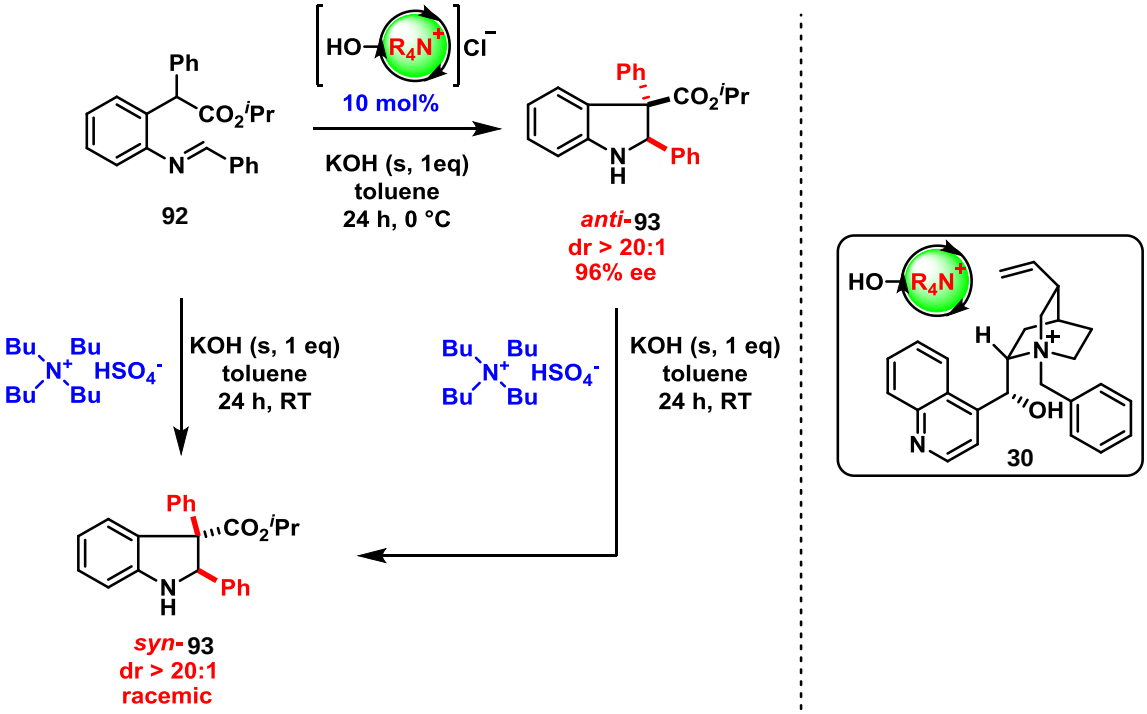
Scheme 45: Diastereoselectivity with ester-substituted benzhydryl system

3.2.1.1 Interconversion Experiments

The observation that the use of different phase-transfer catalysts gave different diastereoselectivity led to experiments in order to investigate if the diastereomers are interconverting under the cyclization conditions.

3.2.1.1.1 Investigations on ester-substituted benzhydryl system

The enantioenriched isomer *anti*-**93** was subjected to the achiral phase-transfer conditions using catalyst TBAHS at room temperature which resulted in the formation of a single isomer *syn*-**93**, suggesting that the diastereomers are interconverting (Scheme **46**). [58] Interestingly the diastereomer *syn*-**93** was obtained as a racemate from the enantio-enriched starting material ***anti*-93**.



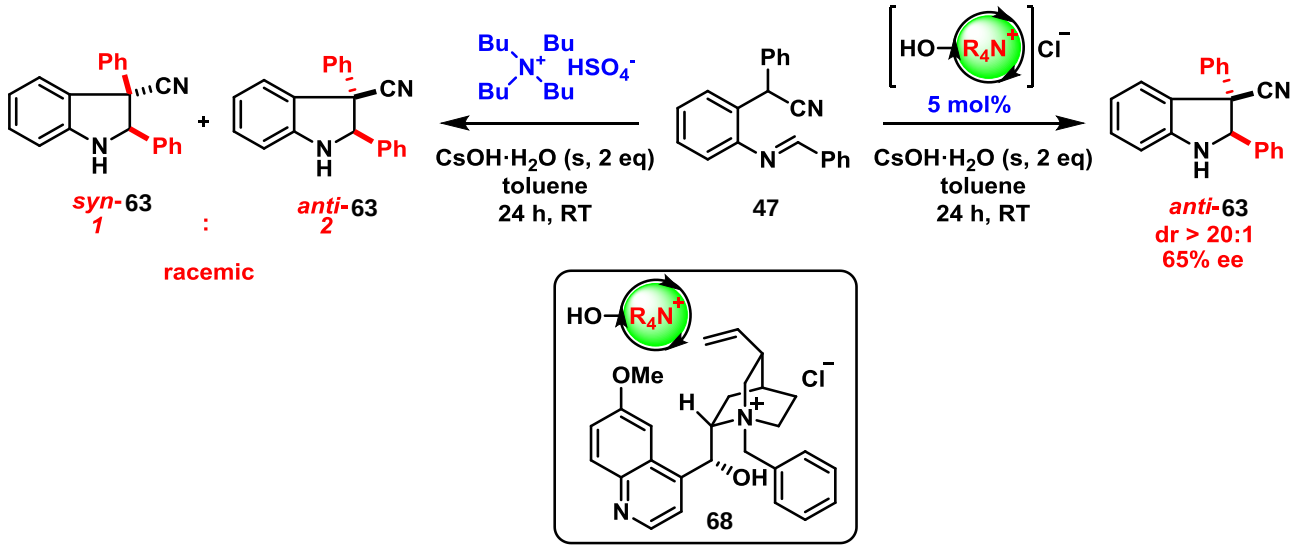
Scheme 46: Interconversion experiments with phenyl-ester system

When racemic *syn*-**93** was subjected to chiral conditions, no change in stereochemistry was observed. Subsequently, racemic *anti*-**93** was also subjected to chiral phase-transfer conditions which similarly resulted in no change of stereochemistry, being consistent with the previous observation.

The observed results suggest that indoline isomer *anti*-**93** is the kinetic isomer which, under achiral phase-transfer conditions, is converted to the thermodynamically more stable isomer *syn*-**93**.

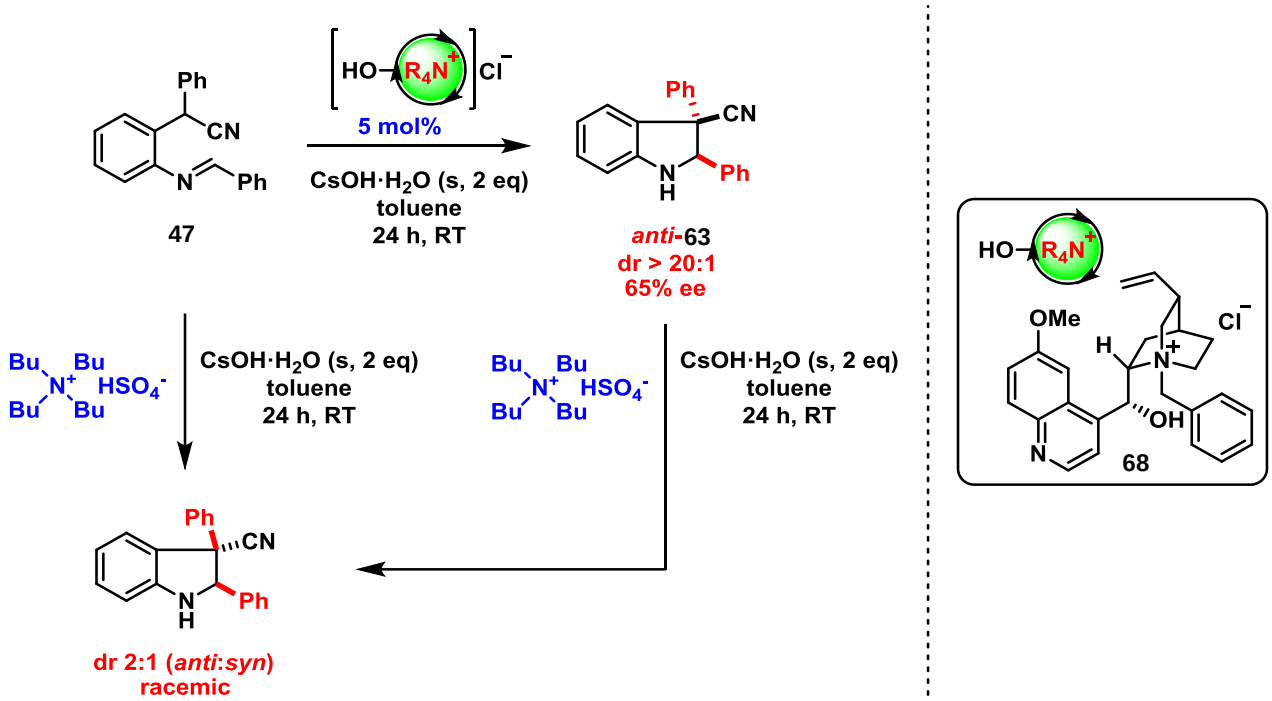
3.2.1.1.2 Investigations on nitrile-substituted benzhydryl system

A similar catalyst dependent diastereoselectivity was observed with the nitrile-substituted benzhydryl system. The presence of the phase-transfer catalyst **68** accelerates the conversion of the imine to the indoline **63** with a high diastereomeric preference. The diastereoselectivity observed is excellent, with greater than 20:1 selectivity at RT in favour of the *anti*-isomer **63** (Scheme **47**).



Scheme 47: Diastereoselectivity with nitrile-substituted benzhydryl system

We subjected the enantioenriched *anti* diastereomer **63** to achiral phase-transfer conditions using TBAHS as a catalyst. Under these conditions the *anti*-isomer **63** underwent partial conversion to the *syn*-isomer **63** giving a mixture of racemic *syn*- and *anti*- isomers in a 1:2 ratio respectively (Scheme **48**).



Scheme 48: Interconversion experiments with phenyl-nitrile system

The stereochemical course of this reaction was probed through X-ray crystallography which confirmed the conversion of the *anti*- to the *syn*-isomer (Figure **13**).

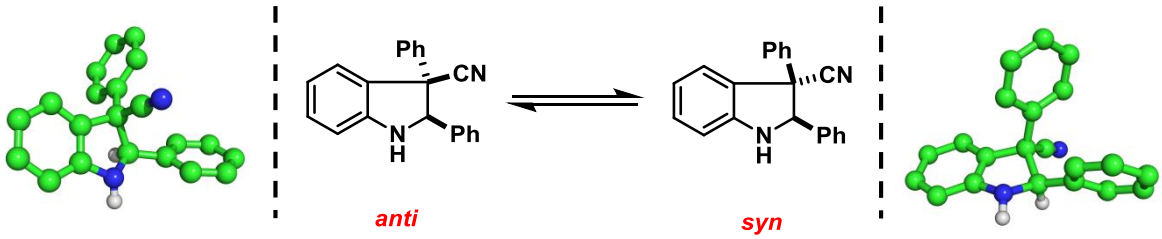
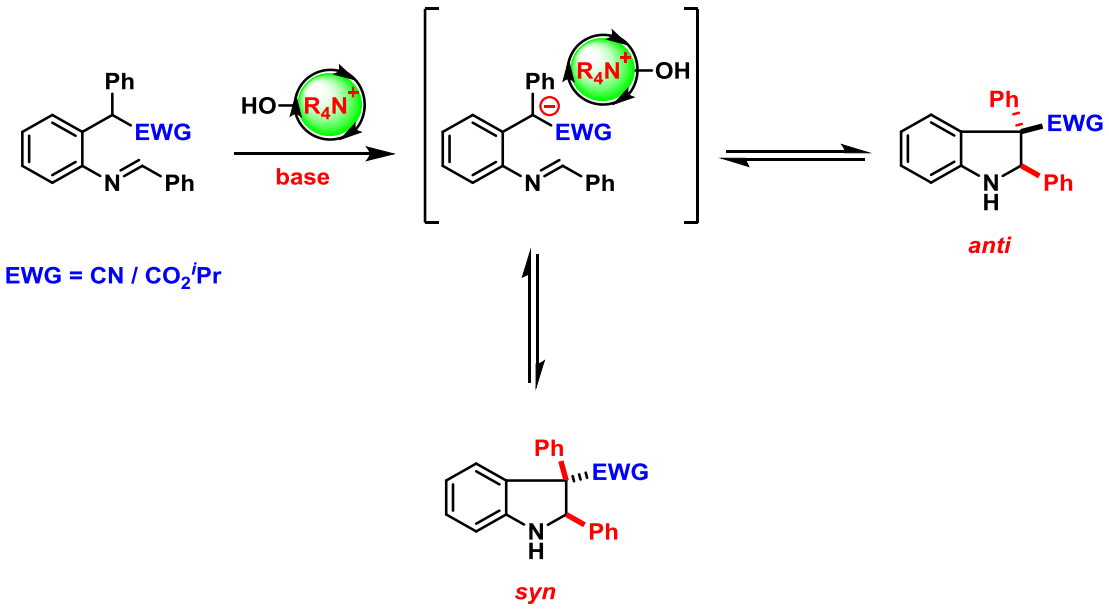


Figure 13: X-ray crystal structures of the diastereomers

Subsequently, this mixture of racemic *anti*-**63** and *syn*-**63** was subjected to the chiral phase-transfer conditions, again using catalyst **68**, with no change in stereochemistry observed. When the imine **47** was subjected to the same achiral phase-transfer conditions, again a 1:2 mixture of the diastereomers *syn*-**63** and *anti*-**63** were formed respectively suggesting that this is the thermodynamic equilibrium ratio of products.

3.2.1.2 Interconversion experiments- Conclusions

There are two possible modes of interconversion between the diastereomers either *via* a cycloreversion mechanism (Scheme **49**), or by deprotonation of the hydrogen at C-2 of the indoline followed by reprotonation. However, since both stereocentres have been affected during the conversion to give racemic *syn*-isomer of indoline, it is likely that cycloreversion is responsible for conversion between the diastereomers as opposed to C-2 deprotonation.



Scheme 49: Cycloreversion

Hence on the basis of the results obtained with these interconversion experiments, we conclude that the chiral phase-transfer catalysts (**30** and **68**) allow the formation of the kinetic, *anti*-indolines (**93** and **63**) but do not facilitate the cycloreversion reaction needed for the formation of the thermodynamic *syn*-isomers. However, the use of achiral phase-transfer catalyst TBAHS facilitates the ring opening and ring closing of the kinetic *anti*-indoline (**93** and **63**) to the thermodynamically more stable *syn*-isomer (**93** and **63**) until equilibrium is reached.

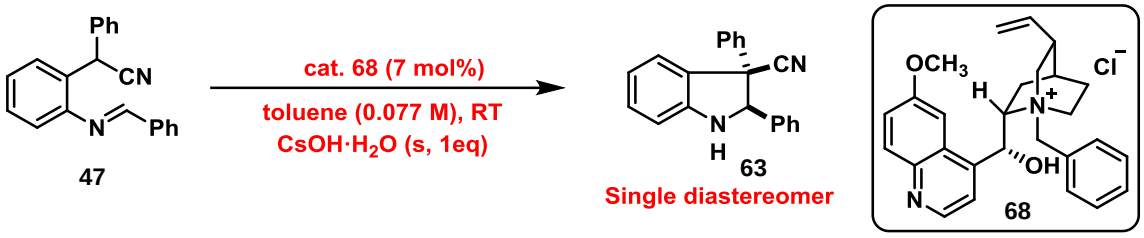
3.2.2 Kinetic Investigations

As stated previously, phase-transfer catalysed reactions can broadly follow two different mechanisms. They can proceed *via* a Starks extraction mechanism, or a Mąkosza interfacial mechanism. We were interested in finding out the type of mechanism followed by our phase-transfer catalysed electrocyclization process. Hence, we decided to investigate our phase-transfer catalysed process by following the kinetics of the reaction.

3.2.2.1 Initial investigations

3.2.2.1.1 Initial attempts at monitoring reaction

Our strategy was to follow the cyclization reaction at room temperature under the optimized conditions by taking out reaction aliquots at particular time intervals followed by filtering through a silica plug to quench the reaction by removing the base and catalyst, and then analysing the aliquots using HPLC to determine the reaction conversion. This would allow us to analyze conversion as a function of reaction time. We instigated the investigations with asymmetric cyclization reaction and performed a test reaction (Scheme **50**). The substrate imine **47** was dissolved in toluene (0.077 M) followed by addition of 7 mol% of chiral phase-transfer catalyst **68** (*N*-benzylquininium chloride), the mixture was left stirring at 500 rpm for 15 minutes to allow a uniform reaction mixture. One equivalent of solid base ($CsOH \cdot H_2O$) was added to the reaction mixture at which point the reaction time was defined as zero. A change in the colour of the reaction mixture from light yellow to red was observed indicating progress of reaction. Reaction mixture aliquots were taken out at five minute intervals and were analysed using a pre-calibrated HPLC (refer section 5.4 for calibration).

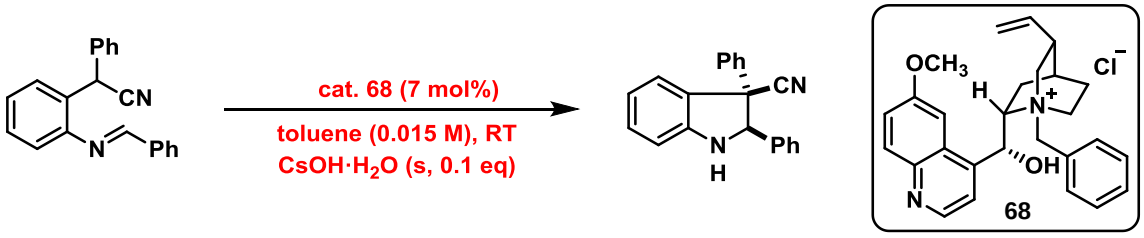


Scheme 50: Asymmetric cyclization- Initial kinetic investigations

The HPLC analysis of the first aliquot (at t = 15 min) indicated that the reaction had already reached completion with no trace of starting material observed.

3.2.2.1.2 Modification of reaction conditions

In an attempt to lower the rate of reaction to facilitate following the reaction kinetics, the reaction conditions were modified. The reaction mixture was diluted fivefold (with toluene) and the amount of base was lowered to 0.1 equivalents (Scheme **51**). A decrease in the reaction rate was observed when the reaction was performed under these modified cyclization conditions.



Scheme 51: Modified asymmetric cyclization

The HPLC trace indicated that the reaction was clean, showing complete conversion of starting material to the product (Figure **14**). A reaction conversion vs. time graph was plotted which surprisingly resulted in a sigmoidal shaped curve with an induction period (Figure **15**). This is superficially suggestive of autocatalysis.

Hence, it was apparent that the mechanism of our cyclization reaction is more complex than that of a simple phase-transfer catalysed process.

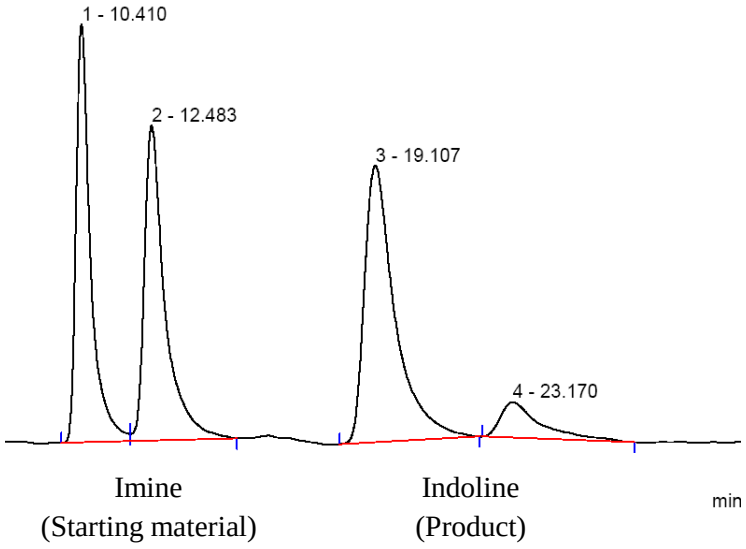


Figure 14: HPLC trace of reaction aliquot taken at t = 1800 seconds

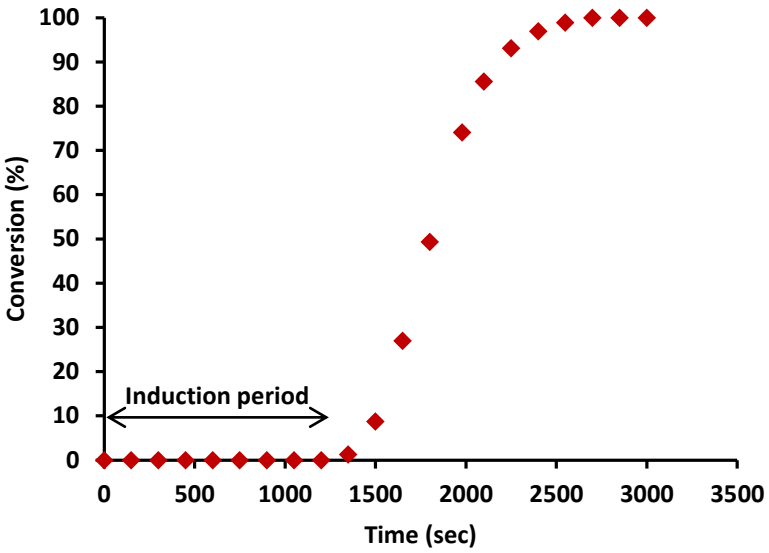


Figure 15: Reaction profile: Plot of product conversion versus time

These observations prompted several questions: (i) what is the origin of the induction period and (ii) the sigmoidal nature of the curve. This compelled us to perform a detailed kinetic study of the reaction.

Our journey towards understanding these unusual characteristics have led to an unravelling of the mystery behind the complex mechanism of this phase-transfer catalysed cyclization process, which will be discussed in this chapter in the following sections.

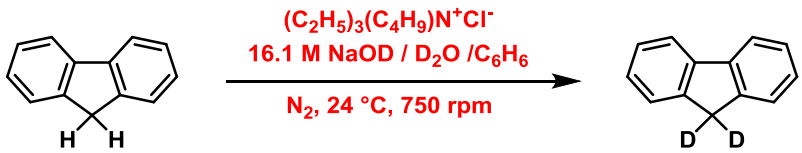
3.2.2.2 Kinetic investigation experiments

3.2.2.2.1 Order of addition experiments

We decided to investigate whether the order of addition of the chiral catalyst has any effect on the induction period of the reaction.

Kinetic investigations carried out by Halpern and Rabinovitz on deuteration of fluorene have demonstrated that an induction period exists when the aqueous base is added last, whereas

no induction period is observed when the catalyst is added last to a pre-equilibrated reaction mixture (Scheme **52**).[59] These results indicate that the phase-transfer catalyst is involved in catalysing the deuterium exchange, but mainly after an equilibration is established between the NaOD/D_2O and the fluorene/benzene system. When this pre-equilibration is not performed, an induction period is observed during which a steady state concentration of [Na^+R^-] ion-pair is generated at the interface. The special steric requirement for interfacial deprotonation and the presence of water molecules at the interface contributes to the low concentration of [Na^+R^-] ion pairs at the interface in the absence of catalyst. The role of the catalyst seems to shift the equilibrium of the interfacial deprotonation step to the right by transferring the fluorenyl anion formed at the interface to the organic phase, thereby greatly increasing the quantity of fluorenyl anion in the system, and hence leading to an increase in the rate of deuteration. This suggest that interfacial deprotonation of the substrate is a fast equilibrium process and constitutes a necessary pre-requisite for catalysis.

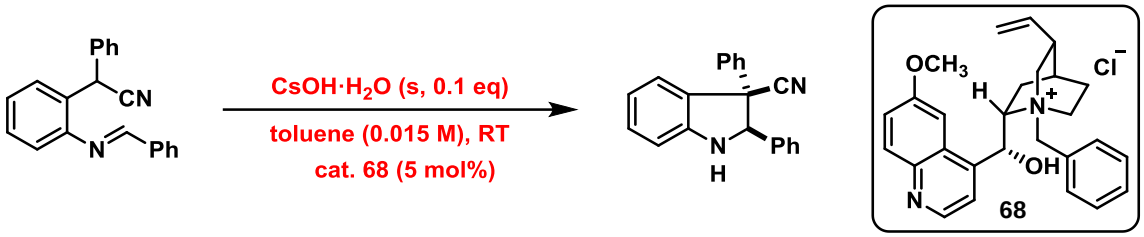


Scheme 52: Deuteration of fluorene

We carried out a similar experiment on our asymmetric cyclization reaction. We started with a stirring mixture of substrate imine **47** and base ($CsOH·H_2O$) dissolved in toluene and added to it chiral phase-transfer catalyst **68** at different times (t = 0 sec, t = 660 sec, t = 1800 sec) in separate reaction flasks. These reactions were monitored and a reaction conversion vs. time graph was plotted (Figure **16**).

The order of addition of the chiral catalyst did not have any marked effect on the induction period. We also observed that if the chiral catalyst is added at any time after the induction period region (i.e. at $t > t_{induction}$), the reaction starts immediately at that particular time giving rise to a sigmoidal shaped reaction profile.

This experiment suggests that the induction period is independent of when the chiral catalyst is added.



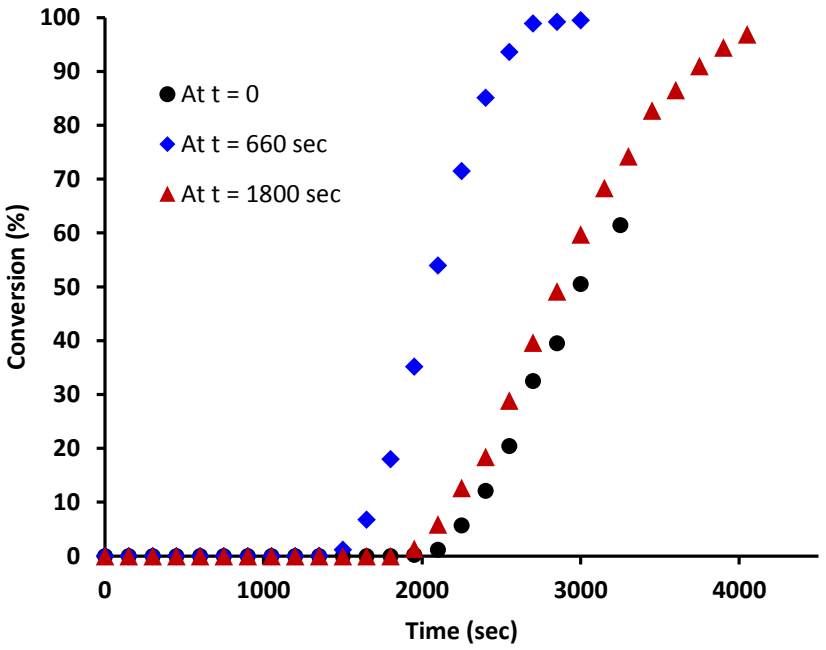
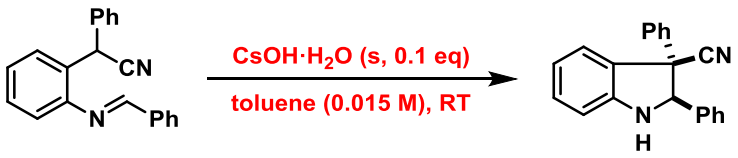


Figure 16: Order of addition experiment

3.2.2.2.2 Background cyclization: Without phase-transfer catalyst

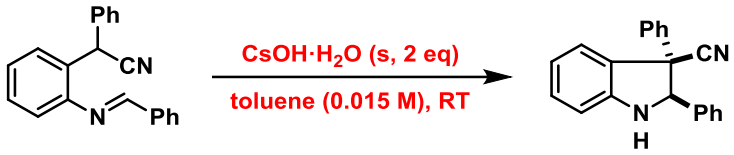
We moved to investigate whether the cyclization occurs in the absence of the phase-transfer catalyst. Substrate imine **47** was treated with base ($CsOH \cdot H_2O$) in toluene without any catalyst under the previous conditions (Scheme **53**). Surprisingly the reaction went to form product indoline but the reaction was very slow. The fact that the reaction takes place even in the absence of the phase-transfer catalyst **68** suggested that substrate imine **47** is deprotonated at the phase-boundary without any mediation of the phase-transfer catalyst.[60] This indicates an interfacial mechanism involving an equilibrium between solid and liquid phases in our asymmetric phase-transfer cyclization reaction.



Scheme 53: Cyclization in the absence of phase-transfer catalyst

3.2.2.2.2.1 Kinetic profile of background cyclization

Kinetic studies were performed on this reaction which indicated that the induction period was approximately 120 minutes ($\pm$ 20 minutes) and the overall reaction takes several days to go to completion. Reaction conditions were modified in order to decrease the time period of this reaction by increasing the amount of base added (Scheme **54**).



Scheme 54: Cyclization under modified conditions

A plot of reaction conversion versus time indicates that the reaction commences after an induction period of 20 minutes with an increasing rate (Figure **17**). The rate of the reaction then decreases after a certain point at around t = 34 minutes and the reaction proceeds with a lower rate.

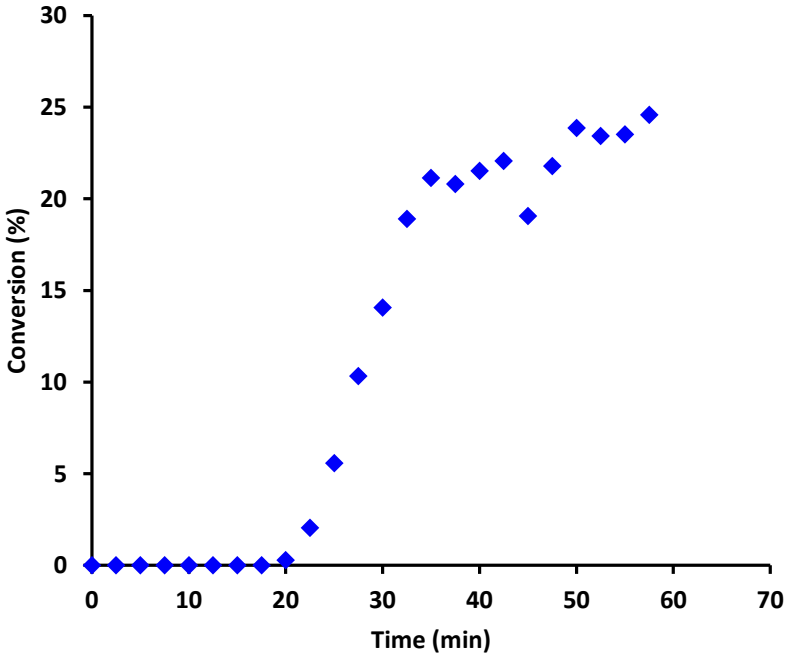
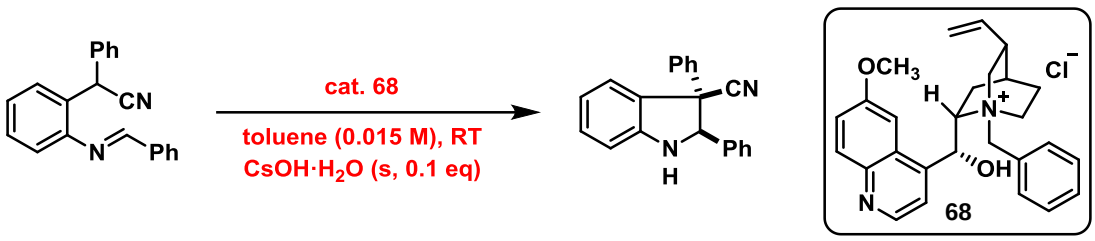


Figure 17: Kinetic studies on background cyclization

3.2.2.2.3 Chiral catalyst loading

The dependence of the reaction rate on chiral catalyst concentration was investigated. The cyclization reaction was performed with different loadings of the chiral catalyst (Scheme **55**) and a reaction conversion vs. time curve was plotted.



Scheme 55: Chiral catalyst loading

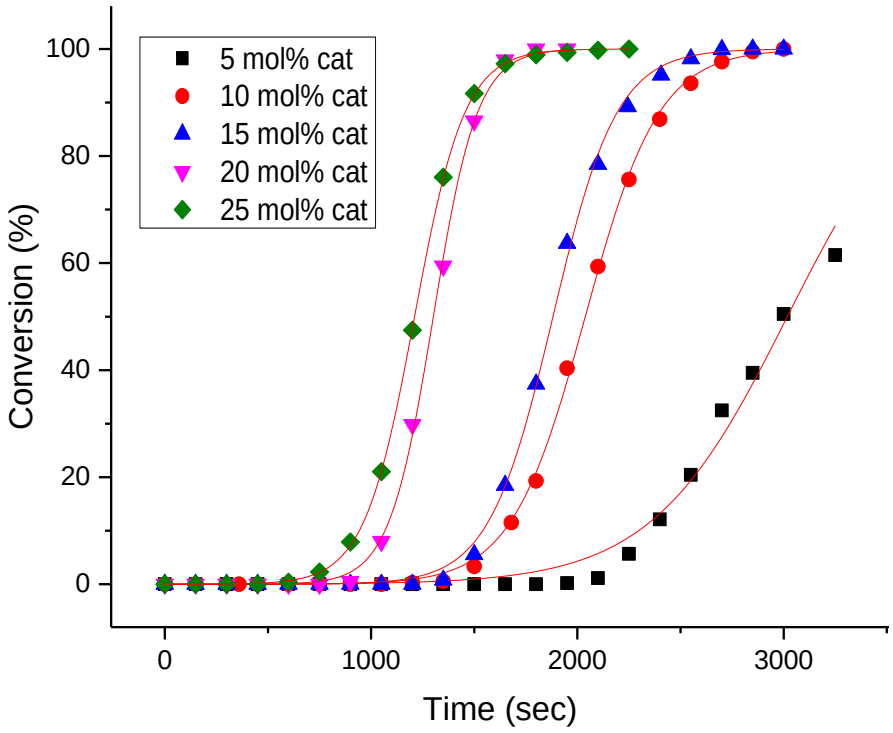


Figure 18: Rate plot- Chiral catalyst loading

Curve fitting of this plot was carried out using OriginPro 8.5 (Figure **18**) which demonstrated that the rate of reaction increases with increase in loading of the chiral catalyst.

The rate of these reactions was measured by calculating the slope of the central linear regime of the curves. A bilogarithmic plot of rate (k) vs. concentration of chiral catalyst ([Cat]) resulted in a straight line with a slope (m) of 0.65 and a regression value (R) of 0.96 indicating a good fit (Figure **19**). This indicated that our cyclization reaction is fractional order with respect to the chiral catalyst and involves complicated reaction kinetics, indicating an interfacial mechanism being operational. This observation is consistent with the mechanism in which the catalyst exists partially as a dimer and has to dissociate to form the active monomer in order to catalyse the cyclization reaction (refer Section **3.1.3.2**).[55]

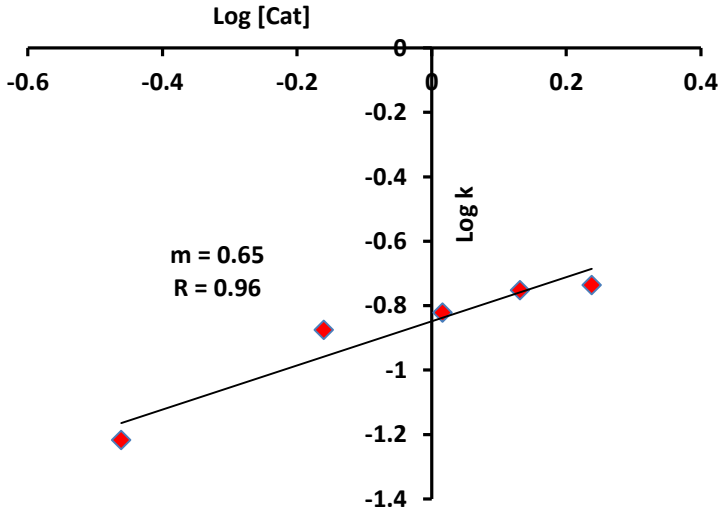


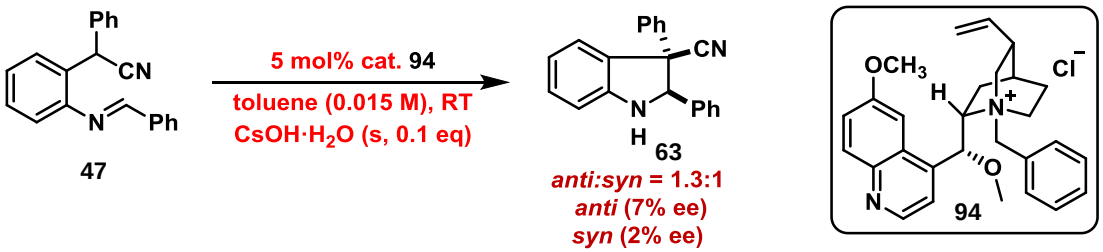
Figure 19: Log [Cat] vs. Log k plot

3.2.2.2.4 Cyclization with –OH protected catalyst

It has been shown that our cyclization reaction is of order 0.65 with respect to the chiral catalyst **68**. As discussed above this observation is consistent with the mechanism proposed by Dolling *et al.* that such catalysts exists partially as a dimer and has to dissociate to form the active monomer in order to catalyse the cyclization reaction.[55] These authors suggested that the dimeric species is significantly more soluble in the organic phase than the monomeric derivative of the catalyst.

To establish whether this process was responsible for the sigmoidal shape of the kinetic profile, we examined the reaction in the presence of C-9 O-alkylated derivative[61] **94** to see whether the presence of a free OH group on the catalyst was a prerequisite (Scheme **56**).

Catalyst **94** affected significantly slower cyclization reaction rates than catalyst **68** (Figure **20**). However it possessed about the same length of induction period which suggests that the process of dimerization of catalyst **68** is not responsible for the presence of the induction period.



Scheme 56: Cyclization with –OH protected catalyst **94**

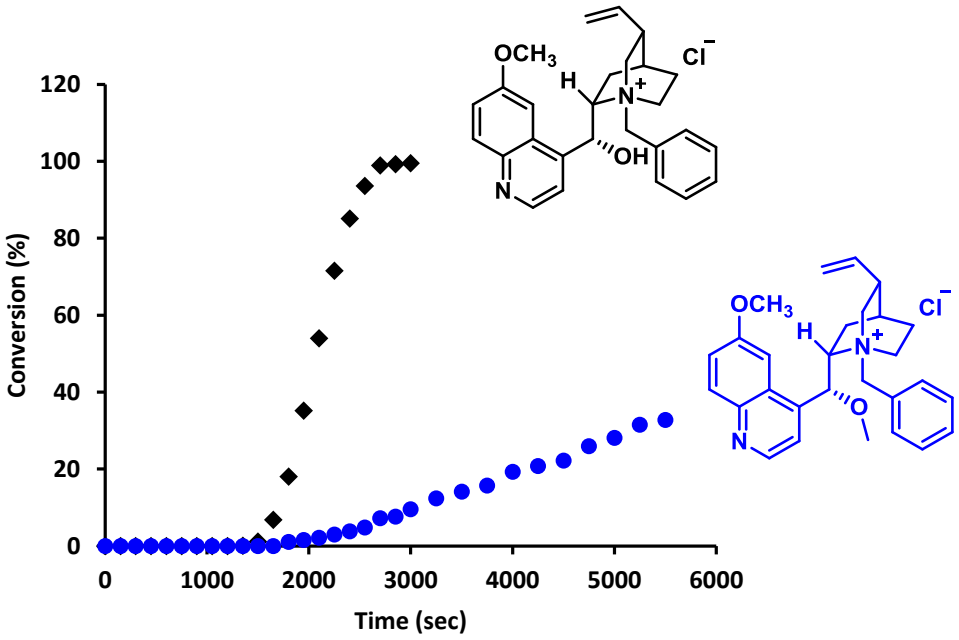
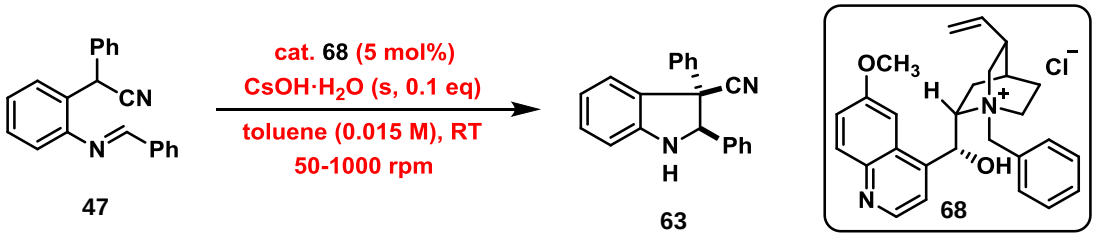


Figure 20: Kinetic profile- Cyclization with –OH protected catalyst

3.2.2.2.5 Stirring rate experiments

The effect of stirring speed on the rate of our cyclization reaction was investigated. The asymmetric cyclization reaction was carried out at different stirring speeds (50, 150, 250, 500, 1000 rpm), the reaction kinetics were monitored and reaction conversion was examined as a function of time (Scheme **57**, Figure **21**).



Scheme 57: Effect of stirring speed

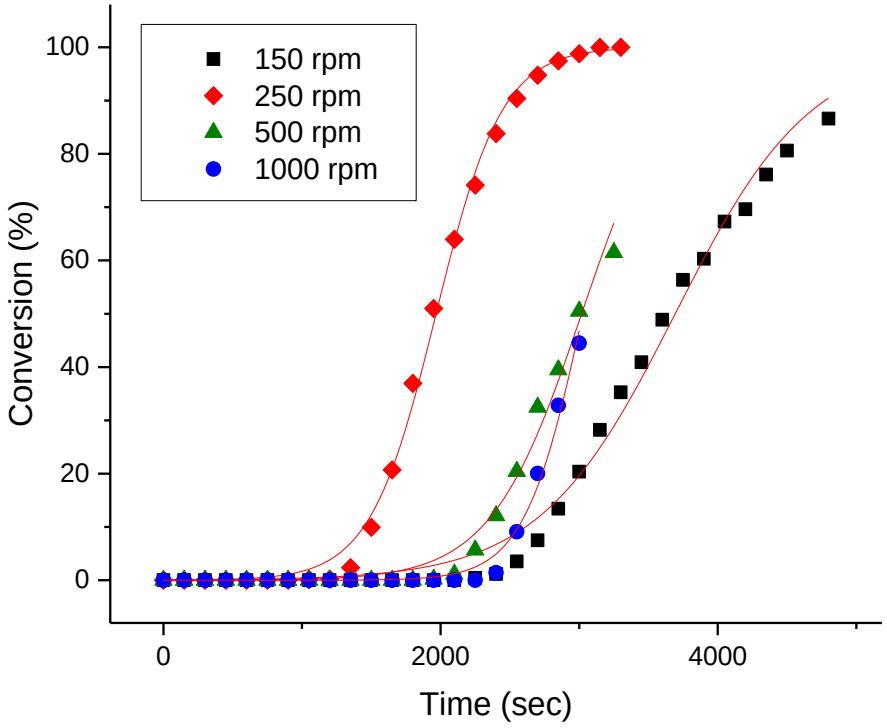


Figure 21: Stirring speed experiment (150-1000 rpm)

We observed that there is only a slight variation in the rate and induction period when the stirring speed is varied from 250-1000 rpm. On the other hand, if the stirring speed is further decreased to 50 rpm the reaction rate decreases considerably along with induction period becoming longer (Figure **22**).

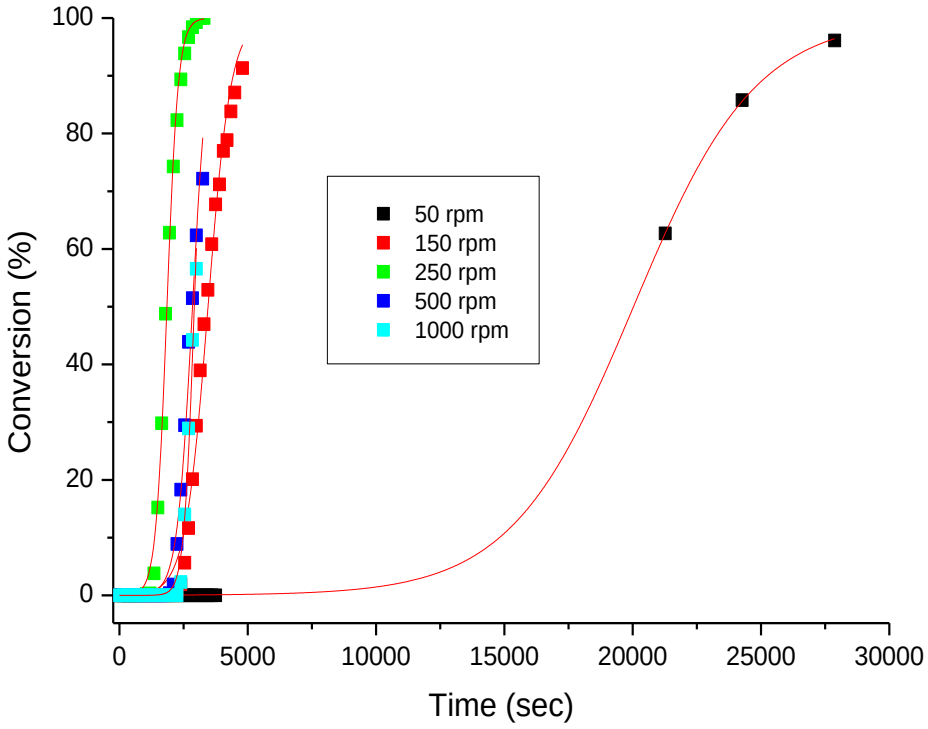


Figure 22: Stirring speed experiment (with 50 rpm)

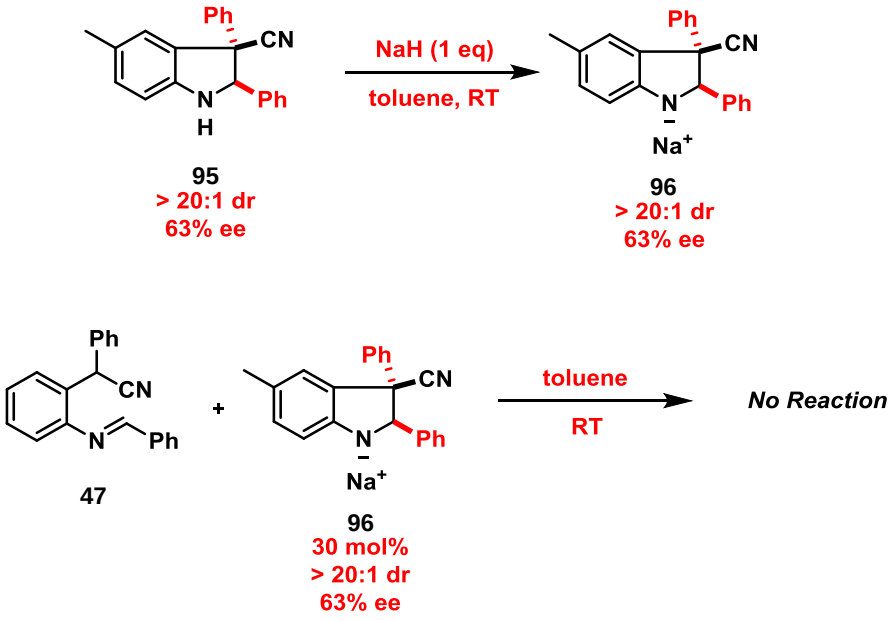
Based on the above results, it was proposed that the cyclization reaction is dependent on the stirring speed up to a threshold (~200 rpm), above which the rate becomes independent of the stirring speed.

3.2.2.2.6 Autocatalysis investigation

A sigmoidal shaped reaction profile with an induction period is superficially suggestive of autocatalysis. We postulated that an autocatalytic reaction might be responsible for this, where the product of cyclization - an indolinyl anion (pK_{aH} ~ 25) – could be catalysing the reaction by deprotonating the substrate imine **47** (pK_a ~ 18) in the organic phase.

3.2.2.2.6.1 Autocatalysis investigation with indolinyl anion 96

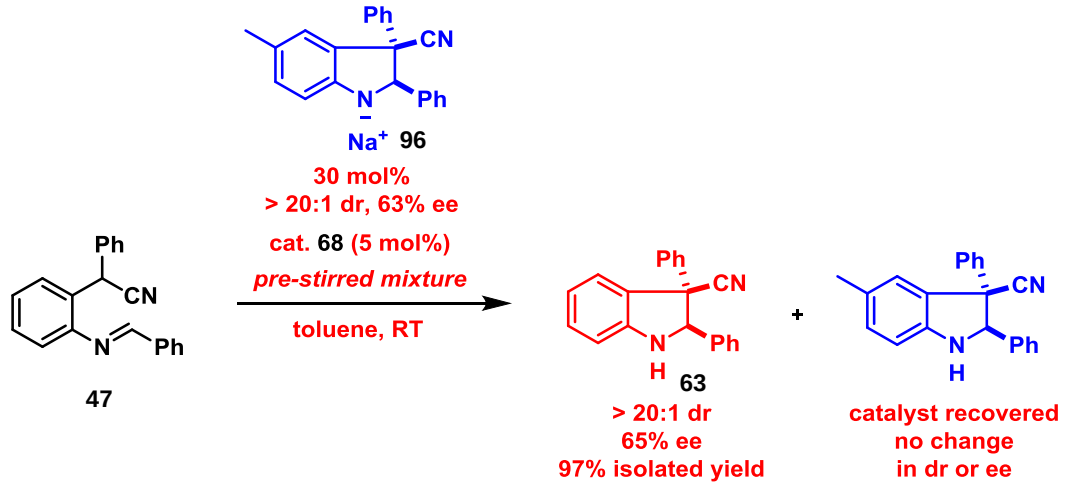
To test this hypothesis we designed an autocatalysis investigation experiment where we subjected the substrate imine **47** to catalytic amounts (30 mol%) of the enantioenriched (63% ee) *anti*- isomer of 4-methyl indolinyl sodium salt **96** in toluene at room temperature (Scheme **58**).



Scheme 58: Autocatalysis investigation

Under these conditions we observed essentially no cyclization over a two hour time scale.

However, when we subjected a stirring solution of imine **47** in toluene to a pre-stirred mixture of 4-methyl indolinyl sodium salt **96** (racemic) and chiral phase-transfer catalyst **68** the cyclization proceeded, with an immediate change in the colour of the reaction mixture (Scheme **59**). Moreover, the reaction was so rapid that it went to completion in just 5 minutes giving product indoline **63** in 97% isolated yield (65% ee, > 20:1 dr).



Scheme 59: Autocatalysis investigation (Pre-stirring)

We were able to follow the conversion of the imine **47** to indoline **63** by sampling every 30 seconds during the first 10 minutes of the reaction. A plot of percentage conversion versus time resulted in a similar reaction profile with effectively no induction period (Figure **23**).

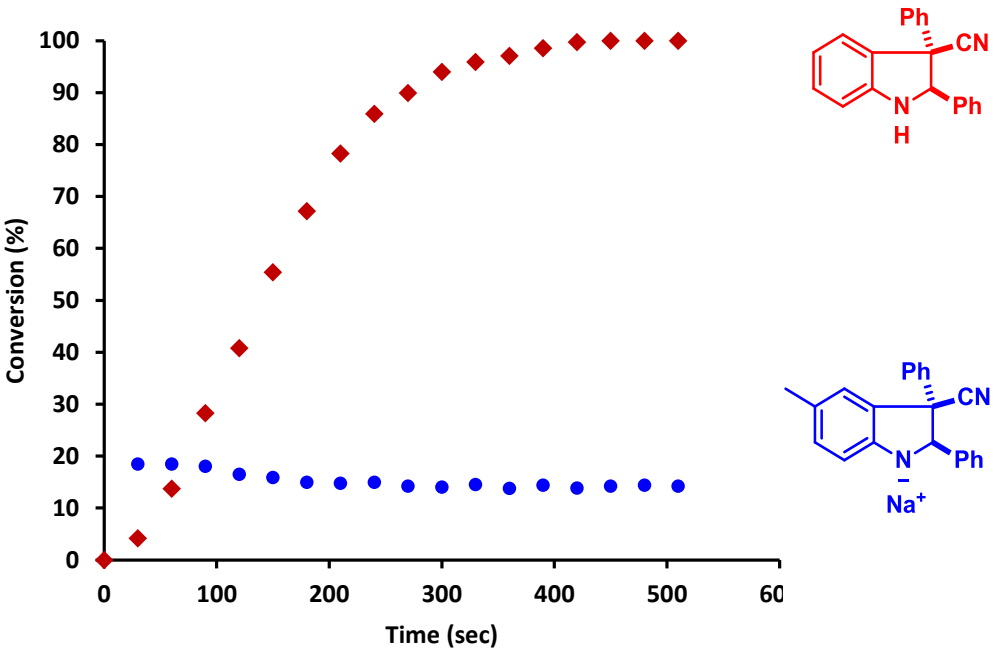


Figure 23: Kinetic rate plot- Autocatalysis investigation (Pre-stirring)

This experiment suggested that the indolinyl anion paired with the phase-transfer ammonium catalyst counterion is the autocatalytic species and is responsible for catalysing the cyclization in the organic phase (Figure **24**).

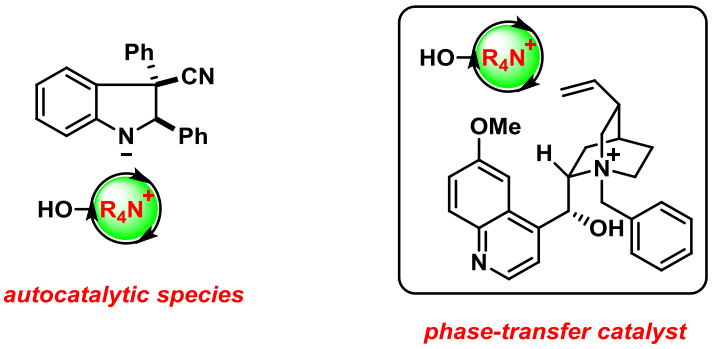
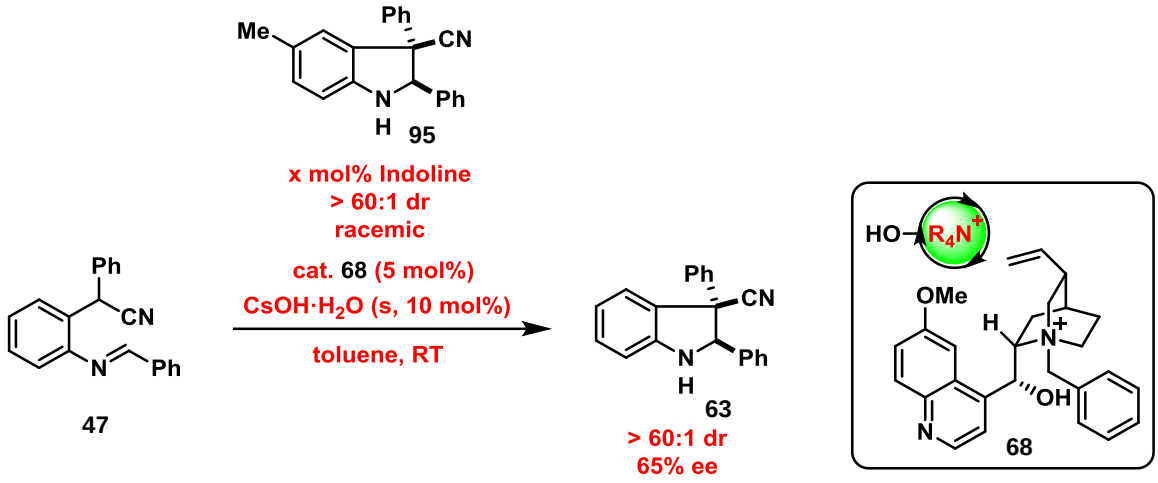


Figure 24: Autocatalytic species

3.2.2.2.6.2 Autocatalysis investigation with product indoline 95

We then attempted to determine whether the catalytically active ion pair described above could be generated from the product *in situ*. We subjected the substrate imine **47** to $CsOH \cdot H_2O$ in the presence of racemic indoline **95** (Figure **25**).



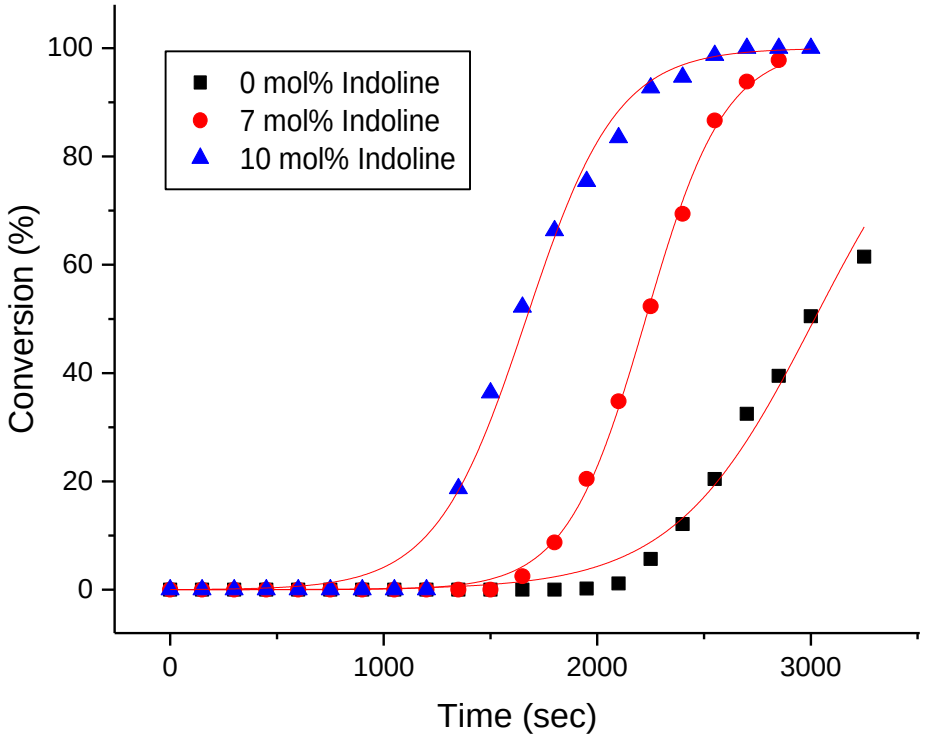


Figure 25: Autocatalysis investigation

It can be observed from the above kinetic rate plot that when the substrate imine **47** is subjected to catalytic amounts of product indoline **95**, the cyclization reaction rate slightly increases and the induction period gets shorter. This confirms that the product indoline **95** can be deprotonated in the presence of base ($CsOH \cdot H_2O$) to give rise to the indolinyl anion **96**, which then forms an ion-pair with the phase-transfer ammonium catalyst cation to act as the autocatalytic species which catalyses the cyclization reaction in the organic phase.

3.2.2.2.6.3 Influence of autocatalytic species' chirality on enantioselectivity of cyclization

It was observed during the autocatalysis experiments that the product indoline **63** was generated with the same ee (65%) irrespective of whether the autocatalytic species was racemic or enantiomerically-enriched.

This suggests that the configuration and enantiopurity of the indoline 'catalyst' component does not have any influence on the enantioselectivity of the overall process and that it is only facilitating the deprotonation of the substrate imine **47**, with asymmetric induction being provided by the chiral counter-cation.

3.2.3 Proposed Mechanism

On the basis of the above results obtained with the kinetic investigations performed, the following mechanism is proposed for our phase-transfer catalysed cyclization process (Figure **26**).

We believe that there are three different phases present in the reaction system - solid, organic and the interface between the two. The base ($CsOH \cdot H_2O$), an inorganic solid, is distributed between the solid phase and the interface. Substrate imine **47** is distributed between the organic phase and interface. Substrate **47** is deprotonated at the phase boundary by the solid cesium hydroxide base to form a cesium cyanocarbanion **97.** This is relatively unreactive towards cyclization in the interfacial region until it exchanges with the quaternary ammonium phase-transfer catalyst **68** cation to give rise to the ammonium-substrate ion pair **98**. The quaternary ammonium phase-transfer catalyst then transfers the substrate anion to the organic phase in the form of ammonium-substrate ion pair for the cyclization to occur. The substrate anion **98** undergoes cyclization in the organic phase controlled by the chiral ammonium cation to generate the autocatalytic species **99** - an enantioenriched indolinyl anion paired with chiral ammonium cation. The product·ammonium complex can then deprotonate another molecule of substrate imine **47**, but this time in the organic phase, and the cycle continues.

We suggest that the catalyst resting state is likely to be dimeric by virtue of our observation that the reaction is fractional order in catalyst, consistent with the proposal of Dolling.[55] Consequently, the reaction can be described as an interfacial phase transfer reaction, but this may not be the most accurate description of the overall process. Once initiated, we believe that the reaction proceeds entirely in the homogenous organic phase, with the autocatalytic component **99** being responsible for turnover. As such, the reaction may be better described

as a phase transfer initiated counterion directed cyclization than a phase transfer catalysed process.

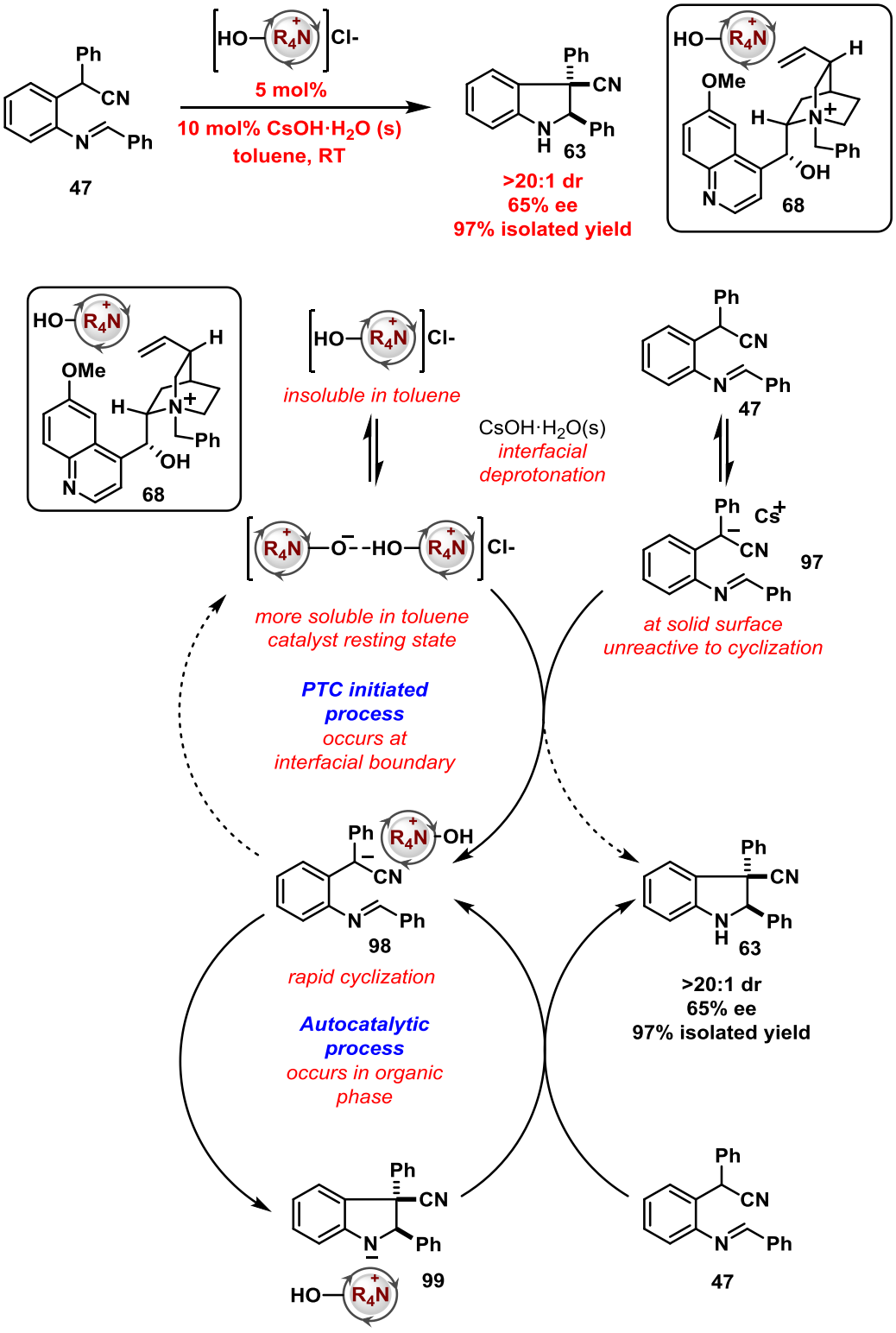


Figure 26: Proposed Catalytic Cycle*

* Dotted lines indicate transformations that are believed to be slow under the reaction conditions.

3.2.3.1 Catalyst-dependent diastereoselectivity

It has been shown before (section 3.2.1.2) that the presence of chiral phase-transfer catalyst **68** allows the formation of the kinetic, *anti*-indoline **63** but does not facilitate the cycloreversion reaction needed for the formation of the thermodynamic *syn*-isomer. However, the use of achiral phase-transfer catalyst TBAHS facilitates the ring opening and ring closing of the kinetic *anti*-indoline **63** to the thermodynamically more stable *syn*-isomer until equilibrium is reached.

This autocatalytic mechanism also allows us to rationalize the difference in the diastereoselectivity observed with different phase-transfer catalysts (tetrabutyl ammonium and quinine derived salt). Based on our proposed autocatalytic mechanism (figure **26**) we postulated that the observed difference in diastereoselectivity arises by a process that occurs entirely in the organic phase and hence ion transport and interfacial processes can be neglected. This assumed that the ammonium salts are concentrated in the organic phase and hence solubility and lipophilicity of the catalyst are less important. Consequently, we considered the intrinsic reactivity of the indoline product•ammonium complexes (Figure **27**).

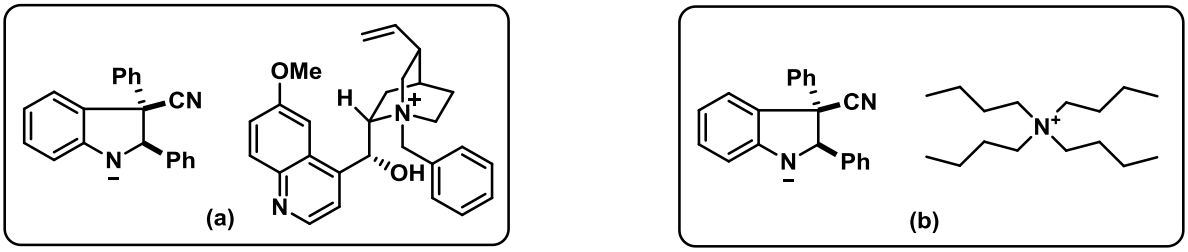
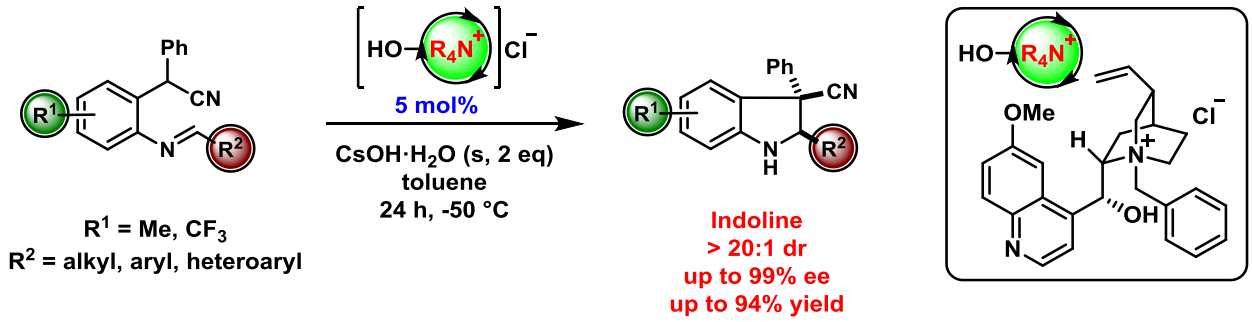


Figure 27: Differences in catalyst reactivity and diastereoselectivity in cyclization.

The reactivity of phase transfer catalysts has been elegantly investigated by Denmark[62,63] who concluded that catalyst cross sectional area and charge accessibility were key factors. This is consistent with our observations; we propose that the charge on the quininium ion (a) is more accessible than that on the quaternary ammonium ion (b) leading to tighter binding of the indolinyl anion. Consequently, the less tightly paired indolinyl anion is more reactive, leading to retrocyclization-cyclization and a change in diastereoselectivity.

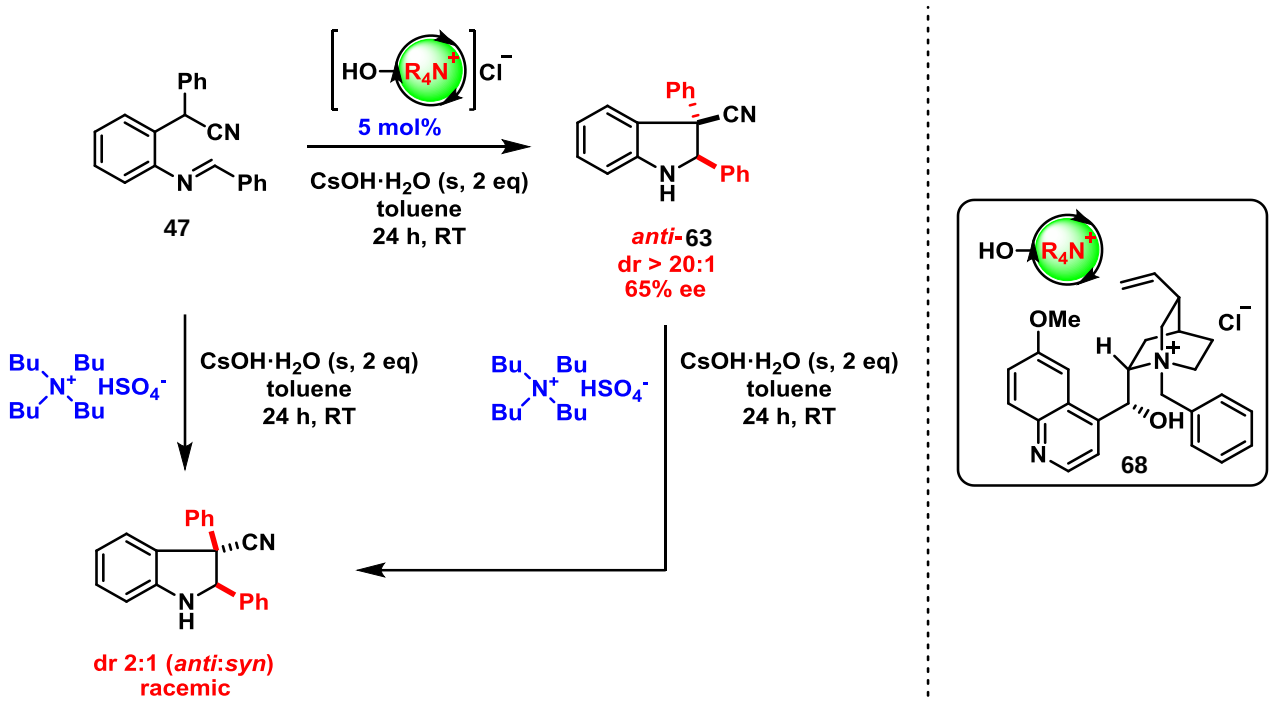
4. Conclusions and future work

By extending the applications of phase-transfer catalysis we have developed a highly diastereo- and enantioselective synthesis of functionalized indolines bearing two contiguous stereocentres, one of which is quaternary and all carbon, in a single synthetic step. The reaction proceeds with complete diastereoselectivity and with high levels of enantioselectivity (up to 99% ee), (Scheme **60**).



Scheme 60: Diastereo- and enantioselective synthesis of indolines

A base-catalysed interconversion of diastereoisomeric indolines (*anti*-**63**, *syn*-**63**) *via* a cycloreversion-cyclization process was observed in the presence of tetrabutyl ammonium phase-transfer catalyst whereas no such interconversion was observed with the quinine derived catalyst **68** (Scheme **61**). It was suggested that the charge on the quinine-derived catalyst **68** is more accessible than that on the tetrabutyl ammonium cation leading to tighter binding of the indolinyl anion. Consequently, the less tightly paired indolinyl anion (with tetrabutyl ammonium ion) is more reactive, leading to retrocyclization-cyclization and a change in diastereoselectivity.



Scheme 61: Catalyst-Dependent Diastereoselectivity

Despite the development of phase-transfer catalysis as a primary synthetic tool in organic synthesis, the mechanistic understanding of these reactions still remains a challenge, due mainly to the difficulty of studying the complex multi-phase systems. Therefore, a further aim of this project was to understand the reaction mechanism of our phase-transfer catalysed transformation. Investigations into the mechanism of our phase-transfer catalysed reaction have been carried out by studying the reaction kinetics. These have shown that the reaction follows a sigmoidal curve with an induction period present. A detailed kinetic investigation was carried out which demonstrated that an autocatalytic mechanism is operational. The ion-pair of product indoline with quaternary ammonium catalyst has been identified as the autocatalytic species (Figure **28**).

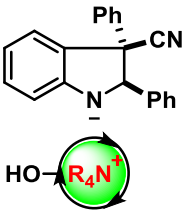


Figure 28: Autocatalytic species

Future work would be to expand the scope of our asymmetric cyclization reaction by allowing a variation of electron-withdrawing groups at the benzylic position of substrate imine.

We will be interested in performing further kinetic isotope labelling experiments in order to determine the rate determining step of our phase-transfer catalyzed cyclization reaction. It will also be interesting to see if the overall phase-transfer process for the synthesis of indolines could be made faster at lower temperatures without compromising with the stereoselectivity, by utilizing the information that the reaction is autocatalytic.

There are two feasible mechanistic pathways for our phase-transfer cyclization reaction: an intramolecular 5-*endo-trig* Mannich process which is kinetically disfavoured by Baldwin's rules[64,65], or by the proposed suprafacial 6π electrocyclic process (Figure **29)**.

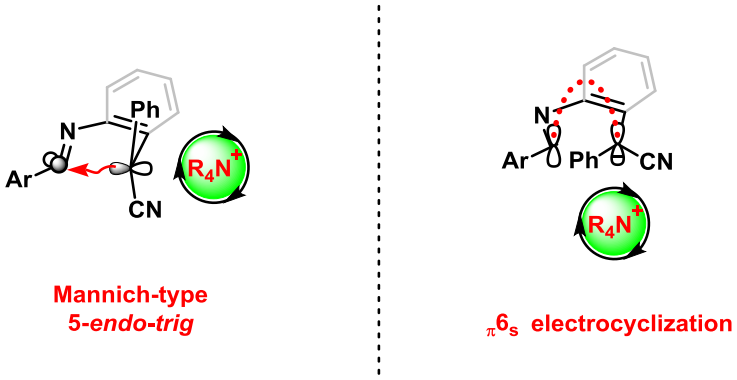


Figure 29: Possible modes of cyclization

Density functional theory calculations are being carried out in collaboration with Professor Dean Tantillo at UC Davis to probe these two mechanistic pathways, which will hopefully lead to an indication whether this process is pericyclic or not.

5. Experimental

5.1 General Information.

5.1.1 Solvents and Reagents

Tetrahydrofuran, dichloromethane, diethyl ether and toluene were purified by pressurized filtration through activated silica columns employing the method of Grubbs *et. al.*[66] Other solvents were used as supplied (analytical or HPLC grade) without prior purification. Petroleum ether refers to the fraction of petroleum ether boiling in the range 40-60 °C. All other reagents and solvents were used as supplied, without prior purification.

5.1.2 Chromatography

Flash column chromatography was carried out using VWR silica gel (40-63 μm particle size). Analytical thin layer chromatography was carried out on Merck Kieselgel 60 F_{254} 0.25 mm precoated aluminium plates. Visualization was carried out by viewing under ultra-violet radiation (254 nm) and appropriate heating with ammonium molybdate. The ammonium molybdate solution was made by dissolving ammonium molybdate (5 g) and ceric sulphate (0.2 g) in 5% aqueous sulphuric acid (100 mL).

5.1.3 NMR Spectroscopy

NMR spectra were recorded on a Bruker DPX 400 (^{1}H: 400 MHz and ^{13}C: 101 MHz), a Bruker Avance Cryo 500 (^{1}H: 500 MHz and ^{13}C: 126 MHz) or a Bruker DPX 200 (^{1}H: 200 MHz) spectrometer. Chemical shifts are quoted in ppm and are referenced to the residual non-deuterated solvent peak, and are reported based on appearance rather than interpretation. ^{1}H spectra are reported as follows: δ_H (*spectrometer frequency*, *solvent*): *ppm* (*no. of protons*, *multiplicity*, *J-coupling constant*(*s*), *assignment*). ^{13}C spectra are reported as follows

δ_C (*spectrometer frequency, solvent*)*: ppm* (*assignment*). Spectral assignment was aided by the results of DEPT, COSY, HMBC and HSQC experiments where appropriate.

5.1.4 IR Spectroscopy

IR spectra were recorded on a Bruker Tensor 27 FTIR spectrometer equipped with an attenuated total reflectance attachment with internal calibration. Absorption maxima (ν_{max}) are quoted in wavenumbers (cm^{-1}).

5.1.5 Mass Spectrometry

Accurate masses were recorded on Bruker MicroTOF and Micromass GCT spectrometers under conditions of ESI and field ionization (FI) respectively. Values are reported as a ratio of mass to charge in Daltons.

5.1.6 Polarimetry

Optical rotations were recorded on a Perkin-Elmer 341 polarimeter with a path length of 1dm.

5.1.7 Melting Points

All melting points were measured on a Reichert melting point stage apparatus and are uncorrected. Solvents are reported in parentheses where solids were purified by recrystallization.

5.1.8 HPLC

Analytical chiral stationary phase HPLC was performed on a Dionex Ultimate 3000 HPLC system comprising a Dionex LPG-3400A pump, WPS-3000SL autosampler, TCC-3000SD column compartment, DAD-3000 diode array detector and the appropriate Daicel Chiralpak

column (dimensions: 0.46 cm × 25 cm) and the corresponding guard column (0.4 cm × 1 cm).

5.1.9 Naming and Numbering of Compounds

Where given, systematic compound names are those generated by ChemBioDraw Ultra 12.0 following IUPAC conventions. The numbering of atoms for spectral assignment purposes is arbitrary and not necessarily consistent with the IUPAC name.

5.2 General Procedures.

General Procedure 1. Synthesis of nitro-compounds via phase transfer S_NAr reaction.

A mixture of phenylacetonitrile in tetrabutylammonium bisulfate, toluene and 50% NaOH was deoxygenated *via* a vacuum-argon cycle repeated twice. To the mixture was added a deoxygenated solution of appropriate 2-fluoronitrobenzene compound in toluene and the reaction mixture was stirred at room temperature for 2 h. The mixture was diluted with dil. HCl and extracted with diethyl ether. The organic solution was dried over magnesium sulfate, filtered, concentrated *in vacuo* and the residue purified by flash column chromatography.

General Procedure 2. Synthesis of aniline derivatives via reduction of nitro-compounds.

Zn powder (10.0 eq.) and ammonium chloride (15.0 eq.) were added to a solution of nitro-compound (1.0 eq) in a 5:1 mixture of acetone:water at RT. After 2 h the reaction mixture was filtered through a pad of Celite® and concentrated *in vacuo.* The residue was extracted with diethyl ether, washed with brine, dried over magnesium sulfate and purified by flash column chromatography.

General Procedure 3. Asymmetric 'one pot' cyclization.

The appropriate aniline (1.0 eq.), aldehyde (1.1 eq.) and magnesium sulphate (5.0 eq.) were stirred for 24 h at RT in toluene (0.2 M concentration of aniline). The resulting mixture was filtered and concentrated *in vacuo*. The imine was redissolved in toluene (0.08 M concentration of imine), *N*-benzylquininium chloride (0.05 eq.) was added and the mixture was cooled to -50 °C for 30 mins before adding cesium hydroxide monohydrate (2.0 eq.). The reaction was stirred at -50 °C for 48 h. The reaction was quenched with saturated aqueous ammonium chloride (40.0 mL/mmol imine) and extracted with dichloromethane

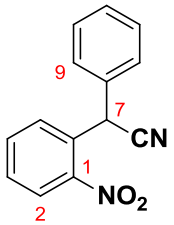
(3 × 40.0 mL/mmol imine). The organic layers were combined, dried over sodium sulfate, filtered and concentrated *in vacuo* and purified by flash column chromatography.

General Procedure 4. Racemic 'one pot' cyclization.

The appropriate aniline (1.0 eq.), aldehyde (1.1 eq.) and magnesium sulphate (5.0 eq.) were stirred for 24 h at RT in toluene (0.2 M concentration of aniline). The resulting mixture was filtered and concentrated *in vacuo*. The imine was redissolved in toluene (0.1 M concentration of imine) and the mixture was cooled to 0 °C before adding potassium *tert*-butoxide (1.0 eq.). The reaction was stirred at 0 °C for 3 h. The reaction was quenched with saturated aqueous ammonium chloride (40.0 mL/mmol imine) and extracted with dichloromethane (3 × 40.0 mL/mmol imine). The organic layers were combined, dried over sodium sulfate, filtered and concentrated *in vacuo* and purified by preparative TLC.

5.3 Experimental procedures and data.

(±)-2-(2-Nitrophenyl)-2-phenylacetonitrile



32a

Prepared according to *general procedure 1*. Phenylacetonitrile (5.85 g, 50.0 mmol), 2-fluoronitrobenzene (7.05 g, 50.0 mmol), tetrabutylammonium bisulfate (16.97 g, 50.0 mmol), 50% aq. NaOH (20.0 mL), toluene (150 mL). Purification *via* flash column chromatography on silica gel (PE/Et_2O = 15:1) gave **32a** as an orange coloured crystalline solid (9.05 g, 76%).

mp: 38 - 40 °C

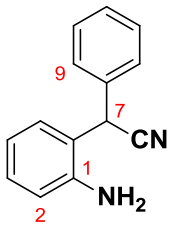
ν_{max} (neat): 2362, 2246 (C≡N), 1524 (NO_2), 1345(NO_2).

δ_H (400 MHz, $CDCl_3$): 8.07 (1H, dd, *J* 8.1, 1.3, H2), 7.77-7.66 (2H, m, H4, H5), 7.56 (1H, app. tt, *J* 8.3, 1.3, H3), 7.42-7.29 (5H, m, Ar-H), 6.18 (1H, s, H7).

δ_C (101 MHz, $CDCl_3$): 147.6 (C1), 134.2 (C4), 134.1 (C8), 130.9 (C5), 130.5 (C6), 129.7 (C3), 129.3 (C10), 128.7 (C11), 127.9 (C9), 125.8 (C2), 118.6 (CN), 39.2 (C7).

HRMS (ES+): found 261.0638; $C_{14}H_{10}N_2O_2Na$ $[M+Na]^+$ requires 261.0634.

(±)-2-(2-Aminophenyl)-2-phenylacetonitrile



33a

Prepared according to *general procedure 2*. Zinc powder (4.73 g, 72.7 mmol), NH_4Cl (5.78 g, 109.1 mmol), **32a** (1.73 g, 7.27 mmol), 5:1 mixture of acetone/H_2O (145.0 mL). Purification *via* flash column chromatography on silica gel (PE/Et_2O = 3:1) gave **33a** as an orange coloured crystalline solid (1.19 g, 79%).

mp: 72 - 74 °C

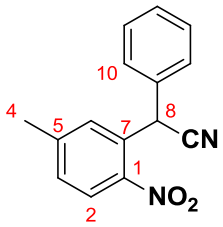
ν_{max} (neat): 3462 (NH_2), 3377, 2247 (C≡N), 1631, 1304.

δ_H (400 MHz, $CDCl_3$): 7.47-7.28 (6H, m, H9, H10, H11, H5), 7.21 (1H, app. td, *J* 7.7, 1.8, H3), 6.89 (1H, app. tt, *J* 7.5, 0.7, H4), 6.74 (1H, d, *J* 7.8, H2), 5.19 (1H, s, H7), 3.54 (2H, br. s, NH_2).

δ_C (101 MHz, $CDCl_3$): 143.8 (C1), 134.0 (C8), 129.6 (C3), 129.5 (C5), 129.4 (C10), 128.5 (C11), 127.7 (C9), 120.0 (CN), 119.6 (C4), 118.9 (C6), 117.5 (C2), 39.0 (C7).

HRMS (ES+): found 231.0891; $C_{14}H_{12}N_2Na$ $[M+Na]^+$ requires 231.0893.

(±)-2-(5-Methyl-2-nitrophenyl)-2-phenylacetonitrile



32b

Prepared according to *general procedure 1*. Phenylacetonitrile (1.11 g, 10.0 mmol), 3-Fluoro-4-nitrotoluene (1.55 g, 10.0 mmol), tetrabutylammonium bisulfate (3.39 g, 10.0 mmol), 50% aq. NaOH (4.0 mL), toluene (30.0 mL). The product was recrystallized from diethyl ether to afford an orange crystalline solid **32b** (2.16 g, 86% yield).

mp: 77 - 80 °C (Et_2O)

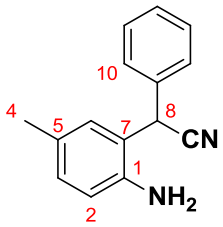
ν_{max} (neat): 2925, 2242 (C≡N), 1521 (NO_2), 1344 (NO_2), 845, 698.

δ_H (400 MHz, $CDCl_3$): 8.01 (1H, d, *J* 8.3, H2), 7.54 (1H, s, H6), 7.35 (6H, m, H10, H11, H12, H3), 6.24 (1H, s, H8), 2.48 (3H, s, H4).

δ_C (101 MHz, $CDCl_3$): 145.8 (C1), 145.3 (C5), 134.2 (C9), 131.4 (C6), 130.5 (C7), 130.2 (C3), 129.3 (C11), 128.6 (C12), 127.8 (C10), 126.0 (C2), 118.9 (CN), 38.3 (C8), 21.6 (C4).

HRMS (ES+): found 275.0791; $C_{15}H_{12}N_2NaO_2$ $[M+Na]^+$ requires 275.0791.

(±)-2-(2-Amino-5-methylphenyl)-2-phenylacetonitrile



33b

Prepared according to *general procedure 2*. Zinc powder (1.28 g, 19.8 mmol), NH_4Cl (1.57 g, 29.7 mmol), **32b** (0.5 g, 1.98 mmol), 5:1 mixture of acetone/H_2O (40 mL). Purification *via* flash column chromatography on silica gel (PE/Et_2O = 3:1) gave **33b** as an orange coloured crystalline solid (0.32 g, 73%).

mp: 97 - 100 °C

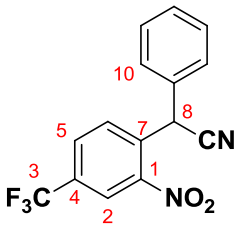
ν_{max} (neat): 3372 (NH_2), 2917, 2360, 2242 (C≡N), 1601, 1494, 697.

δ_H (400 MHz, $CDCl_3$): 7.45-7.31 (5H, m, H10, H11, H12), 7.17 (1H, s, H6), 7.02 (1H, d, *J* 7.8, H3), 6.66 (1H, d, *J* 8.1, H2), 5.19 (1H, s, H8), 3.4 (2H, br. s, NH_2), 2.3 (3H, s, H4).

δ_C (101 MHz, $CDCl_3$): 141.1 (C1), 134.2 (C9), 130.2 (C3), 129.8 (C6), 129.4 (C11), 129.2 (C5), 128.5 (C12), 127.7 (C10), 120.4 (CN), 119.1 (C7), 117.9 (C2), 39.0 (C8), 21.0 (C4).

HRMS (ES+): found 245.1054; $C_{15}H_{14}N_2Na$ $[M+Na]^+$ requires 245.1049.

(±)-2-(2-Nitro-4-(trifluoromethyl)phenyl)-2-phenylacetonitrile



32c

Prepared according to *general procedure 1*. Phenylacetonitrile (1.75 g, 15.0 mmol), 4-fluoro-3-nitrobenzotrifluoride (3.13 g, 15.0 mmol), tetrabutylammonium bisulfate (5.09 g, 15.0 mmol), 50% aq. NaOH (6.0 mL), toluene (45.0 mL). Purification *via* flash column chromatography on silica gel (PE/Et_2O = 8:1) gave **32c** as a yellow oil (3.53 g, 77%).

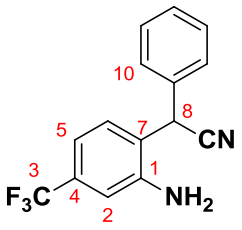
ν_{max} (neat): 2250 (C≡N), 1540 (NO_2), 1324 (NO_2), 1133, 1089, 666.

δ_H (400 MHz, $CDCl_3$): 8.33 (1H, s, H2), 8.02-7.88 (2H, m, H5, H6), 7.47-7.28 (5H, m, H10, H11, H12), 6.21 (1H, s, H8).

δ_C (101 MHz, $CDCl_3$): 147.7 (C1), 134.4 (Ar C), 133.2 (Ar C), 132.0 (C6), 130.6 (q, *J* 3.7, C5), 129.6 (C11), 129.1 (C12), 127.9 (C10), 122.4 (q, *J* 272, C3), 123.1 (q, *J* 4, C2), 121.0 (CN), 117.9 (Ar C), 38.3 (C8).

HRMS (ES+): found 329.0499; $C_{15}H_9F_3N_2O_2Na$ $[M+Na]^+$ requires 329.0508.

(±)-2-(2-Amino-4-(trifluoromethyl)phenyl)-2-phenylacetonitrile



33c

Prepared according to *general procedure 2*. Zinc powder (5.44 g, 83.7 mmol), NH_4Cl (6.64 g, 125.4 mmol), **32c** (2.56 g, 8.3 mmol), 5:1 mixture of acetone/H_2O (167.0 mL). Purification *via* flash column chromatography on silica gel (PE/Et_2O = 6:1) gave **33c** as an orange coloured crystalline solid (1.34 g, 60%).

mp: 48 - 50 °C

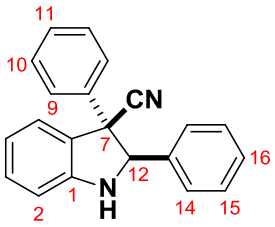
ν_{max} (neat): 3379 (NH_2), 2245 (C≡N), 1633, 1437, 1336 (CF), 1119, 697.

δ_H (400 MHz, $CDCl_3$): 7.48-7.37 (6H, m, H10, H11, H12, H6), 7.12 (1H, d, *J* 7.8, H5), 6.97 (1H, s, H2), 5.21 (1H, s, H8), 3.76 (2H, br. s, NH_2).

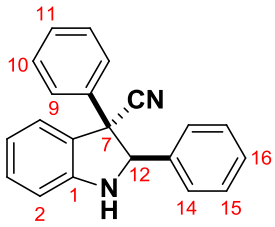
δ_C (101 MHz, $CDCl_3$): 144.3 (C1), 132.9 (C9), 132.1 (C4), 130.0 (C6), 129.6 (C11), 129.0 (C12), 127.6 (C10), 123.8 (q, *J* 272, C3), 123.0 (C7), 118.4 (CN), 115.8 (q, *J* 3.7, C5), 113.9 (q, *J* 4, C2), 38.9 (C8).

HRMS (ES+): found 299.0759; $C_{15}H_{11}F_3N_2Na$ $[M+Na]^+$ requires 299.0767.

2,3-Diphenylindoline-3-carbonitrile



***anti*-64**



***syn*-64**

Asymmetric: Prepared according to *general procedure 3*. Aniline **33a** (41 mg, 0.20 mmol), aldehyde **34** (23 mg, 0.22 mmol), *N*-benzylquininium chloride (5 mg, 0.01 mmol), $CsOH \cdot H_2O$ (67 mg, 0.40 mmol), toluene (2.6 mL), T = -50 °C. Reaction time: 48 h. Crude ^1H NMR shows >60:1 d.r. Purification *via* flash column chromatography on silica gel (PE/Et_2O = 30:1) gave indoline ***anti*-64** as a colourless crystalline solid (44 mg, 75%, single diastereoisomer, 89% e.e.).

Racemic: Potassium *tert*-butoxide (16 mg, 0.14 mmol) added to a stirring solution of aniline **19a** (30 mg, 0.14 mmol), aldehyde **34** (16 mg, 0.15 mmol) and THF (1.4 mL) at 0 °C. The reaction was warmed to RT and left to stir. The reaction was quenched with saturated aqueous ammonium chloride (5 mL) and extracted with dichloromethane (3 × 5 mL). The organic layers were combined, dried (Na_2SO_4), filtered and concentrated *in vacuo*. Reaction time: 2 h. Purification *via* flash column chromatography on silica gel (PE/Et_2O = 30:1) gave indoline **64** as a colourless crystalline solid (35 mg, 83% combined yield of diastereomers, 2.0:1.9 d.r.).

mp: 150 - 154 °C

ν_{max} (neat): 3371 (NH), 1599, 1466, 1360, 1257, 785, 742, 700.

***anti*-33**

δ_H (400 MHz, $CDCl_3$): 7.42 (5H, s, H9, H10, H11), 7.39-7.24 (6H, m, Ar-H), 7.05 (1H, dd, *J* 7.7, 1.1, H5), 6.91-6.85 (2H, m, H2, H4), 5.04 (1H, d, *J* 2.8, H12), 4.31 (1H, br. s, NH).

δ_C (101 MHz, $CDCl_3$): 150.3 (C1), 137.6 (C8), 136.3 (C13), 130.2 (C3), 129.0 (C11), 128.7 (C9), 128.4 (C16), 128.4 (Ar CH), 127.6 (C14), 127.6 (Ar CH), 127.1 (C6), 125.7 (C5), 120.5 (C4), 118.8 (CN), 110.4 (C2), 77.7 (C12), 58.3 (C7).

HRMS (ES+): found 319.1207; $C_{21}H_{16}N_2Na$ $[M+Na]^+$ requires 319.1206.

Chiral HPLC (Chiralpak OD-H, 8% IPA; 92% hexane, 1.0 mL.min^{-1}, λ = 209 nm) t_R (major) = 20.1, t_R (minor) = 24.4.

$[\alpha]_D^{20.0}$ + 4.6 (*c* = 0.58, $CHCl_3$).

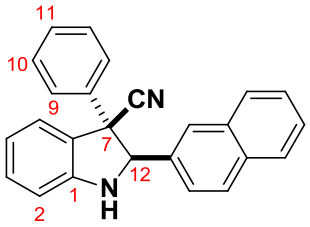
***syn*-33 (racemic)**

δ_H (500 MHz, $CDCl_3$): 7.35-7.26 (3H, m, H9, Ar-H), 7.20-7.10 (5H, m, Ar-H), 7.06-7.01 (2H, m, Ar-H), 6.98-6.85 (2H, m, H2, H4), 6.78-6.65 (2H, m, Ar-H), 5.57 (1H, s, H12), 4.21 (1H, br. s, NH).

δ_C (126 MHz, $CDCl_3$): 150.2 (C1), 135.6 (C8), 134.3 (C13), 130.2 (C3), 128.4 (Ar CH), 128.0 (Ar CH), 127.9 (Ar CH), 127.8 (Ar CH), 127.7 (Ar CH), 127.4 (Ar CH), 125.6 (C5), 121.7 (C6), 120.7 (C4), 120.5 (CN), 110.4 (C2), 74.6 (C12), 55.3 (C7).

Chiral HPLC (Chiralpak OD-H, 8% IPA; 92% hexane, 1.0 mL.min^{-1}, λ = 209 nm) t_R = 18.8, t_R = 23.5.

2-(Naphthalen-2-yl)-3-phenylindoline-3-carbonitrile



73

Asymmetric: Prepared according to *general procedure 3*. Aniline **33a** (32 mg, 0.15 mmol), aldehyde **35** (26 mg, 0.17 mmol), *N*-benzylquininium chloride (3 mg, 0.01 mmol), $CsOH{\cdot}H_2O$ (26 mg, 0.15 mmol), toluene (2.0 mL), T = -50 °C. Reaction time: 48 h. Crude ^1H NMR shows >60:1 d.r. Purification *via* flash column chromatography on silica gel (PE/Et_2O = 15:1) gave indoline **73** as a colourless crystalline solid (45 mg, 84%, single diastereoisomer, 80% e.e.).

Racemic: Prepared according to *general procedure 4*. Aniline **33a** (15 mg, 0.07 mmol), aldehyde **35** (38 mg, 0.24 mmol), potassium *tert*-butoxide (8 mg, 0.07 mmol), toluene (0.7 mL). Crude ^1H NMR shows >60:1 d.r. Purification *via* preparative TLC gave indoline **73** as an oil.

mp: 58 - 61 °C

ν_{max} (neat): 3362 (NH), 3058, 2360, 2238 (C≡N), 1629, 1483, 1258, 908, 741, 699.

δ_H (400 MHz, $CDCl_3$): 7.88-7.77 (4H, m, Ar-H), 7.52-7.48 (2H, m, Ar-H), 7.43 (5H, s, H9, H10, H11), 7.35-7.29 (2H, m, H3, Ar-H), 7.07 (1H, d, *J* 7.8, H5), 6.95-6.86 (2H, m, H2, H4), 5.19 (1H, s, H12), 4.33 (1H, br. s, NH).

δ_C (101 MHz, $CDCl_3$): 150.4 (C1), 137.7 (C8), 133.9 (C13), 133.7 (Ar C), 133.0 (Ar C), 130.3 (C3), 129.9 (d, *J* 2.4, Ar CH), 128.8 (C10), 128.6 (Ar CH), 128.2 (Ar CH), 128.1 (Ar

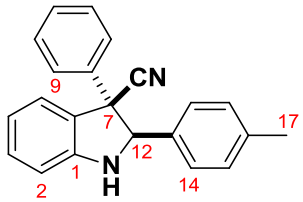
CH), 127.8 (Ar CH), 127.7 (C9), 127.3 (C6), 127.0 (Ar CH), 126.4 (Ar CH), 126.3 (Ar CH), 125.8 (Ar CH), 120.6 (C4), 118.9 (CN), 110.5 (C2), 77.9 (C12), 58.4 (C7).

HRMS (ES+): found 369.1355; $C_{25}H_{18}N_2Na$ $[M+Na]^+$ requires 369.1362.

Chiral HPLC (Chiralpak AD-H, 12% IPA; 88% hexane, 1.0 $mL.min^{-1}$, λ = 227 nm) t_R (major) = 30.5, t_R (minor) = 24.1.

$[\alpha]_D^{20.0}$ + 23.4 (*c* = 0.35, $CHCl_3$).

2-(4-Methyl)-3-phenylindoline-3-carbonitrile



74

Asymmetric: Prepared according to *general procedure 3*. Aniline **33a** (23 mg, 0.11 mmol), aldehyde **36** (15 mg, 0.12 mmol), *N*-benzylquininium chloride (2 mg, 0.01 mmol), $CsOH{\cdot}H_2O$ (37 mg, 0.22 mmol), toluene (1.5 mL), T = -50 °C. Reaction time: 48 h. Crude ^1H NMR shows >60:1 d.r. Purification *via* flash column chromatography on silica gel (PE/Et_2O = 16:1) gave indoline **74** as a colourless crystalline solid (30 mg, 86%, single diastereoisomer, 90% e.e.).

Racemic: Prepared according to *general procedure 4*. Aniline **19a** (19 mg, 0.09 mmol), aldehyde **36** (12 mg, 0.1 mmol), potassium *tert*-butoxide (11 mg, 0.09 mmol), toluene (0.9 mL). Crude ^1H NMR shows >60:1 d.r. Purification *via* preparative TLC gave indoline **74** as an oil.

mp: 58 - 60 °C

ν_{max} (neat): 3357 (NH), 2360 (C≡N), 2341, 1607, 1468, 1258, 822, 747, 698.

δ_H (400 MHz, $CDCl_3$): 7.41 (5H, s, H9, H10, H11), 7.27 (1H, app. td, *J* 7.7, 1.3, H3), 7.21-7.12 (4H, m, Ar-H), 7.05 (1H, app. dt, *J* 7.5, 0.8, H5), 6.91-6.83 (2H, m, H2, H4), 5.01 (1H, s, H12), 4.12 (1H, br. s, NH), 2.37 (3H, s, H17).

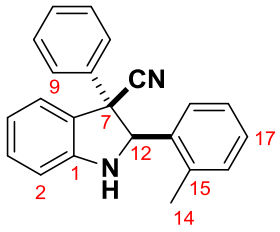
δ_C (101 MHz, $CDCl_3$): 150.4 (C1), 138.8 (C8), 137.7 (C16), 133.2 (C13), 130.2 (C3), 129.1 (Ar CH), 128.7 (Ar CH), 128.4 (C11), 127.6 (Ar CH), 127.5 (Ar CH), 127.2 (C6), 125.8 (C5), 120 (C4), 119 (CN), 110.4 (C2), 77.5 (C12), 58.4 (C7), 21.3 (C17).

HRMS (ES+): found 333.1350; $C_{22}H_{18}N_2Na$ $[M+Na]^+$ requires 333.1362.

Chiral HPLC (Chiralpak ODH, 2% IPA; 98% hexane, 1.0 $mL.min^{-1}$, λ = 211 nm) t_R (major) = 45.0, t_R (minor) = 40.1.

$[\alpha]_D^{20.0}$ + 5.0 (*c* = 0.64, $CHCl_3$).

2-(2-Methyl)-3-phenylindoline-3-carbonitrile



75

Asymmetric: Prepared according to *general procedure 3*. Aniline **33a** (94 mg, 0.45 mmol), aldehyde **37** (59 mg, 0.49 mmol), *N*-benzylquininium chloride (10 mg, 0.02 mmol), $CsOH{\cdot}H_2O$ (151 mg, 0.9 mmol), toluene (5.9 mL), T = -50 °C. Reaction time: 48 h. Crude ^1H NMR shows > 20:1 d.r. Purification *via* flash column chromatography on silica gel (PE/Et_2O = 16:1) gave indoline **75** as a colourless crystalline solid (139 mg, 97%, single diastereoisomer, 71% e.e.).

Racemic: Prepared according to *general procedure 4*. Aniline **33a** (21 mg, 0.10 mmol), aldehyde **37** (13 mg, 0.11 mmol), potassium *tert*-butoxide (11 mg, 0.10 mmol), toluene (1.4 mL). Crude ^1H NMR shows > 20:1 d.r. Purification *via* preparative TLC gave indoline **75** as an oil.

mp: 116 - 118 °C

ν_{max} (neat): 3359 (NH), 2360 (C≡N), 2341, 1607, 1468, 1259, 750.

δ_H (400 MHz, $CDCl_3$): 7.83 (1H, dd, *J* 7.7, 1.3, Ar-H), 7.37-7.24 (5H, m, Ar-H), 7.19-7.12 (3H, m), 7.00-6.92 (2H, m, Ar-H), 6.80-6.71 (2H, m, H2, H4), 5.21 (1H, s, H12), 4.12 (1H, br. s, NH), 1.51 (3H, s, H14).

δ_C (101 MHz, $CDCl_3$): 150.6 (C1), 138.2 (C8), 136.5 (C15), 135.1 (C13), 130.5 (Ar CH), 130.3 (Ar CH), 129.2 (Ar CH), 129.0 (Ar CH), 128.7 (Ar CH), 128.6 (ArCH), 128.1 (Ar

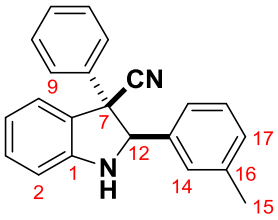
CH), 128.0 (Ar CH), 127.3 (Ar CH), 127.2 (C6), 126.4 (Ar CH), 125.7 (Ar CH), 120.4 (C4), 119.2 (CN), 110.2 (C2), 73.1 (C12), 58.4 (C7), 19.0 (C14).

HRMS (ES+): found 333.1369; $C_{22}H_{18}N_2Na$ $[M+Na]^+$ requires 333.1362.

Chiral HPLC (Chiralpak ODH, 2% IPA; 98% hexane, 1.0 mL.min^{-1}, λ = 211 nm) t_R (major) = 45.0, t_R (minor) = 40.1.

$[\alpha]_D^{20.0}$ + 20.3 (*c* = 1.25, $CHCl_3$).

2-(3-Methyl)-3-phenylindoline-3-carbonitrile



76

Asymmetric: Prepared according to *general procedure 3*. Aniline **33a** (94 mg, 0.45 mmol), aldehyde **38** (59 mg, 0.49 mmol), *N*-benzylquininium chloride (10 mg, 0.02 mmol), $CsOH{\cdot}H_2O$ (151 mg, 0.9 mmol), toluene (5.9 mL), T = -50 °C. Reaction time: 48 h. Crude ^1H NMR shows > 20:1 d.r. Purification *via* flash column chromatography on silica gel (PE/Et_2O = 16:1) gave indoline **76** as a colourless crystalline solid (133 mg, 95%, single diastereoisomer, 60% e.e.).

Racemic: Prepared according to *general procedure 4*. Aniline **33a** (21 mg, 0.10 mmol), aldehyde **38** (13 mg, 0.11 mmol), potassium *tert*-butoxide (11 mg, 0.10 mmol), toluene (1.4 mL). Crude ^1H NMR shows > 20:1 d.r. Purification *via* preparative TLC gave indoline **76** as an oil.

mp: 120 - 122 °C

ν_{max} (neat): 3357 (NH), 2360 (C≡N), 2342, 1607, 1469, 1258, 748.

δ_H (400 MHz, $CDCl_3$): 7.33 (5H, s, H9, H10, H11), 7.20-7.08 (4H, m, Ar-H), 7.00-6.91 (2H, m, Ar-H), 6.83-6.76 (2H, m, H2, H4), 4.92 (1H, s, H12), 4.20 (1H, br. s, NH), 2.25 (3H, s, H15).

δ_C (101 MHz, $CDCl_3$): 150.4 (C1), 138.1 (C8), 137.8 (C16), 136.4 (C13), 130.3 (Ar CH), 129.8 (Ar CH), 129.1 (Ar CH), 128.8 (Ar CH), 128.5 (ArCH), 128.3 (Ar CH), 128.2 (Ar

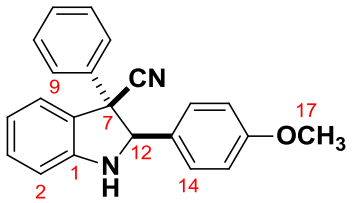
CH), 127.8 (Ar CH), 127.7 (Ar CH), 127.3 (C6), 125.8 (Ar CH), 124.7 (Ar CH), 120.5 (C4), 118.9 (CN), 110.4 (C2), 77.7 (C12), 58.4 (C7), 21.5 (C15).

HRMS (ES+): found 333.1369; $C_{22}H_{18}N_2Na$ $[M+Na]^+$ requires 333.1362.

Chiral HPLC (Chiralpak ODH, 2% IPA; 98% hexane, 1.0 mL.min^{-1}, λ = 211 nm) t_R (major) = 45.0, t_R (minor) = 40.1.

$[\alpha]_D^{20.0}$ + 11.6 (*c* = 1.06, $CHCl_3$).

2-(4-Methoxyphenyl)-3-phenylindoline-3-carbonitrile



78

Asymmetric: Prepared according to *general procedure 3*. Aniline **33a** (21 mg, 0.10 mmol), aldehyde **39** (15 mg, 0.11 mmol), *N*-benzylquininium chloride (2 mg, 0.01 mmol), $CsOH{\cdot}H_2O$ (18 mg, 0.10 mmol), toluene (1.6 mL), T = -50 °C. Reaction time: 48 h. Crude ^1H NMR shows >60:1 d.r. Purification *via* flash column chromatography on silica gel (PE/Et_2O = 8:1) gave indoline **78** as a white crystalline solid (29 mg, 83%, single diastereoisomer, 90% e.e.).

Racemic: Prepared according to *general procedure 4*. Aniline **33a** (35 mg, 0.17 mmol), aldehyde **39** (25 mg, 0.19 mmol), potassium *tert*-butoxide (19 mg, 0.17 mmol), toluene (1.7 mL). Crude ^1H NMR shows >60:1 d.r. Purification *via* preparative TLC gave indoline **78** as an oil.

mp: 112 - 114 °C

ν_{max} (neat): 3355 (NH), 2918, 2360 (C≡N), 1608, 1513, 1467, 1248, 1031, 748.

δ_H (400 MHz, $CDCl_3$): 7.40 (5H, s, H9, H10, H11), 7.30-7.16 (3H, m, H3, H14), 7.05 (1H, d, *J* 7.8, H5), 6.93-6.82 (4H, m, H2, H4, H15), 4.98 (1H, s, H12), 4.23 (1H, br. s, NH), 3.82 (3H, app. d, *J* 1, H17).

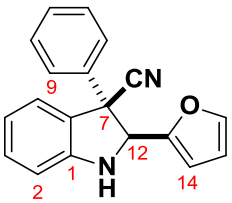
δ_C (101 MHz, $CDCl_3$): 160.1 (C16), 150.4 (C1), 137.6 (C8), 130.2 (C3), 128.8 (Ar CH), 128.7 (Ar CH), 128.4 (C11), 128.2 (C6), 127.6 (Ar CH), 127.1 (C13), 125.8 (C5), 120.4 (C4), 119.0 (CN), 113.7 (C15), 110.3 (C2), 77.4 (C12), 58.4 (C7), 55.2 (C17).

HRMS (ES+): found 349.1297; $C_{22}H_{18}N_2NaO$ $[M+Na]^+$ requires 349.1311.

Chiral HPLC (Chiralpak OD-H, 7% IPA; 93% hexane, 1.0 mL.min^{-1}, λ = 204 nm) t_R (major) = 32.4, t_R (minor) = 25.6.

$[\alpha]_D^{20.0}$ + 19.1 (*c* = 0.46, $CHCl_3$).

2-(Furan-2-yl)-3-phenylindoline-3-carbonitrile



79

Asymmetric: Prepared according to *general procedure 3*. Aniline **33a** (50 mg, 0.24 mmol), aldehyde **40** (25 mg, 0.26 mmol), *N*-benzylquininium chloride (5 mg, 0.01 mmol), $CsOH{\cdot}H_2O$ (41 mg, 0.24 mmol), toluene (3.1 mL), T = -50 °C. Reaction time: 48 h. Crude ^1H NMR shows >60:1 d.r. Purification *via* flash column chromatography on silica gel (PE/Et_2O = 5:1) gave indoline **79** as a yellow crystalline solid (63 mg, 91%, single diastereoisomer, 98% e.e.).

Racemic: Prepared according to the *general procedure 4*. Aniline **33a** (33 mg, 0.16 mmol), aldehyde **40** (16 mg, 0.17 mmol), potassium *tert*-butoxide (18 mg, 0.16 mmol), toluene (1.6 mL). Crude ^1H NMR shows >60:1 d.r. Purification *via* preparative TLC gave indoline **79** as a yellow oil.

mp: 108 - 110 °C

ν_{max} (neat): 3357 (NH), 2239 (C≡N), 1605, 1468, 739.

δ_H (400 MHz, $CDCl_3$): 7.53-7.33 (6H, m, H9, H10, H11, H16), 7.27 (1H, app. td, *J* 7.7, 1.3, H3), 7.11 (1H, d, *J* 7.6, H5), 6.95-6.81 (2H, m, H2, H4), 6.52 (1H, d, *J* 3.3, H14), 6.42 (1H, app. dt, *J* 2.8, 1.2, H15), 5.07 (1H, s, H12), 4.24 (1H, br. s, NH).

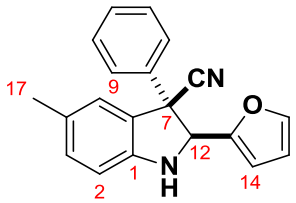
δ_C (101 MHz, $CDCl_3$): 151.0 (C1), 149.7 (C13), 143.1 (C16), 138.2 (C8), 130.3 (C3), 129.0 (C10), 128.5 (C11), 127.1 (C6), 127.0 (C9), 125.7 (C5), 120.7 (C4), 118.8 (CN), 110.0 (C2, C15), 108.9 (C14), 70.7 (C12), 57.0 (C7).

HRMS (ES+): found 309.0992; $C_{19}H_{14}N_2NaO$ $[M+Na]^+$ requires 309.0998.

Chiral HPLC (Chiralpak ODH, 5% IPA; 95% hexane, 1.0 $mL.min^{-1}$, λ = 208 nm) t_R (major) = 24.3, t_R (minor) = 18.3.

$[\alpha]_D^{20.0}$ + 83.2 (*c* = 0.51, $CHCl_3$).

2-(Furan-2-yl)-5-methyl-3-phenylindoline-3-carbonitrile



80

Asymmetric: Prepared according to *general procedure 3*. Aniline **33b** (27 mg, 0.13 mmol), aldehyde **40** (14 mg, 0.14 mmol), *N*-benzylquininium chloride (3 mg, 0.01 mmol), $CsOH{\cdot}H_2O$ (23 mg, 0.13 mmol), toluene (1.8 mL), T = -50 °C. Reaction time: 48 h. Crude ^1H NMR shows >60:1 d.r. Purification *via* flash column chromatography on silica gel (PE/Et_2O = 5:1) gave indoline **80** as a yellow crystalline solid (36 mg, 89%, single diastereoisomer, 97% e.e.).

Racemic: Prepared according to the *general procedure 4*. Aniline **33b** (15 mg, 0.07 mmol), aldehyde **40** (10 mg, 0.1 mmol), potassium *tert*-butoxide (8 mg, 0.07 mmol), toluene (0.7 mL). Crude ^1H NMR shows >60:1 d.r. Purification *via* preparative TLC gave indoline **80** as a yellow oil.

mp: 104 - 108 °C

ν_{max} (neat): 3356 (NH), 2863, 2240 (C≡N), 1617, 1496, 1250, 1147, 1011, 739.

δ_H (400 MHz, $CDCl_3$): 7.52-7.34 (6H, m, H9, H10, H11, H16), 7.08 (1H, dt, *J* 8.1, 1, H3), 6.92 (1H, s, H5), 6.78 (1H, d, *J* 8.1, H2), 6.50 (1H, d, *J* 3.3, H14), 6.41 (1H, dd, *J* 3.3, 1.8, H15), 5.05 (1H, s, H12), 3.78 (1H, br. s, NH), 2.27 (3H, s, H17).

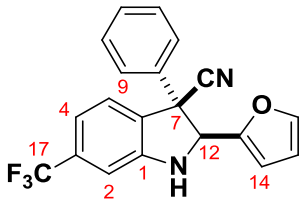
δ_C (101 MHz, $CDCl_3$): 151.2 (C1), 147.5 (C13), 143.1 (C16), 138.3 (C8), 130.9 (C3), 130.5 (C4), 128.9 (C10), 128.5 (C11), 127.4 (C6), 127.0 (C9), 126.0 (C5), 118.9 (CN), 110.7 (C2), 110.6 (C15), 108.8 (C14), 70.9 (C12), 57.2 (C7), 20.8 (C17).

HRMS (ES+): found 323.1147; $C_{20}H_{16}N_2NaO$ $[M+Na]^+$ requires 323.1155.

Chiral HPLC (Chiralpak ODH, 5% IPA; 95% hexane, 1.0 $mL.min^{-1}$, λ = 206 nm) t_R (major) = 30.5, t_R (minor) = 15.0.

$[\alpha]_D^{20.0}$ + 73.3 (*c* = 0.56, $CHCl_3$).

2-(Furan-2-yl)-3-phenyl-6-(trifluoromethyl)indoline-3-carbonitrile



81

Asymmetric: Prepared according to *general procedure 3*. Aniline **33c** (25 mg, 0.12 mmol), aldehyde **40** (13 mg, 0.13 mmol), *N*-benzylquininium chloride (3 mg, 0.01 mmol), $CsOH \cdot H_2O$ (20 mg, 0.12 mmol), toluene (1.5 mL), T = -50 °C. Reaction time: 48 h. Crude ^1H NMR shows >60:1 d.r. Purification *via* flash column chromatography on silica gel (PE/Et_2O = 5:1) gave indoline **81** as a yellow oil (34 mg, 81%, single diastereoisomer, 95% e.e.).

Racemic: Prepared according to the *general procedure 4*. Aniline **33c** (10 mg, 0.05 mmol), aldehyde **40** (5 mg, 0.06 mmol), potassium *tert*-butoxide (6 mg, 0.05 mmol), toluene (0.5 mL). Crude ^1H NMR shows >60:1 d.r. Purification *via* preparative TLC gave indoline **81** as a yellow oil.

ν_{max} (neat): 3361 (NH), 2366 (C≡N), 1619, 1324 (CF), 1222, 1125, 1055, 742.

δ_H (400 MHz, $CDCl_3$): 7.46-7.40 (6H, m, H9, H10, H11, H16), 7.24-7.19 (1H, m, H4), 7.17-7.12 (1H, m, H5), 7.08 (1H, s, H2), 6.53 (1H, d, *J* 3.3, H14), 6.43 (1H, dt, *J* 2.8, 1.2, H15), 5.15 (1H, s, H12), 3.79 (1H, br. s, NH).

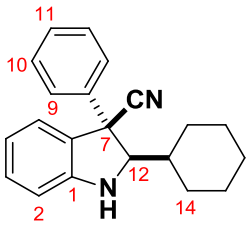
δ_C (101 MHz, $CDCl_3$): 150.4 (C1), 149.9 (C13), 143.4 (C16), 137.6 (C8), 132.9 (C3), 130.7 (C6), 129.2 (C10), 128.9 (C11), 126.8 (C9), 126.1 (C5), 118.1 (CN), 117.5 (q, *J* 4.2, C4), 110.7 (C15), 109.2 (C14), 107.1 (q, *J* 3.5, C2), 70.7 (C12), 56.7 (C7).

HRMS (ES+): found 377.0863; $C_{20}H_{13}F_3N_2NaO$ $[M+Na]^+$ requires 377.0872.

Chiral HPLC (Chiralpak IA, 5% IPA; 95% hexane, 1.0 $mL.min^{-1}$, λ = 207 nm) t_R (major) = 21.3, t_R (minor) = 16.2.

$[\alpha]_D^{20.0}$ + 89.6 (*c* = 0.50, $CHCl_3$).

2-Cyclohexyl-3-phenylindoline-3-carbonitrile



82

Asymmetric: Prepared according to *general procedure 3*. Aniline **33a** (35 mg, 0.17 mmol), aldehyde **41** (21 mg, 0.19 mmol), *N*-benzylquininium chloride (4 mg, 0.01 mmol), $CsOH{\cdot}H_2O$ (58 mg, 0.35 mmol), toluene (2.3 mL), T = -50 °C. Reaction time: 48 h. Crude ^1H NMR shows >60:1 d.r. and 66% conversion of starting material to product. Purification *via* flash column chromatography on silica gel (PE/Et_2O = 10:1) gave indoline **82** as a yellow crystalline solid (16 mg, 32%, single diastereoisomer, 94% e.e.).

Racemic: Prepared according to *general procedure 4*. Aniline **33a** (16 mg, 0.08 mmol), aldehyde **41** (10 mg, 0.09 mmol), potassium *tert*-butoxide (9 mg, 0.08 mmol), toluene (0.8 mL). Crude ^1H NMR shows >60:1 d.r. Purification *via* preparative TLC gave indoline **82** as a yellow oil.

mp: 154 - 158 °C

ν_{max} (neat): 3355 (NH), 3339, 2924, 2849, 2236 (C≡N), 1605, 1448, 1227, 745.

δ_H (400 MHz, $CDCl_3$): 7.58-7.50 (2H, m, Ar-H), 7.43-7.27 (5H, m, Ar-H), 7.15 (1H, t, *J* 1.0, H3), 6.83-6.68 (3H, m, Ar-H), 4.15 (1H, br. s, NH), 3.88 (1H, d, *J* 8.5, H12), 2.20-2.05 (1H, m, H13), 1.97 (1 H, ddt, *J* 12.3, 3.7, 1.7, Alk-H), 1.81-1.61 (3H, m, Alk-H), 1.44-1.28 (2H, m, Alk-H), 1.14-0.98 (3H, m, Alk-H), 0.59 (1H, qd, *J* 12.3, 3.4, H14).

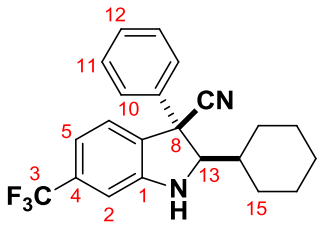
δ_C (126 MHz, $CDCl_3$): 149.3 (C1), 139.8 (C8), 130.0 (C6), 129.9 (C3), 128.7 (C10), 127.9 (C11), 127.3 (C9), 125.0 (C5), 120.0 (C4), 118.9 (CN), 110.0 (C2), 77.2 (C12), 55.0 (C7), 41.6 (C13), 30.3 (C14), 30.0 (C14'), 26.0 (C16), 25.6 (C15).

HRMS (ES+): found 325.1672; $C_{21}H_{22}N_2Na$ $[M+Na]^+$ requires 325.1675.

Chiral HPLC (Chiralpak ODH, 2% IPA; 98% hexane, 1.0 $mL.min^{-1}$, λ = 207 nm) t_R (major) = 14.2, t_R (minor) = 11.4.

$[\alpha]_D^{20.0}$ + 54.4 (*c* = 2.90, $CHCl_3$).

2-Cyclohexyl-3-phenyl-6-(trifluoromethyl)indoline-3-carbonitrile



83

Asymmetric: Prepared according to *general procedure 3*. Aniline **33c** (35 mg, 0.17 mmol), aldehyde **41** (21 mg, 0.19 mmol), *N*-benzylquininium chloride (4 mg, 0.01 mmol), $CsOH \cdot H_2O$ (28 mg, 0.17 mmol), toluene (2.2 mL), T = -50 °C. Reaction time: 48 h. Crude ^1H NMR shows >60:1 d.r. Purification *via* flash column chromatography on silica gel (PE/Et_2O = 15:1) gave indoline **83** as a yellow crystalline solid (48 mg, 78%, single diastereoisomer, 99% e.e.).

Racemic: Prepared according to *general procedure 4*. Aniline **19c** (17 mg, 0.08 mmol), aldehyde **41** (10 mg, 0.09 mmol), potassium *tert*-butoxide (9 mg, 0.08 mmol), toluene (0.8 mL). Crude ^1H NMR shows >60:1 d.r. Purification *via* preparative TLC gave indoline **83** as a yellow oil.

mp: 146 - 149 °C

ν_{max} (neat): 3456 (NH), 3348, 3016, 2970, 2941, 1738, 1367 (CF), 1228.

δ_H (200 MHz, $CDCl_3$): 7.56-7.27 (5H, m, H10, H11, H12), 7.03-6.82 (3H, m, H2, H5, H6), 3.95 (1H, d, *J* 8.7, H13), 3.40 (1H, br. s, NH), 3.83-2.97 (1H, m, H13), 2.25-2.03 (1H, m, H14), 2.02-0.85 (9H, m, H15, H16, H17), 0.60 (1H, qd, *J* 12.1, 2.9, H15).

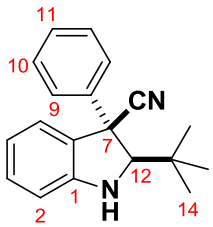
δ_C (101 MHz, $CDCl_3$): 149.4 (C1), 139.0 (C9), 133.3 (C7), 129.3 (d, *J* 7.6, C4), 128.9 (C11), 128.3 (C12), 127.2 (C10), 125.4 (C6), 123.9 (q, *J* 272, C3), 118.3 (CN), 116.8 (q, *J* 3.8, C5), 106.5 (q, *J* 3.8, C2), 77.4 (C13), 54.6 (C8), 41.6 (C14), 30.1 (C15), 29.9 (C15'), 25.9 (C17), 25.5 (C16).

HRMS (ES+): found 393.1544; $C_{22}H_{21}F_3N_2Na$ $[M+Na]^+$ requires 393.1549.

Chiral HPLC (Chiralpak IA, 5% IPA; 95% hexane, 1.0 $mL.min^{-1}$, λ = 209 nm) t_R (major) = 16.8, t_R (minor) = 13.2.

$[\alpha]_D^{20.0}$ + 66.0 (*c* = 0.30, $CHCl_3$).

2-(*tert*-Butyl)-3-phenylindoline-3-carbonitrile



84

Asymmetric: Prepared according to *general procedure 3*. Aniline **33a** (40 mg, 0.19 mmol), aldehyde **42** (18 mg, 0.21 mmol), *N*-benzylquininium chloride (4 mg, 0.01 mmol), $CsOH \cdot H_2O$ (65 mg, 0.39 mmol), toluene (2.5 mL), T = -50 °C. Reaction time: 48 h. Crude ^1H NMR shows >60:1 d.r. Purification *via* flash column chromatography on silica gel (PE/Et_2O = 8:1) gave indoline **84** as a yellow oil (15 mg, 30%, single diastereoisomer, 67% e.e.).

Racemic: Prepared according to the *general procedure 4*. Aniline **33a** (65 mg, 0.31 mmol), aldehyde **42** (29 mg, 0.34 mmol), potassium *tert*-butoxide (35 mg, 0.31 mmol), toluene (3.0 mL). Crude ^1H NMR shows >60:1 d.r. Purification *via* preparative TLC gave indoline **84** as a yellow oil.

ν_{max} (neat): 3363 (NH), 2963, 2849, 2360, 2234 (C≡N), 1606, 1488, 1264, 744.

δ_H (400 MHz, $CDCl_3$): 7.53-7.49 (2H, m, H9), 7.41-7.30 (3H, m, H10, H11), 7.17 (1H, t, *J* 7.8, H3), 6.91-6.84 (1H, m, H5), 6.80-6.72 (2H, m, H4, H2), 4.14 (1H, br. s, NH), 3.88 (1H, s, H12), 1.11 (9H, s, H14).

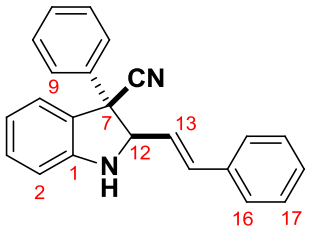
δ_C (126 MHz, $CDCl_3$): 149.5 (C1), 141.5 (C8), 129.9 (C6), 129.8 (C3), 128.6 (C10), 127.8 (C11), 127.3 (C9), 125.2 (C5), 120.8 (CN), 119.9 (C4), 109.7 (C2), 81.8 (C12), 52.3 (C7), 35.0 (C13), 26.9 (C14).

HRMS (ES+): found 299.1527; $C_{19}H_{20}N_2Na$ $[M+Na]^+$ requires 299.1519.

Chiral HPLC (Chiralpak ODH, 2% IPA; 98% hexane, 1.0 $mL.min^{-1}$, λ = 207 nm) t_R (major) = 12.0, t_R (minor) = 10.4.

$[\alpha]_D^{20.0}$ + 31.3 (*c* = 0.42, $CHCl_3$).

3-Phenyl-2-((*E*)-styryl)indoline-3-carbonitrile



85

Asymmetric: Prepared according to *general procedure 3*. Aniline **33a** (42 mg, 0.20 mmol), aldehyde **43** (29 mg, 0.22 mmol), *N*-benzylquininium chloride (5 mg, 0.01 mmol), $CsOH \cdot H_2O$ (68 mg, 0.40 mmol), toluene (2.6 mL), T = -50 °C. Reaction time: 48 h. Crude ^1H NMR shows >60:1 d.r. and partial conversion of starting material to product. Purification *via* flash column chromatography on silica gel (PE/Et_2O = 15:1) gave indoline **85** as a red oil (33 mg, 50%, single diastereoisomer, 90% e.e.).

Racemic: Prepared according to the *general procedure 4*. Aniline **33a** (12 mg, 0.06 mmol), aldehyde **43** (9 mg, 0.07 mmol), potassium *tert*-butoxide (7 mg, 0.06 mmol), toluene (0.6 mL). Crude ^1H NMR shows >60:1 d.r. Purification *via* flash column chromatography on silica gel (PE/Et_2O = 15:1) gave indoline **85** as a red oil (16 mg, 81%, single diastereoisomer).

ν_{max} (neat): 3375 (NH), 2360, 2342, 1606, 1482, 1260, 1222, 749, 695.

δ_H (400 MHz, $CDCl_3$): 7.53-7.47 (2H, m, Ar-H), 7.45-7.21 (9H, m, H3, Ar-H), 7.10 (1H, d, *J* 7.6, H13), 6.92-6.79 (2H, m, H2, H4), 6.55-6.49 (2H, m, H5, H14), 4.48 (1H, d, *J* 1, H12), 4.45 (1H, br. s, NH).

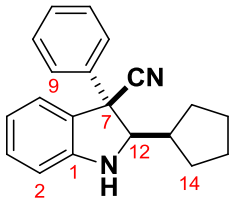
δ_C (101 MHz, $CDCl_3$): 150.0 (C1), 137.6 (C8), 135.9 (C15), 135.4 (C14), 130.3 (C3), 128.9 (Ar CH), 128.7 (Ar CH), 128.4 (Ar CH), 128.3 (Ar CH), 127.3 (Ar CH), 127.2 (C6), 126.9 (Ar CH), 125.7 (C13), 124.7 (C5), 120.4 (C4), 118.9 (CN), 110.7 (C2), 75.7 (C12), 56.6 (C7).

HRMS (ES+): found 345.1368; $C_{23}H_{18}N_2Na$ $[M+Na]^+$ requires 345.1362.

Chiral HPLC (Chiralpak ADH, 12% IPA; 88% hexane, 1.0 $mL.min^{-1}$, λ = 207 nm) t_R (major) = 25.8, t_R (minor) = 31.2.

$[\alpha]_D^{20.0}$ + 63.9 (c = 0.740, $CHCl_3$).

2-Cyclopentyl-3-phenylindoline-3-carbonitrile



86

Asymmetric: Prepared according to *general procedure 3*. Aniline **33a** (40 mg, 0.19 mmol), aldehyde **44** (21 mg, 0.21 mmol), *N*-benzylquininium chloride (4 mg, 0.01 mmol), $CsOH{\cdot}H_2O$ (65 mg, 0.39 mmol), toluene (2.5 mL), T = -50 °C. Reaction time: 48 h. Crude ^1H NMR shows >60:1 d.r. Purification *via* flash column chromatography on silica gel (PE/Et_2O = 10:1) gave indoline **86** as an oil (16 mg, 29%, single diastereoisomer, 70% e.e.).

Racemic: Prepared according to the *general procedure 4*. Aniline **33a** (19 mg, 0.09 mmol), aldehyde **44** (10 mg, 0.10 mmol), potassium *tert*-butoxide (10 mg, 0.09 mmol), toluene (0.9 mL). Crude ^1H NMR shows >60:1 d.r. Purification *via* preparative TLC gave indoline **86** as an oil.

ν_{max} (neat): 3464 (NH), 2954, 2360, 2231 (C≡N), 1615, 1249, 750, 700.

δ_H (400 MHz, $CDCl_3$): 7.69-7.25 (6H, m, Ar-H), 7.17 (1H, t, *J* 7.6, H3), 6.87-6.81 (1H, m, H5), 6.80-6.72 (1H, m, Ar-H), 3.88 (1H, d, *J* 9.6, H12), 3.09 (1H, br. s, NH), 2.60-2.46 (1H, m, H14), 2.12-1.95 (1H, m, H13), 1.84-1.69 (1H, m, Al-H), 1.66-1.19 (4H, m, Al-H), 0.98-0.55 (2H, m, Al-H).

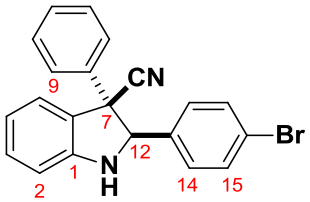
δ_C (101 MHz, $CDCl_3$): 150.9 (C1), 140.1 (C8), 129.9 (C6), 129.2 (C3), 128.6 (Ar CH), 128.1 (Ar CH), 127.6 (Ar CH), 125.3 (C5), 120.3 (C4), 118.2 (CN), 110.3 (C2), 78.5 (C12), 43.7 (C13), 31.4 (All CH_2), 29.2 (Alk CH_2), 25.4 (Alk CH_2), 24.8 (Alk CH_2).

HRMS (ES+): found 311.1515; $C_{20}H_{20}N_2Na$ $[M+Na]^+$ requires 311.1519.

Chiral HPLC (Chiralpak IA, 5% IPA; 95% hexane, 1.0 $mL.min^{-1}$, λ = 207 nm) t_R (major) = 14.3, t_R (minor) = 12.1.

$[\alpha]_D^{20.0}$ + 8.6 (c = 0.255, $CHCl_3$).

2-(4-Bromophenyl)-3-phenylindoline-3-carbonitrile



87

Asymmetric: Prepared according to *general procedure 3*. Aniline **33a** (42 mg, 0.20 mmol), aldehyde **45** (41 mg, 0.22 mmol), *N*-benzylquininium chloride (4 mg, 0.01 mmol), $CsOH{\cdot}H_2O$ (67 mg, 0.40 mmol), toluene (2.6 mL), T = -50 °C. Reaction time: 48 h. Crude ^1H NMR shows >60:1 dr. Purification *via* flash column chromatography on silica gel (PE/Et_2O = 30:1) gave indoline **87** as a yellow oil (57 mg, 76%, single diastereoisomer, 55% ee).

Racemic: Prepared according to the *general procedure 4*. Aniline **33a** (21 mg, 0.1 mmol), aldehyde **45** (20 mg, 0.11 mmol), potassium *tert*-butoxide (11 mg, 0.10 mmol), toluene (1.0 mL). Crude ^1H NMR shows >60:1 dr. Purification *via* preparative TLC gave indoline **87** as an oil.

ν_{max} (neat): 3352 (NH), 2236 (C≡N), 1605, 1484, 1010, 748, 697.

δ_H (400 MHz, $CDCl_3$): 7.48 (2H, d, *J* 8.3, H15), 7.41 (5H, s, H9, H10, H11), 7.27-7.26 (1H, m, H3), 7.16 (2H, d, *J* 8.6, H14), 7.03 (1H, d, *J* 7.6, H5), 6.93-6.86 (2H, m, H2, H4), 5.0 (1H, s, H12), 4.28 (1H, br. s, NH).

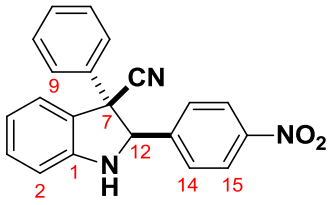
δ_C (101 MHz, $CDCl_3$): 150.2 (C1), 137.1 (Ar C), 135.2 (Ar C), 131.6 (C15), 130.4 (C3), 129.3 (Ar CH), 128.9 (Ar CH), 128.7 (C11), 127.7 (Ar CH), 127.0 (C6), 125.8 (C5), 123.2 (C16), 120.8 (C4), 118.6 (CN), 110.6 (C2), 77.3 (C12), 58.3 (C7).

HRMS (ES+): found 397.0297; $C_{21}H_{15}{}^{79}BrN_2Na$ $[M+Na]^+$ requires 397.0311.

Chiral HPLC (Chiralpak ADH, 10% IPA; 90% hexane, 1.0 mL.min^{-1}, λ = 207 nm) t_R (major) = 34.2, t_R (minor) = 19.1.

$[\alpha]_D^{20.0}$ + 6.9 (c = 0.995, $CHCl_3$).

2-(4-Nitrophenyl)-3-phenylindoline-3-carbonitrile



88

Asymmetric: Prepared according to *general procedure 3*. Aniline **33a** (63 mg, 0.30 mmol), aldehyde **46** (50 mg, 0.33 mmol), *N*-benzylquininium chloride (7 mg, 0.02 mmol), $CsOH{\cdot}H_2O$ (101 mg, 0.6 mmol), toluene (3.9 mL), T = -50 °C. Reaction time: 48 h. Crude ^1H NMR shows >60:1 d.r. Purification *via* flash column chromatography on silica gel (PE/Et_2O = 10:1) gave indoline **88** as a yellow crystalline solid (65 mg, 64%, single diastereoisomer, 55% e.e.).

Racemic: Prepared according to the *general procedure 4*. Aniline **33a** (12 mg, 0.06 mmol), aldehyde **46** (10 mg, 0.07 mmol), potassium *tert*-butoxide (7 mg, 0.06 mmol), toluene (0.6 mL). Crude ^1H NMR shows >60:1 d.r. Purification *via* preparative TLC gave indoline **88** as an oil.

mp: 98 - 103 °C

ν_{max} (neat): 3374 (NH), 1604, 1514 (NO_2), 1342 (NO_2), 855, 750, 700.

δ_H (400 MHz, $CDCl_3$): 8.31-8.10 (2H, m, H15), 7.52-7.37 (7H, m, H9, H10, H11, H14), 7.31 (1H, t, *J* 7.6, H3), 7.07-7.01 (1H, m, H5), 6.96-6.91 (2H, m, H2, H4), 5.16 (1H, s, H12), 4.36 (1H, br. s, NH).

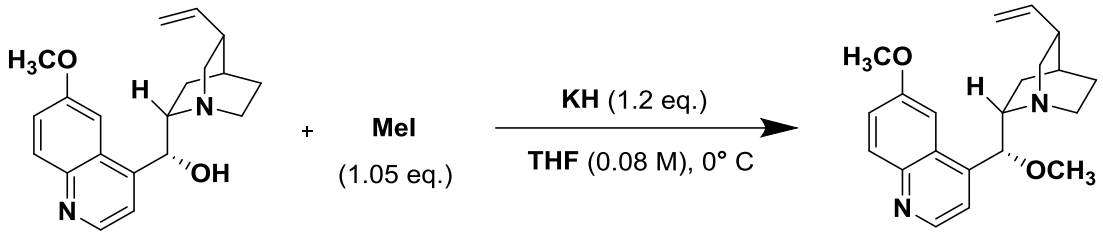
δ_C (101 MHz, $CDCl_3$): 149.9 (C1), 148.4 (C16), 143.5 (C13), 136.7 (C8), 130.6 (C3), 129.1 (Ar CH), 129.0 (C11), 128.6 (Ar CH), 127.7 (Ar CH), 126.7 (C6), 125.7 (C5), 123.6 (C15), 121.2 (C4), 118.2 (CN), 110.9 (C2), 77.1 (C12), 58.4 (C7).

HRMS (ES+): found 364.1051; $C_{21}H_{15}N_3NaO_2$ $[M+Na]^+$ requires 364.1056.

Chiral HPLC (Chiralpak ADH, 15% IPA; 85% hexane, 1.0 $mL.min^{-1}$, λ = 208 nm) t_R (major) = 34.3, t_R (minor) = 17.1. `

$[\alpha]_D^{20.0}$ + 15.3 (c = 0.435, $CHCl_3$).

Preparation of *O*-Methylquinine



Potassium hydride (287 mg, 4.22 mmol, 1.2 eq) was placed in a 50 mL round-bottom flask filled with nitrogen. A solution of quinine (1.14 g, 3.52 mmol) in THF (35 mL) was then added slowly *via* syringe under nitrogen at 0° C. The reaction mixture was stirred for 30 minutes. Methyl iodide (230 uL, 3.69 mmol, 1.05 eq) was then added *via* syringe and the mixture was stirred for 5 h at 0° C.

The reaction mixture was quenched by adding sat. aq. NH_4Cl solution (~2 mL) until the pH of solution was 9-11. The residue was extracted with a mixture of chloroform and isopropyl alcohol (30:1). The organic extract was dried over $MgSO_4$, filtered and concentrated *in vacuo* to afford the crude product. The product was purified by silica gel flash chromatography (DCM/MeOH = 20:1) to afford 120 mg (10%) of *O*-Methylquinine as a solid.

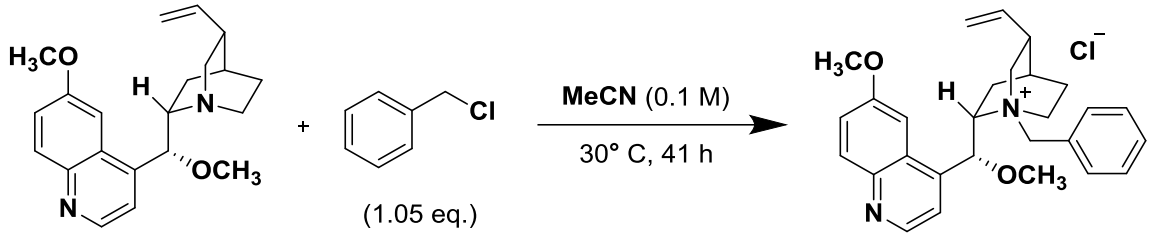
mp: 102 - 104 °C

δ_H (400 MHz, $CDCl_3$): 8.68-8.58 (1H, m), 7.91 (1H, dd, *J* 9.05, 3.67), 7.37-7.23 (3H, m), 5.91 (1H, s), 5.54-5.41 (1H, m), 4.96-4.83 (2H, m), 3.97 (3H, d, *J* 3.42), 3.85 (1H, s), 3.31 (3H, d, *J* 2.69), 3.18 (1H, t, *J* 8.80), 2.99 (1H, t, *J* 11.49), 2.89 (1H, d, *J* 12.72), 2.50 (1H, s), 1.93 (4H, m), 1.70 (1H, s), 1.36 (1H, t, *J* 10.27).

δ_C (101 MHz, $CDCl_3$): 158.9, 147.2, 144.8, 141.1, 138.2, 131.9, 127.0, 122.9, 118.4, 116.8, 100.7, 90.2, 88.9, 61.3, 59.9, 58.1, 57.1, 55.4, 53.5, 43.9, 37.6, 27.7, 27.2, 25.1, 20.0.

HRMS (ES+): found 339.2068; $C_{21}H_{27}N_2O_2$ $[M]^+$ requires 339.2067.

Preparation of *O*-Methyl-*N*-(Benzyl)quininium Chloride



94

O-Methylquinine (60 mg, 0.18 mmol), MeCN (2 mL) were taken in a 10 mL round-bottom flask filled with nitrogen. Benzyl chloride (21.0 uL, 0.19 mmol, 1.05 eq) was then added to it. The reaction mixture was allowed to stir for 41 hrs. The solvent was removed on a rotavap and the residue was purified by silica gel flash chromatography (DCM/MeOH = 10:1) to afford 30 mg (40%) of **94** as a white, crystalline solid.

mp: 167 - 169 °C

δ_H (400 MHz, $CDCl_3$): 8.74 (1H, d, *J* 4.40), 7.96 (1H, d, *J* 9.05), 7.83 (2H, d, *J* 5.38), 7.63 (2H, m), 7.47-7.28 (4H, m), 6.09 (1H, m), 5.68 (1H, ddd, *J* 16.99, 10.15, 6.85), 5.23 (1H, s), 5.01-4.83 (2H, m), 4.75 (1H, d, *J* 11), 4.57 (1H, s), 4.13 (3H, s), 3.47 (3H, s), 3.38-3.22 (1H, m), 3.15 (1H, t, *J* 11.74), 2.50 (1H, s), 2.39-2.07 (3H, m), 2.00 (1H, s), 1.74 (1H, s), 1.57-1.40 (1H, m).

δ_C (101 MHz, $CDCl_3$): 159.0, 156.5, 146.9, 144.9, 140.0, 138.5, 136.4, 135.8, 134.2, 131.8, 130.5, 129.2, 127.4, 127.3, 125.1, 122.9, 120.7, 118.3, 101.5, 92.2, 67.4, 62.9, 59.6, 57.0, 53.5, 51.1, 42.8, 38.0, 27.2, 25.3, 22.4, 19.8.

HRMS (ES+): found 429.2540; $C_{28}H_{33}N_2O_2$ $[M]^+$ requires 429.2537.

5.4 Calibration of HPLC system for kinetic analysis.

A calibration of Dionex Ultimate 3000 HPLC system was performed prior to the kinetic studies.

Samples containing a mixture of imine **47** and indoline **63** in different proportions (1:1, 1:2, 2:1, 1:3 and 3:1) were analysed with the HPLC. The area under the peak of imine **47** and indoline **63** were calculated. The ratio of the areas under the peaks was plotted against the ratio of concentration of the two species present in the sample mixture (Figure **30**).

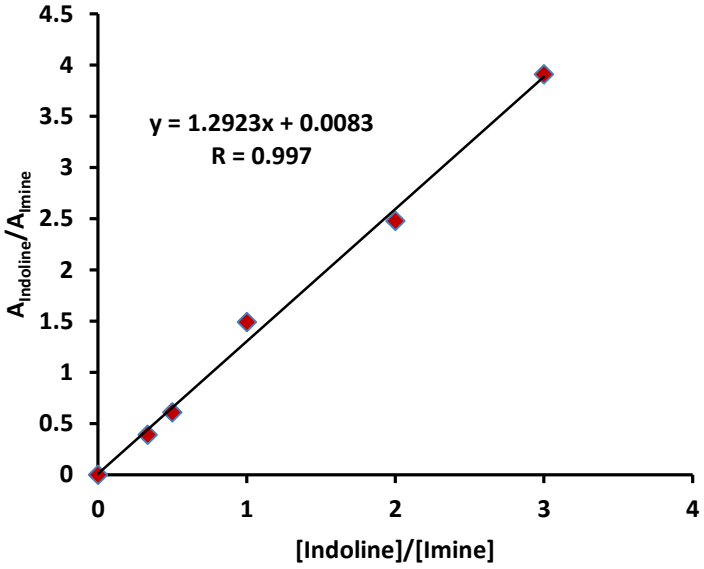


Figure 30: HPLC calibration plot

A best fit line was made and its slope was calculated. The slope of the line (m = 1.29) was the required conversion factor.

$[Pr]/[SM] = (1/K)*A_{Pr}/A_{SM}$ (i)

Where K = 1.29 (Conversion factor)

[Pr] = actual value of indoline concentration in the reaction mixture at time t

[SM] = actual value of imine concentration in the reaction mixture at time t

A_{Pr} = area under the peak of indoline

A_{SM} = area under the peak of imine

At time t, $[Pr] + [SM] = [SM]_o$, where $[SM]_o$ – Conc. of imine at time t = 0

Substituting in (i)

$[Pr]/[SM]_o = A_{Pr}/(K*A_{SM} + A_{Pr})$

Percentage conversion of the reaction at a time t is given by,

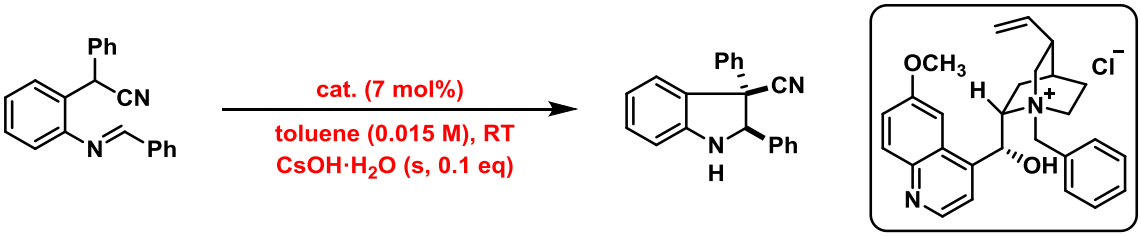
$[Pr]/[SM]_o*100$

Therefore, percentage reaction conversion at time t is

$A_{Pr}/(1.29*A_{SM} + A_{Pr})*100$

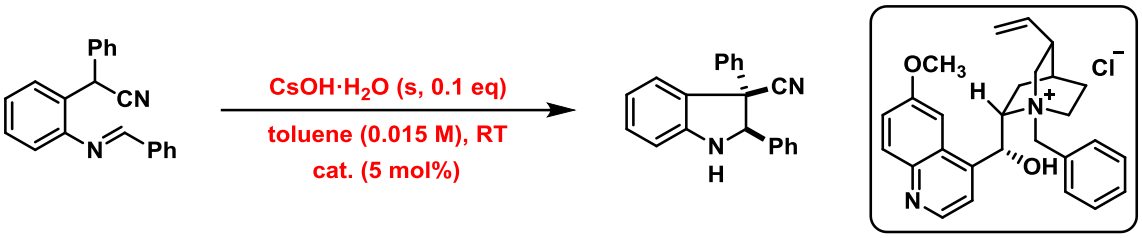
5.5 Kinetic Experiments Data

5.5.1 Modified asymmetric cyclization



Time (sec)	A_{Pr} (HPLC)	% Conversion
0	0	0
150	0	0
300	0	0
450	0	0
600	0	0
750	0	0
900	0	0
1050	0	0
1200	0	0
1350	1.03	0.800303
1500	7.06	5.561131
1650	22.64	18.49154
1800	43.54	37.41405
1980	69.36	63.69988
2100	82.44	78.44525
2250	91.44	89.22508
2400	96.17	95.11357
2550	98.57	98.16292
2700	99.92	99.89682
2850	100	100
3000	100	100

5.5.2 Order of addition



5.5.2 (a) At t = 0 sec

Time (sec)	A_{Pr} (HPLC)	% Conversion
0	0	0
150	0	0
300	0	0
450	0	0
600	0	0
750	0	0
900	0	0
1050	0	0
1200	0	0
1350	0	0
1500	0	0
1650	0	0
1800	0	0
1950	0.3	0.232715
2100	1.5	1.166725
2250	7.2	5.673222
2400	15.1	12.11674
2550	24.9	20.44688
2700	38.3	32.48709
2850	45.7	39.48266
3000	56.8	50.47633

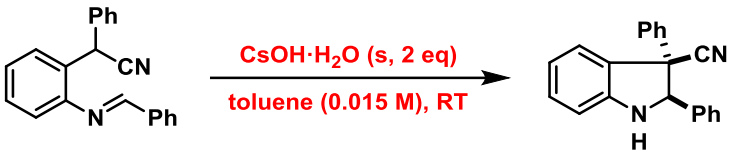
5.5.2 (b) At t = 660 sec

Time (sec)	A_{Pr} (HPLC)	% Conversion
0	0	0
150	0	0
300	0	0
450	0	0
600	0	0
750	0	0
900	0	0
1050	0	0
1200	0	0
1350	0.04	0.031011
1500	1.46	1.13551
1650	8.55	6.757798
1800	22.05	17.98451
1950	41.16	35.16037
2100	60.18	53.94997
2250	76.4	71.50612
2400	88.07	85.12493
2550	94.97	93.60459
2700	99.14	98.89336
2850	99.39	99.21449
3000	99.63	99.52321

5.5.2 (c) At t = 1800 sec

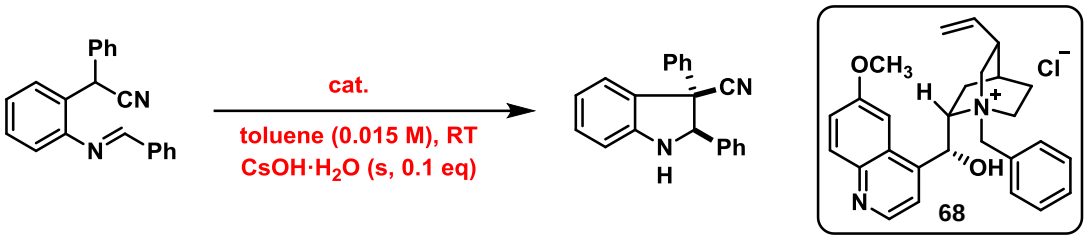
Time (sec)	A_{Pr} (HPLC)	% Conversion
0	0	0
150	0	0
300	0	0
450	0	0
600	0	0
750	0	0
900	0	0
1050	0	0
1200	0	0
1350	0	0
1500	0	0
1650	0	0
1800		0
1950	1.69	1.315074
2100	7.45	5.873565
2250	15.7	12.61581
2400	22.51	18.3797
2550	34.36	28.86531
2700	45.86	39.63679
2850	55.48	49.13613
3000	65.68	59.73472

5.5.3 Background cyclization



Time (sec)	A_{Pr} (HPLC)	% Conversion
0	0	0
150	0	0
300	0	0
450	0	0
600	0	0
750	0	0
900	0	0
1050	0	0
1200	0.38	0.294826
1350	2.62	2.043041
1500	7.09	5.585144
1650	12.94	10.33155
1800	17.44	14.07105
1950	23.11	18.89645
2100	25.69	21.13535
2250	25.32	20.81258
2400	26.14	21.52868
2550	26.75	22.06322
2700	23.3	19.0604
2850	26.43	21.78261
3000	28.8	23.8711

5.5.4 Chiral catalyst loading



5.5.4 (a) 5 mol% catalyst 68

Time (sec)	A_{Pr} (HPLC)	% Conversion
0	0	0
150	0	0
300	0	0
450	0	0
600	0	0
750	0	0
900	0	0
1050	0	0
1200	0	0
1350	0	0
1500	0	0
1650	0	0
1800	0	0
1950	0.3	0.232715
2100	1.5	1.166725
2250	7.2	5.673222
2400	15.1	12.11674
2550	24.9	20.44688
2700	38.3	32.48709
2850	45.7	39.48266
3000	56.8	50.47633

5.5.4 (b) 10 mol% catalyst 68

Time (sec)	A_{Pr} (HPLC)	% Conversion
0	0	0
150	0	0
360	0	0
450	0	0
600	0	0
750	0	0
900	0	0
1050	0	0
1200	0.37	0.28706
1350	0.7	0.543491
1500	4.25	3.326355
1680	14.39	11.52796
1800	23.58	19.30227
1950	46.62	40.37056
2100	65.3	59.32966
2250	80	75.61437
2400	89.52	86.87956
2550	94.95	93.57953
2700	98.14	97.61347
2850	99.61	99.49747
3000	100	100

5.5.4 (c) 15 mol% catalyst 68

Time (sec)	A_{Pr} (HPLC)	% Conversion
0	0	0
150	0	0
300	0	0
450	0	0
600	0	0
750	0	0
900	0	0
1050	0	0
1200	0	0
1350	1.03	0.800303
1500	7.06	5.561131
1650	22.64	18.49154
1800	43.54	37.41405
1950	69.36	63.69988
2100	82.44	78.44525
2250	91.44	89.22508
2400	96.17	95.11357
2550	98.57	98.16292
2700	99.92	99.89682
2850	100	100
3000	100	100

5.5.4 (d) 20 mol% catalyst 68

Time (sec)	A_{Pr} (HPLC)	% Conversion
0	0	0
150	0	0
300	0	0
450	0	0
600	0	0
750	0	0
900	0.65	0.504613
1050	10.08	7.995127
1200	35.41	29.82369
1350	65.4	59.43617
1500	89.23	86.52749
1650	98.4	97.94553
1800	100	100
1950	100	100

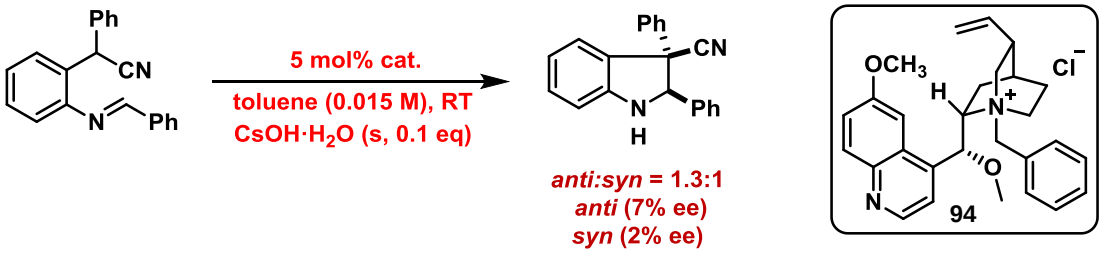
5.5.4 (d) 25 mol% catalyst 68

Time (sec)	A_{Pr} (HPLC)	% Conversion
0	0	0
150	0	0
300	0	0
450	0	0
600	0.5	0.388033
750	2.95	2.302089
900	9.94	7.881545
1050	25.58	21.03933
1200	53.83	47.47362
1350	80.38	76.05275
1500	93.43	91.68316
1650	97.84	97.23095
1800	99.15	98.9062
1950	99.5	99.35593
2100	99.8	99.74215
2250	100	100

5.5.5 Log [Cat] vs. Log k plot

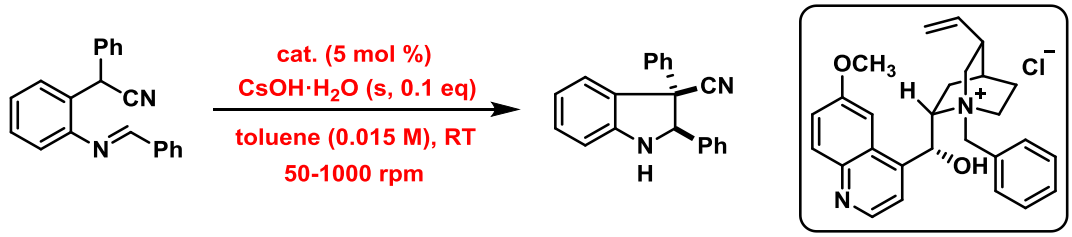
[Cat]	k	Log [Cat]	Log k
0.3459	0.064	-0.46105	-1.19382
0.4841	0.1373	-0.31506	-0.86233
0.6918	0.133	-0.16002	-0.87615
1.0378	0.151	0.016114	-0.82102
1.353	0.177	0.131298	-0.75203

5.5.6 Cyclization with –OH protected catalyst 94



Time (sec)	A_{Pr} (HPLC)	% Conversion
0	0	0
150	0	0
300	0	0
450	0	0
600	0	0
750	0	0
900	0	0
1050	0	0
1200	0	0
1350	0	0
1500	0	0
1650	0	0
1800	1.3	1.010706
1950	2	1.55739
2100	2.7	2.105805
2250	3.8	2.971118
2400	4.86	3.809058
2550	6.04	4.746622
2700	9.07	7.177353
2850	9.58	7.589814
3000	11.97	9.535668
3250	15.37	12.34115
3500	17.5	14.12144
3750	19.31	15.64829
4000	23.54	19.2677
4250	25.25	20.75158
4500	26.92	22.21247
4750	31.11	25.92973
5000	33.46	28.04774
5250	37.24	31.50582
5500	38.6	32.76573

5.5.7 Stirring rate experiments



5.5.7 (a) 150 rpm

Time (sec)	A_{Pr} (HPLC)	% Conversion
0	0	0
150	0	0
300	0	0
450	0	0
600	0	0
750	0	0
900	0	0
1050	0	0
1200	0	0
1350	0	0
1500	0	0
1650	0	0
1800	0	0
1950	0	0
2100	0	0
2250	0.6	0.754822
2400	1.54	1.932662
2550	4.52	5.629047
2700	9.48	11.65747
2850	16.66	20.12008
3000	24.81	29.3663
3150	33.64	38.97729
3300	41.26	46.9509
3450	47.15	52.92137
3600	55.21	60.83236
3750	62.49	67.73261
3900	66.21	71.17253
4050	72.62	76.9686
4200	74.72	78.83229
4350	80.42	83.80603
4500	84.27	87.09706
4800	89.3	91.3162

5.5.7 (b) 250 rpm

Time (sec)	A_{Pr} (HPLC)	% Conversion
0	0	0
150	0	0
300	0	0
450	0	0
600	0	0
750	0	0
900	0	0
1050	0.18	0.139591
1200	0.27	0.209429
1350	3.04	2.372805
1500	12.47	9.945471
1650	25.19	20.69931
1800	43.05	36.94787
1950	57.29	50.97615
2100	69.61	63.97208
2250	78.7	74.12151
2400	86.97	83.80332
2550	92.38	90.38272
2700	95.88	94.74795
2850	98	97.43488
3000	99.06	98.7907
3150	99.97	99.9613
3300	100	100

5.5.7 (c) 500 rpm

Time (sec)	A_{Pr} (HPLC)	% Conversion
0	0	0
150	0	0
300	0	0
450	0	0
600	0	0
750	0	0
900	0	0
1050	0	0
1200	0	0
1350	0	0
1500	0	0
1650	0	0
1800	0	0
1950	0.3	0.232715
2100	1.5	1.166725
2250	7.2	5.673222
2400	15.1	12.11674
2550	24.9	20.44688
2700	38.3	32.48709
2850	45.7	39.48266
3000	56.8	50.47633

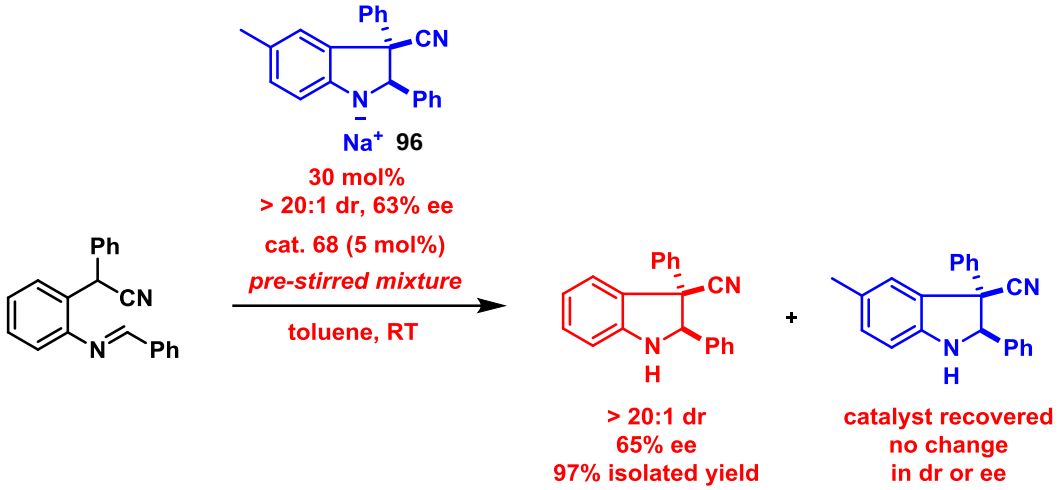
5.5.7 (d) 1000 rpm

Time (sec)	A_{Pr} (HPLC)	% Conversion
0	0	0
150	0	0
300	0	0
450	0	0
600	0	0
750	0	0
900	0	0
1050	0	0
1200	0	0
1350	0	0
1500	0	0
1650	0	0
1800	0	0
1950	0	0
2100	0	0
2250	0	0
2400	1.84	1.432281
2550	11.45	9.110475
2700	24.41	20.02114
2850	38.64	32.80292
3000	50.81	44.46677

5.5.7 (e) 50 rpm

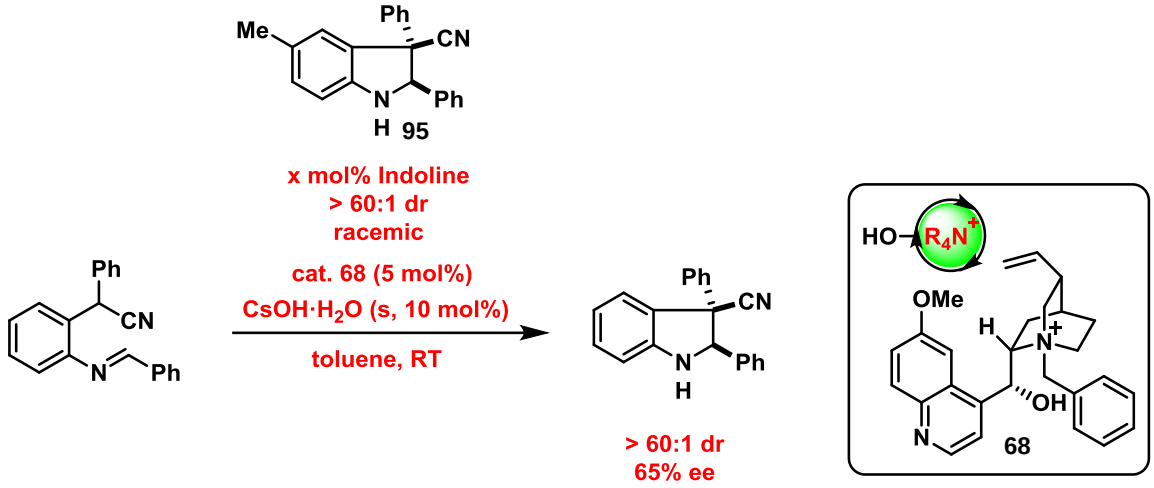
Time (sec)	A_{Pr} (HPLC)	% Conversion
0	0	0
150	0	0
300	0	0
450	0	0
600	0	0
750	0	0
900	0	0
1050	0	0
1200	0	0
1350	0	0
1500	0	0
1650	0	0
1800	0	0
1950	0	0
2100	0	0
2250	0	0
2400	0	0
2550	0	0
2700	0	0
2850	0	0
3000	0	0
3150	0	0
3300	0	0
3450	0	0
3600	0	0
3750	0	0
21270	62.7029	56.58281
24270	85.7616	82.36081
27870	96.0957	95.01984

5.5.8 Autocatalysis investigation (Pre-stirring)



Time (sec)	A_{Pr} (HPLC)	% Conversion
0	0	0
30	5.33	4.181891
60	17	13.70194
90	33.68	28.24726
120	47.05	40.78696
150	61.59	55.41714
180	72.5	67.14517
210	82.3	78.2818
240	88.7	85.88553
270	92	89.914
300	95.29	94.00597
330	96.8	95.90996
360	97.7	97.05266
390	98.86	98.53425
420	99.8	99.74215
450	100	100
480	100	100
510	100	100

5.5.9 Autocatalysis investigation with product indoline 95



5.5.9 (a) 7 mol% indoline 95

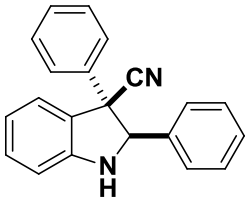
Time (sec)	A_{Pr} (HPLC)	% Conversion
0	0	0
150	0	0
300	0	0
450	0	0
600	0	0
750	0	0
900	0	0
1050	0	0
1200	0	0
1350	0	0
1500	0	0
1650	3.189189	2.490092
1800	10.97297	8.721317
1950	24.92973	20.47274
2100	40.75676	34.78116
2250	58.60541	52.32418
2400	74.51892	69.39124
2550	89.30811	86.62226
2700	95.13514	93.81163
2850	98.27027	97.77979

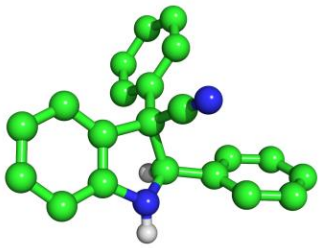
5.5.9 (b) 10 mol% indoline 95

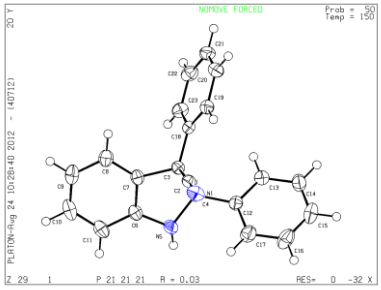
Time (sec)	A_{Pr} (HPLC)	% Conversion
0	0	0
150	0	0
300	0	0
1350	22.8913	18.70793
1500	42.44565	36.37448
1650	58.47826	52.19348
1800	71.76087	66.32896
1950	79.80435	75.38901
2100	86.69565	83.47497
2250	94.23913	92.69059
2400	95.81522	94.66636
2550	98.97826	98.68585
2700	100	100
2850	100	100
3000	100	100

5.6 X-Ray Crystallographic Data

anti-2,3-Diphenylindoline-3-carbonitrile



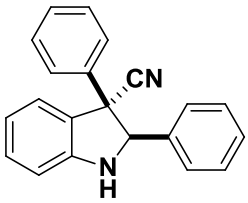


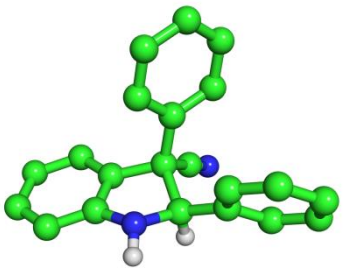


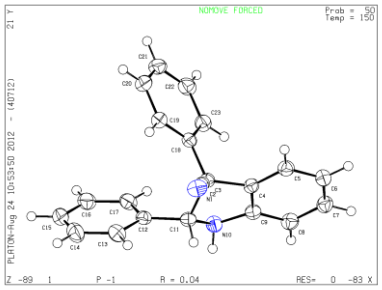
Key data and refinement for compound *anti*-64	
Empirical formula	$C_{21}H_{16}N_2$
Formula weight	296.37
Temperature	150 K
Wavelength	0.71073 Å
Crystal system	Orthorhombic
Space group	P 21 21 21
Unit cell dimensions	a = 9.5487 Å α = 90°
	b = 11.6601 Å β = 90°
	c = 14.4501 Å γ = 90°
Volume	1608 .0 $Å^3$
Z	4
Density (calculated)	1.223 Mg/m^3
Absorption coeffitient	0.072 mm^{-1}
F (000)	624
Crystal size	0.12 × 0.32 × 0.39 mm^3
Theta range for data collected	5.100 to 27.490°
Reflections collected	3668

Independent reflections	2092
Completeness to theta = 27.490°	99.0%
Refinement method	Full-matric least-squares on F^2
Data / restraint / parameters	2092/0/208
Goodness-of-fit on F^2	1.036

***syn*-2,3-Diphenylindoline-3-carbonitrile**







Key data and refinement for compound *syn*-64	
Empirical formula	$C_{21}H_{16}N_2$
Formula weight	296.37
Temperature	150 K
Wavelength	0.71073 Å
Crystal system	Triclinic
Space group	P - 1
Unit cell dimensions	a = 7.9846 Å α = 94.732°
	b = 9.7916 Å β = 106.024°
	c = 10.3173 Å γ = 91.140°
Volume	771.88 $Å^3$
Z	2
Absorption coeffitient	0.075 mm^{-1}
F (000)	312
Crystal size	0.24 × 0.52 × 0.56 mm^3
Theta range for data collected	5.000 to 27.000°
Reflections collected	6749
Independent reflections	3522
Completeness to theta = 27.490°	99.0%

Refinement method	Full-matric least-squares on F^2
Data / restraint / parameters	3522/0/208
Goodness-of-fit on F^2	0.910

5.7 Crystallographic information files (.cif)

The crystallographic information files (.cif) for all of the X-ray structures provided in this thesis are included in the attached CD.

6. References

1. Fleming, I. *Pericyclic Reactions*, Oxford University Press: Oxford, UK **1999**.

2. Fleming, I. Molecular Orbitals and Organic Chemical Reactions **2009**, Wiley.

3. Doering, W. von E.; Roth, W. R. *Tetrahedron* **1962**, *18*, 67-74.

4. Woodward, R. B. Aromaticity: an international symposium, *Chemical Society: London* **1967**, 217-249.

5. Woodward, R. B.; Hoffmann, R. *Angew. Chem. Int. Ed.* **1969**, *8*, 781-853.

6. Hoffmann, R.; Woodward, R. B. *Acc. Chem. Res.* **1968**, *1*, 17–22.

7. Woodward, R. B.; Hoffmann, R. The Conservation of Orbital Symmetry, *Verlag Chemie*, Weinheim, **1970**.

8. a) Woodward, R. B.; *Pure Appl. Chem.* **1968**, *17*, 519; b) Todd, A. R.; Cornforth, J. W. *Biogr. Mem. Fellows R. Soc.* **1981**, *27*, 628.

9. Beaudry, C. M.; Malerich, J. M.; Trauner, D. *Chem. Rev.* **2005**, *105*, 4757.

10. Müller, P. *Pure Appl. Chem.* **1994**, *66*, 1077–1184.

11. Thompson, S.; Coyne, A. G.; Knipe, P. C.; Smith, M. D. *Chem. Soc. Rev.* **2011**, *40*, 4217-4231.

12. For reviews, see: (a) Habermas, K. L.; Denmark, S. E.; Jones, T. K. *Org. React.* **1994**, *45*, 1. (b) Santelli-Rouvier, C.; Santelli, M. *Synthesis* **1983**, 429.

13. Liang, G.; Gradl, S. N.; Trauner, D. *Org. Lett.* **2003**, *5*, 4931–4934.

14. Liang, G. X.; Trauner, D. *J. Am. Chem. Soc.* **2004**, *126*, 9544–9545.

15. Aggarwal, V. K.; Belfield, A. J. *Org. Lett.* **2003**, *5*, 5075–5078.

16. (a) Evans, D. A.; Rovis, T.; Kozlowski, M. C.; Tedrow, J. S. *J. Am. Chem. Soc.* **1999**, *121*, 1994-1995; (b) Evans, D. A.; Rovis, T.; Kozlowski, M. C.; Downey, C. W.; Tedrow, J. S. *J. Am. Chem. Soc.* **2000**, *122*, 9134-9142.

17. Rueping, M.; Ieawsuwan, W.; Antonchick, A. P.; Nachtsheim, B. J. *Angew. Chem. Int. Ed.* **2007**, *46*, 2097–2100.

18. Magomedov, N. A.; Ruggiero, P. L.; Tang, Y. *Org. Lett.* **2004**, *19*, 3373–3379.

19. Magomedov, N. A.; Ruggiero, P. L.; Tang, Y. *J. Am. Chem. Soc.* **2004**, *126*, 1624–1625.

20. Yu, T.-Q.; Fu, Y.; Liu, L.; Guo, Q.-X. *J. Org. Chem.* **2006**, *71*, 6157–6164.

21. Bishop, L. M.; Barbarow, J. E.; Bergman, R. G.; Trauner, D. *Angew. Chem. Int. Ed.* **2008**, *47*, 8100–8103.

22. Bishop, L. M.; Roberson, R. E.; Bergman, R. G.; Trauner, D. *Synthesis* **2010**, 2233.

23. Vijn, R. J.; Speckamp, W. N.; Dejong, B. S.; Hiemstra, H. *Angew. Chem. Int. Ed.* **1984**, *23*, 165–166.

24. Speckamp, W. N.; Veenstra, S. J.; Dijkink, J.; Fortgens, R. *J. Am. Chem. Soc.* **1981**, *103*, 4643-4645.

25. Müller, S.; List, B. *Angew. Chem. Int. Ed.* **2009**, *48*, 9975–9978.

26. Maciver, E. E.; Thompson, S.; Smith, M. D. *Angew. Chem. Int. Ed.* **2009**, *48*, 9979–9982.

27. For reviews of asymmetric phase-transfer catalysis see; a) Donnell, M. J. *Catalytic Asymmetric Synthesis, 2nd ed.*, Wiley-VCH, Weinheim, 2000, p. 727; b) Ooi, T.; Maruoka, K. *Angew. Chem. Int. Ed.* **2007**, *23*, 4222.

28. Paqui Grande Carmona, Summer research project report, **2011**.

29. Mąkosza, M.; Tomashewskij, A. A. *J. Org. Chem.* **1995**, *60*, 5425.

30. MacMillan, K. S.; Nguyen, T.; Hwang, I.; Boger, D. L. *J. Am. Chem. Soc.* **2009**, *131*, 1187.

31. Goetz, F. J.; Hirsch, J. A.; Augustine, R. J. *J. Org. Chem.* **1983**, 2468.

32. Corey, E. J.; Xu, F.; Noe, M. C. *J. Am. Chem. Soc.* **1997**, *119*, 12414.

33. These were synthesized by Dr Meiling Li.

34. Many thanks to Dr Russell Driver for help with X-ray crystallography.

35. Lygo, B.; Andrews, B. I. *Acc. Chem. Res.* **2004**, 37, 518.

36. Starks, C. M. *J. Am. Chem. Soc.* **1971**, *93*, 195.

37. Starks, C. M.; Liotta, C. L.; Halpern, M. *Phase-transfer catalysis: Fundamentals, Applications, and Industrial perspectives*, Springer, **1994**.

38. Starks, C. M.; Liotta, C. L. *Phase-transfer catalysis: Principles and Techniques*, Academic Press, UK, **1978**.

39. Rabinovitz, M.; Cohen, Y.; Halpern, M. *Angew. Chem. Int. Ed.* **1986**, *25*, 960–970.

40. Jones, R. A. *Quaternary Ammonium Salts: Their use in phase-transfer catalysis*, Academic Press, UK, **2001**.

41. Landini, D.; Maia, A.; Montanari, F. *J.C.S. Chem. Comm.* **1977**, 112-113.

42. Freedman, H. H. *Pure Appl. Chem. Soc.* **1986**, *58*, 857.

43. A. Brandstrom, Principles of Phase Transfer Catalysis by Quaternary Ammonium Salts, in Advances in Physical Organic Chemistry, Academic Press, London and New York (1977).
44. Naik, S. D.; Doraiswamy, L. K. *AIChE* **1998**, *44*, 612-646.

45. Mąkosza, M. *Pure Appl. Chem.* **1975**, *43*, 439.

46. Solaro, R.; D'Antone, S.; Chiellini, E. *J. Org. Chem.* **1980**, *45*, 4179.

47. Halpern, M.; Sasson, Y.; Rabinovitz, M. *Tetrahedron* **1982**, *38*, 3183.

48. Herriott, A.; Picker, D. *Tetrahedron Lett.* **1972**, 4521.

49. Dehmlow, E.; Dehmlow, S. *Phase-Transfer Catalysis* **1983**, Verlag Chemie, Weinheim, pp. 14-15.

50. Menger, F. *J. Am. Chem. Soc.* **1970**, *92*, 5965.

51. Halpern, M.; Sasson, Y.; Rabinovitz, M. *J. Org. Chem.* **1983**, *48*, 1022.

52. Landini, D.; Maia, A.; Montanari, F. *J. Am. Chem. Soc.* **1978**, *100*, 2796.

53. Starks, C. M.; Owens, R. M. *J. Am. Chem. Soc.* **1973**, *95*, 3613.

54. Dolling, U.-H.; Davis, P.; Grabowski, E. J. J. *J. Am. Chem. Soc.* **1984**, *106*, 446-447.

55. Hughes, D. L.; Dolling, U.-H.; Ryan, K. M.; Schoenewaldt, E. F.; Grabowski, E. J. J. *J. Org. Chem.* **1987**, *52*, 4745-4752.

56. Denmark, S. E.; Weintraub, R. C.; Gould, N. D. *J. Am. Chem. Soc.* **2012**, *134*, 13415.

57. Wang, M.; Yang, H. *Ind. Eng. Chem. Res.* **1990**, *29*, 522-526.

58. This investigation was initially performed by a part II student David Yeo in the Smith group at University of Oxford, **2010**.

59. Halpern, M.; Cohen, Y.; Sasson, Y.; Rabinovitz, M. *Nouv. J. Chim.* **1984**, *8*, 443.

60. Mąkosza, M.; Bialecka, E. *Tetrahedron Lett.* **1977**, 183.

61. Denmark, S. E.; Weintraub, R. C. *Heterocycles* **2011**, *82*, 1527-1540.

62. Denmark, S. E.; Gould, N. D.; Wolf, L. M. *J. Org. Chem.* **2011**, *76*, 4260-4336.

63. Denmark, S. E.; Gould, N. D.; Wolf, L. M. *J. Org. Chem.* **2011**, *76*, 4337-4357.

64. Baldwin, J. E. *J. Chem. Soc. Chem. Commun.* **1976**, 734.

65. Baldwin, J. E.; Kruse, L. I. *J. Chem. Soc. Chem. Commun.* **1977**, 233.

66. Pangborn, A. B., Gairdello, M. A., Grubbs, R. H., Rosen, R. K., Timmers, F. J., *Organometallics*, **1996**, *15*, 1518.